TOXICITY OF ENGINEERED NANOPARTICLES TO ANAEROBIC WASTEWATER TREATMENT PROCESSES AND APPROACHES FOR TOXICITY ATTENUATION

by

Jorge Gonzalez-Estrella

_____

A dissertation submitted to the Faculty of the

DEPARTMENT OF CHEMICAL AND ENVIRONMENTAL ENGINEERING

In Partial Fulfillment of the Requirements

For the Degree of

DOCTOR OF PHILOSOPHY

WITH A MAJOR IN ENVIRONMENTAL ENGINEERING

In the Graduate College

THE UNIVERSITY OF ARIZONA

2014

THE UNIVERSITY OF ARIZONA

GRADUATE COLLEGE

As members of the Dissertation Committee, we certify that we have read the dissertation prepared by Jorge Gonzalez-Estrella entitled "*Toxicity of engineered nanoparticles to anaerobic wastewater treatment processes*", and recommend that it be accepted as fulfilling the dissertation requirement for the Degree of Doctor of Philosophy.

_____12/12/2014

María Reyes Sierra-Álvarez

_____12/12/2014

James A. Field

_____12/12/2014

Farhang Shadman

_____12/12/2014

Joan E. Curry

Final approval and acceptance of this dissertation is contingent upon the candidate's submission of the copies of the dissertation to the Graduate College. I hereby certify that I have read this dissertation prepared under my direction and I recommend that it be accepted as fulfilling the dissertation requirement

_____12/12/2014

Dissertation Director: María Reyes Sierra-Álvarez

_____12/12/2014

Dissertation Director: James A. Field

STATEMENT BY AUTHOR

This dissertation has been submitted in partial fulfillment of the requirements for an advanced degree at the University of Arizona and deposited in the University Library to be made available to borrowers under rules of the Library.

Brief quotations of this dissertation are allowable without special permission, provided that accurate acknowledgment of source is made. Requests for permission for extended quotation from or reproduction of this manuscript in whole or in part may be granted by the head of the major department or the Dean of the Graduate College when in his or her judgment the proposed use of the material is in the interests of scholarship. In all other instances, however, permission must be obtained from the author.

SIGNED: Jorge Gonzalez-Estrella

Acknowledgements

This thesis could not have been written without the constant support of Dr. Jim Field and Dr. Reyes Sierra Alvarez. Their advice not only has important implications in this document, but also in my development as a researcher, as well as a great influence in my future career. I am truly grateful to have been part of their research group.

I want to acknowledge the important role of Dr. Daniel Puyol in this thesis. His passion for research, energy, and knowledge have encouraged me to make the most of my studies. As well, the supportive work of Sara Gallagher in the busiest days of this journey greatly facilitated the progress of this research.

My friends in Tucson from outside and inside of the University, which I will not name for fear of leaving some off the list, made of this four years a very unique and memorable experience. I am very thankful for all of your talks, the time spent together, and continual support. You are one of the best parts of Tucson, and I am looking forward to continuing our friendship in the future. I am going to make sure to express my thankfulness personally when I see each of you.

Thank you, Amy, for your incredible support during these years. You are not only the best witness of the effort invested in this process, but also a partner that has pushed me to accomplish this goal. Without your tangible help, kindness, love, friendship, and patience, this would had been a completely different experience. I am very thankful for you. You are for sure the best outcome of graduate school.

Gracias Patty y Mario, por siempre creer en mí y darme su apoyo. Gracias Mamá y Papá por darme la libertad de escoger mi camino y motivarme a seguirlo. Siempre estaré agradecido con todos ustedes. Los amo.

Finally, I express my gratitude to the Semiconductor Research Corporation (SRC)/Sematech Engineering Research Center for Environmentally Benign Semiconductor and CONACyT for their financial support.

A Patty, Mario, Mamá, y Papá,

A Amy,

Contents

List of Figures

List of Tables

Abstract

Nanotechnology is an increasing market. Engineered nanoparticles (NPs), materials with at least one dimension between 1 and 100 nm, are produced on a large scale. NPs are vastly used in industrial processes and consumer products and they are most likely discharged into wastewater treatment plants after being used. Activated Sludge is one of the most applied biological wastewater treatment processes for the degradation of organic matter in sewage. Activated sludge produces an excess of sludge that is commonly treated and stabilized by anaerobic digestion. Recent studies have found that NPs accumulate in the activated sludge; thus, there is a potential for the concentrations of NPs to magnify as concentrated waste sludge is fed into the anaerobic digestion process. For this reason, it is important to study the possible toxic effects of NPs on the microorganisms involved in the anaerobic digestion process and the approaches to overcome toxicity if necessary. The present work evaluates the toxic effect of NPs on anaerobic wastewater treatment processes and also presents approaches for toxicity attenuation.

The first objective of this dissertation (Chapter III) was to evaluate the toxicity of high concentrations (1, 500 mg L^{-1}) of Ag^0, Al_2O_3, CeO_2, Cu^0, CuO, Fe^0, Fe_2O_3, Mn_2O_3, SiO_2, TiO_2, and ZnO NPs to acetoclastic and hydrogenotrophic methanogens and the effect of a dispersant on the NPs toxicity to methanogens. The findings indicated that only Cu^0 and ZnO NPs caused severe toxicity to hydrogenotrophic methanogens and Cu^0, CuO, and ZnO NPs to acetoclastic methanogens. The dispersant did not impact the NPs toxicity. The concentrations of Cu^0 and ZnO causing 50% of inhibition (IC_{50}) to hydrogenotrophic methanogens were 68 and 250 mg L^{-1}, respectively. Whereas the IC_{50} values for acetoclastic methanogens were 62, 68, and 179 for Cu^0, ZnO, and CuO-Cu NPs respectively. These findings indicate that acetoclastic methanogens are more sensitive to NP toxicity compared to hydrogenotrophic methanogens and that Cu^0 and ZnO NPs are highly toxic to both. Additionally, it was observed that the toxicity of any given metal was highly correlated with its final dissolved concentration in the assay irrespective of whether it was initially added

as a NP or chloride salt, indicating that corrosion and dissolution of metals from NPs may have been responsible for the toxicity.

The second objective of this dissertation (Chapter IV) was to evaluate the Cu^0 NP toxicity to anaerobic microorganisms of wastewater treatment processes. Cu^0 is known to be toxic to methanogens; nonetheless, little is known about its toxic effects on microorganisms of upper trophic levels of anaerobic digestion or other anaerobic process used for nitrogen removal. This specific objective evaluated Cu^0 NP toxicity to glucose fermentation, syntrophic propionic oxidation, methanogenesis, denitrification and anaerobic ammonium oxidation (anammox). Chapter IV showed that anammox and glucose fermentation were the least and most inhibited processes with inhibition constants (K_i) values of 0.324 and 0.004 mM of added Cu^0 NPs, respectively. The *Ki* values obtained from the residual soluble concentration of the parallel experiments using $CuCl_2$ indicated that Cu^0 NP toxicity is most likely caused by the release of soluble ions for each one of the microorganisms tested. The results taken as a whole demonstrate that Cu^0 NPs are toxic to a variety of anaerobic microorganisms of wastewater treatment processes.

The third objective of this document (Chapter V) was to study the role of biogenic sulfide in attenuating Cu^0 and ZnO NP toxicity to acetoclastic methanogens. Previous literature results and research presented in this dissertation indicated that the release of soluble ions from Cu and ZnO NPs cause toxicity to methanogens. In the past, the application of sulfide to precipitate heavy metals as inert non-soluble sulfides was used to attenuate the toxicity of Cu and Zn salts. Building on this principle, Chapter V evaluated the toxicity of Cu^0 and ZnO NPs in sulfate-containing (0.4 mM) and sulfate-free conditions. The results show that Cu^0 and ZnO were 7 and 14x less toxic in sulfate-containing than in sulfate-free assays as indicated by the differences in K_i values. The K_i values obtained based on the residual metal concentration of the sulfate-free and sulfate-containing assays were very similar, indicating that the

toxicity is well correlated with the release of soluble ions. Overall, this study demonstrated that biogenic sulfide is an effective attenuator of Cu^0 and ZnO NP toxicity to acetoclastic methanogens.

Finally, the last objective (Chapter VI) of this dissertation was to evaluate the effect of iron sulfide (FeS) on the attenuation of Cu^0 and ZnO toxicity to acetoclastic methanogens. FeS is formed by the reaction of iron(II) and sulfide. This reaction is common in anaerobic sediments where the reduction of iron(III) to iron(II) and sulfate to sulfide occurs. FeS plays a key role controlling the soluble concentrations of heavy metals and thus their toxic effects in aquatic sediments. This study evaluated the application of FeS as an approach to attenuate Cu^0 and ZnO NP toxicity and their salt analogs to acetoclastic methanogens. Two particle sizes, coarse FeS (FeS-c, 500-1200 μm) and fine FeS (FeS-f, 25-75 μm) were synthesized and used in this study. The results showed 2.5x less FeS-f than FeS-c was required to recover the methanogenic activity to the same extent from the exposure to highly inhibitory concentrations of $CuCl_2$ and $ZnCl_2$ (0.2 mM). The results also showed that a molar ratio of FeS-f/Cu^0, FeS-f/ZnO, FeS-f/Zn Cl_2, and FeS-f/$CuCl_2$ of 3, 3, 6, and 12 respectively, was necessary to provide a high recovery of methanogenic activity (>75%). The excess of FeS needed to overcome the toxicity indicates that not all the sulfide in FeS was readily available to attenuate the toxicity. Overall, Chapter VI demonstrated that FeS is an effective attenuator of the toxicity of Cu^0 NP and ZnO NPs and their salt analogs to methanogens, albeit molar excesses of FeS were required.

CHAPTER I- INTRODUCTION

1.1 Nanotechnology

Nanotechnology is the science of the manipulation and restructuring of materials by applying size- and structure-dependent properties and phenomena intrinsic of the nanoscale range (1-100nm) (Hansen et al., 2007). Nanotechnology facilitates the creation of devices, materials and systems that provide fundamental new properties and functions due to their small size (Roco, 2011). The worldwide market value of nanotechnology has been estimated at ~$3,000 billion by 2020 (Roco et al., 2011). Due to its great potential for application in numerous aspects of daily life, nanotechnology requires the alliance of chemical, biological, physical, electronic, and engineering processes for the understanding and fabrication of materials in the nanoscale range. Nanotechnology is comprised of four main sectors (Aitken et al., 2006): 1) nano-medicine, 2) nano-fabrication, 3) nano-metrology, and 4) engineered nanoparticles (NPs). The latter sector, engineered nanoparticles, has had a great impact in several applications during the last years.

1.2 Characteristics and applications of NPs

NPs are manmade materials with at least one dimension between 1-100 nm that have unique properties not shared by materials with the same chemical composition but of a different size scale (Hansen et al., 2007). Even though their small size does not provide a new chemical composition, the atypical structure of NPs may enhance processes such as dissolution or generation of reactive oxygen species among other processes (Aruoja et al., 2009; Carlson et al., 2008). The number of atoms localized on the surface of the material exponentially increases in sizes smaller than 20-30 nm, which results in

substantially different qualities than those observed in larger materials (Auffan et al., 2009). At this scale, quantum properties are more important than other characteristics observed at microscale, which has led to the fabrication of a new generation of materials (Hansen et al., 2007).

NPs are used in a broad spectrum of high-tech, consumer, and cosmetic products, custom design and pharmacological applications. Four groups of NPs can be defined according to their chemical composition (Karlsson et al., 2015): 1) metallic-intermetallic, 2) ceramic, 3) polymeric/organic, and 4) composite systems. The first group encompasses the materials that are the main focus of this dissertation: zero-valent metal and metal oxide NPs.

Inorganic NPs are used in wide variety of applications. For example, Ag NPs are well-known antimicrobial materials (Carlson et al., 2008; Choi et al., 2008). Cu-based NPs are commonly used in products such as wood preservatives, catalysts, or printable electronics (Wang et al., 2013). Other materials, such as TiO_2 or ZnO NPs, are components of goods that come into direct contact with the human body in forms such as toothpaste or sunscreen (Chen & Mao, 2007; Reed et al., 2012). Although NPs have shown great benefits in multiple processes and products, their extensive use has created new questions and concerns regarding their fate in and effects on the environment.

1.3 NPs in the environment

There is scientific consensus that NPs are released into the environment. Recently, Gottschalk and Nowack (2011) defined four possible release scenarios of NPs: 1) Release from production, 2) release from manufacturing processes, 3) release from products, and 4) release from technical facilities. NPs are mostly discharged into the environment from non-point sources (e.g. products) like most other contaminants

(Nowack & Bucheli, 2007). For example, TiO_2 or ZnO NPs, present in sunscreens, are very likely to be unintentionally disposed into the environment after being washed off of the skin (Westerhoff et al., 2013).

Studies modeling the life cycle of NPs and their environmental fate have concluded that sewage sludge, waste water treatment plants, and incineration plants are facilities that accumulate large amounts of NPs (Gottschalk & Nowack, 2011). Among these facilities, waste water treatment plants have a very important role in water quality and, therefore, human health. Thus, the accumulation and effect of NPs on wastewater treatment plants and the resulting water quality has attracted the attention of the scientific community in recent years (Brar et al., 2010).

1.4 NPs in wastewater treatment plant processes

Accumulation of NPs in wastewater treatment plants is expected due to the physical and chemical interactions of organic matter with NPs (Brar et al., 2010). One of the most commonly applied wastewater treatment processes is activated sludge. Figure 1 shows the typical configuration of activated sludge. This biological wastewater process is preceded by a primary sedimentation tank which removes most of the suspended inorganic and organic materials. It is followed by an aeration tank which provides the biological conditions for the growth of microorganisms that use biodegradable organic compounds as source of energy and carbon; and finally, a secondary sedimentation tank which recovers the heterotrophs for their recirculation to the aeration tank. All operations of the activated sludge process produce an excess of sludge (biosolids) as a byproduct that needs to be stabilized (Metcalf et al., 2003).

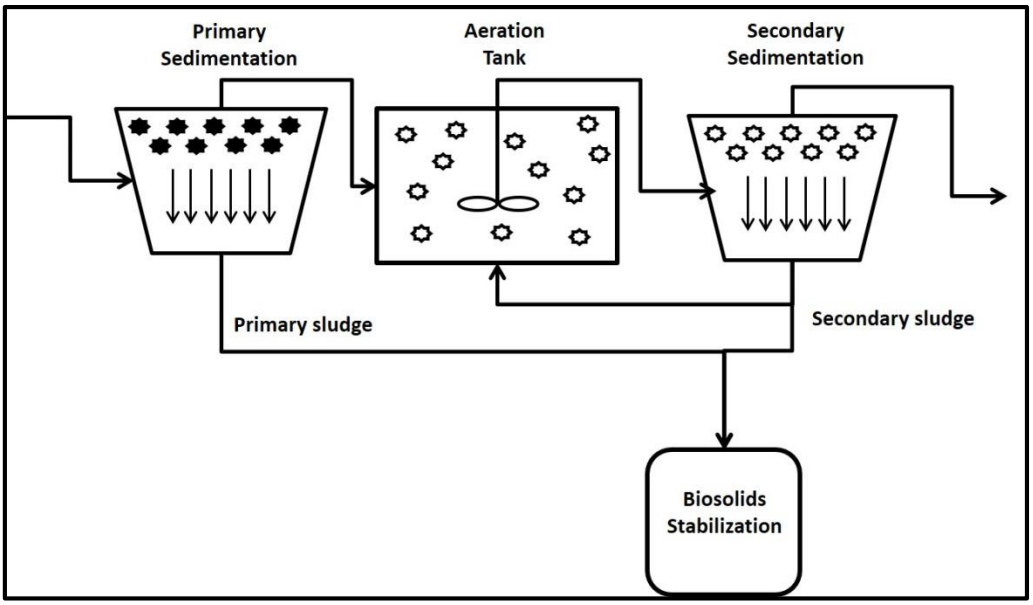

Figure 1.1 Typical aerobic sludge treatment configuration

Recent studies have evaluated the fate of NPs in activated sludge. The findings demonstrated that in a lab-scale activated sludge system, CeO_2 NPs were mainly removed (~97%) by settling, aggregation and association with the sludge (Gomez-Rivera et al., 2012). Another study revealed that a full-scale activated sludge treatment plant retained TiO_2 in the heterotrophic biomass (Kiser et al., 2009). This evidence indicates that other NPs used in consumer products may also be retained in different sections of activated sludge processes. It has been estimated that >90% of all NPs may be retained in wastewater treatment plants (Westerhoff et al., 2013). Therefore, the retention of NPs in the activated sludge process may lead to a substantial increase in the concentration of NPs in unit operations designed for the stabilization of biosolids, such as anaerobic digestion.

Anaerobic digestion is a well-established process for the stabilization of biosolids which consists of the transformation of organic matter to methane (Rittmann & McCarty, 2001). Figure 1.2 shows the general metabolic pathway of anaerobic digestion. The process involves a variety of microorganisms due

to the different metabolic steps that are needed for the full conversion of organic matter to methane. Anaerobic digestion can be subdivided in four different steps (Reith & Wijffels, 2003): 1) hydrolysis, conversion of biopolymers to soluble organic compounds; 2) acidogenesis, degradation of soluble organic compounds for the production of volatile fatty acids and carbon dioxide (CO_2); 3) acetogenesis, conversion of volatile fatty acids to acetate and hydrogen (H_2), and 4) methanogenesis, production of methane via degradation of acetate or by the reduction of CO_2 using H_2 as an electron donor.

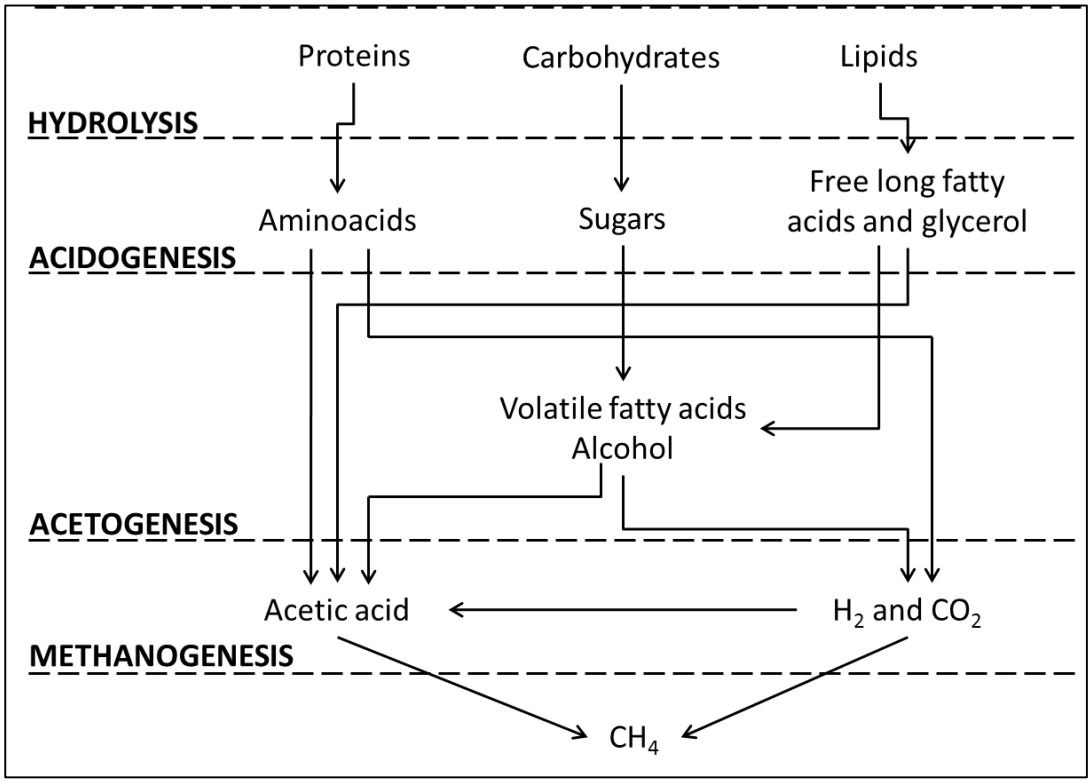

Figure 1.2 General schematic pathway of anaerobic digestion. Adapted from Reith and Wijffels (2003).

As anaerobic digestion is a biological process where non-biodegradable wastewater constituents are concentrated; non-biodegradable constituents such as NPs may accumulate in this process. The

accumulation of NPs may have toxic effects on the microorganisms responsible for the stabilization of biosolids; thus, new research has begun evaluating the toxic effects of NPs on anaerobic digestion.

1.5 Nanoparticle toxicity and toxicity attenuation

One of the main disadvantages of anaerobic digestion is its relatively high sensitivity to a variety of substances and chemical, biological, and physical conditions (Chen et al., 2008). Increased use of NPs may potentially enhance the toxic effect of some materials that are already known to be toxic to methanogens in bulk soluble form. For instance, heavy metals are highly inhibitory to anaerobic digestion (Chen et al., 2014), thus the application of ZnO or Cu NPs in different consumer products or processes could also potentially have severe inhibitory effects in this biological process.

A study comparing the toxic effect of CuO (~30 nm),and ZnO (50-70nm) NPs with that of CuO (~5µm) and ZnO (~1µm) microparticles on methanogens revealed that the toxic effect was increased by approximate 10-fold for CuO NP and 2-fold for ZnO NPs when comparing to their respective bulk particle analog (Luna-delRisco et al., 2011). This study found significantly higher solubility of CuO NPs than CuO bulk particles, whereas no significant difference in solubility was found between the two sizes of AnO tested despite its high solubility. Thus, the difference in the increase of the toxic effect may be attributed to the rate of dissolution. The small size of NPs may increase the rates of process such as dissolution, redox reactions, or generation of reactive oxygen species (Auffan et al., 2009).

Even though NPs have the potential to affect microorganisms via the generation of reactive oxygen species, adsorption to cell membranes (lipids and proteins) or by transporting toxic substances through the membrane (Auffan et al., 2009), the adverse effects of NPs on anaerobic digestion microorganisms have been mostly attributed to the release of soluble toxic ions (Luna-delRisco et al., 2011; Mu et al.,

2011; Otero-González et al., 2014a). Therefore, it can be expected that a decrease in the solubility of NPs would have a positive effect on reducing their toxicity.

In the past, the toxicity of Cu^{2+} and Zn^{2+} soluble cations to methanogens has been attenuated by precipitating these soluble ions as low soluble sulfide salts. This methodology has been applied by reacting the soluble ions with sulfide (S^{2-}) produced by the biological anaerobic reduction of sulfate (SO_4^{2-}) (Lawrence & McCarty, 1965) or by a direct addition of sulfide to the reactors containing these toxic metals (Zayed & Winter, 2000). One study demonstrated that sulfide decreased considerably the dissolution of ZnO NPs by the formation of ZnS (Ma et al., 2013b). Recently, it was demonstrated that the formation of Ag_2S prevent Ag^0 NP toxicity to four different types of aquatic and terrestrial eukaryotic organisms. All these results indicate that similar principles can be applied to attenuate potential NP toxicity to anaerobic digestion.

Until recently, very little research had been carried out investigating the toxic effect of NPs to anaerobic processes of wastewater treatment systems. The present study evaluated the toxicity of NPs to anaerobic processes and investigated approaches for toxicity attenuation of the most toxic NPs. The next chapter describes in detail the objectives of this doctoral dissertation.

CHAPTER II - OBJECTIVES

The main objective of this study was to investigate the toxicity of engineered nanoparticles to microorganisms in anaerobic wastewater treatment processes and to study approaches to attenuate the antimicrobial effects for the most toxic NPs. For that purpose this work has the following specific objectives:

1. Investigate the inhibitory effect of inorganic NPs on the methanogenic activity of acetoclastic and hydrogenotrophic methanogens in anaerobic granular sludge and the effect of the NPs aggregation on the toxicity effect.

2. Evaluate the toxic effect of Cu^0 NPs on the main microbial trophic groups involved in the anaerobic digestion of carbonaceous substrates and as well anaerobic trophic groups important for N-removal.

3. Investigate the role of biogenic sulfide in attenuating ZnO- and Cu^0-NP toxicity to acetoclastic methanogens.

4. Assess the attenuation of Cu^0 and ZnO toxicity to acetoclastic methanogens by iron sulfide

CHAPTER III - TOXICITY ASSESSMENT OF INORGANIC NANOPARTICLES TO ACETOCLASTIC AND HYDROGENOTROPHIC METHANOGENIC ACTIVITY IN ANAEROBIC GRANULAR SLUDGE

Jorge Gonzalez-Estrella*, Reyes Sierra-Alvarez, James A. Field

Department of Chemical and Environmental Engineering, University of Arizona,

P.O. Box 210011, Tucson, AZ 85721, USA

*Corresponding author: Jorge Gonzalez-Estrella

Department of Chemical and Environmental Engineering
The University of Arizona,
P.O. Box 21011, Tucson, AZ 85721, United States
Phone: +1-520-621 6162
E-mail: jorgegonzaleze@email.arizona.edu

Abstract

Release of engineered nanoparticles (NPs) to municipal wastewater from industrial and residential sources could impact biological systems in wastewater treatment plants. Methanogenic inhibition can cause failure of anaerobic waste(water) treatment. This study investigated the inhibitory effect of a wide array of inorganic NPs (Ag^0, Al_2O_3, CeO_2, Cu^0, CuO, Fe^0, Fe_2O_3, Mn_2O_3, SiO_2, TiO_2, and ZnO supplied up to 1,500 mg L^{-1}) to acetoclastic and hydrogenotrophic methanogenic activity of anaerobic granular sludge. Of all the NPs tested, only Cu^0 and ZnO caused severe methanogenic inhibition. The 50% inhibiting concentrations determined towards acetoclastic and hydrogenotrophic methanogens were 62 and 68 mg L^{-1} for Cu^0 NP; and 87 and 250 mg L^{-1} for ZnO NP, respectively. CuO NPs also caused inhibition of acetoclastic methanogens. Cu^{2+} and Zn^{2+} salts caused similar levels of inhibition as Cu^0- and ZnO NPs based on equilibrium soluble metal concentrations measured during the assays, suggesting that the toxicity was due to the release of metal ions by NP-corrosion. A commercial dispersant, Dispex, intended to increase NP stability did not affect the inhibitory impact of the NPs. The results taken as a whole suggest that Zn- and Cu-containing NPs can release metal ions that are inhibitory for methanogenesis.

Keywords: Copper, Engineered Nanoparticles, Inhibition, Methanogenesis, Zinc Oxide

3.1 Introduction

The advance of nanotechnology has led to an increase in the production of engineered nanoparticles (NPs). NPs are defined as having at least one-dimension smaller than 100 nm (Hansen et al., 2007). Nanotechnology is rapidly developing and is becoming applied in several industrial sectors such as medicine and semiconductor manufacturing. NPs are already utilized in consumer products like cosmetics, personal-care products, paints and coatings (Brar et al., 2010; Kahru et al., 2008). The nanotechnology market is projected to be $1 trillion in 2015, employing 2 million people (Aitken et al., 2006).

Concerns about the environmental and health impacts of NPs are increasing. However, compared to NP synthesis and applications, relatively little research has been focused on environmental and health impacts (Brar et al., 2010). The small size of NPs may enhance processes like dissolution, redox reactions or generation of reactive oxygen species, impacting environmental and human health (Auffan et al., 2009; Handy et al., 2008). NPs disposed via wastewater streams will often end up in wastewater treatment plants with biological treatment operations (Brar et al., 2010); where little is known about their fate (Gomez-Rivera et al., 2012; Kiser et al., 2010; Zhang et al., 2008). The extent of NP removal, NP-toxicity to biological treatment, and potential sorption of NPs onto biosolids remain largely unknown (Nyberg et al., 2008). Additionally, variable wastewater composition can influence the physicochemical properties of NPs differently (Boxall et al., 2007; Brar et al., 2010).

NPs may impact several key unit operations at wastewater treatment plants. Some studies found that NPs remain partly retained in the sludge of the aerobic activated sludge process (Gomez-Rivera et al., 2012; Liang et al., 2010). Thus, NPs are expected to enter unit operations used for treating waste activated sludge. Anaerobic digestion (involving methanogenesis) is one of the most frequently applied methods of stabilizing excess wastewater sludge (Rittmann & McCarty, 2001). With the exception of a

few preliminary studies (Garcia et al., 2012; Luna-delRisco et al., 2011; Mu et al., 2011; Nyberg et al., 2008; Yang et al., 2012a), little is known regarding the toxicity of NPs to methanogens. The aim of this study was to investigate the inhibitory effect of inorganic NPs on the methanogenic activity of acetoclastic and hydrogenotrophic methanogens in anaerobic granular sludge. Likewise, this study evaluated the aggregation properties of NPs in an anaerobic basal medium. Lastly, the impact of a surfactant intended to stabilize NP dispersions on NP toxicity was evaluated.

3.2 Materials and methods

3.2.1 Chemicals

The commercial ammonium polyacrylate dispersant (Dispex A40, average MW ~ 4,000) was obtained from BASF (Freeport, TX, USA). Sodium acetate (99.9%) was purchased from Sigma Aldrich (St. Louis, MO, USA). H_2/CO_2 (80/20, v/v) gas mix was delivered by Airweld (Phoenix, AZ, USA). N_2/CO_2 (80/20, v/v) gas mix and CH_4 standard gas (99%) were acquired from Air Liquid America (Plumstedsville, PA, USA)**.** Sodium bicarbonate was purchased from Fisher Scientific (Pittsburgh, PA, USA).

3.2.2 Nanoparticles and stability of NP dispersions

Ag^0, Al_2O_3, Cu^0, CuO, CeO_2, Fe^0, Fe_2O_3, Mn_2O_3, SiO_2, TiO_2, and ZnO NPs were tested as inhibitors of methanogenic activity with and without the use of Dispex. The source of the NPs and the manufacturer reported size and purity are as follows: Ag^0 (size of < 100 nm, purity of 99.5%), Al_2O_3 (< 50 nm, 99%), CeO_2 (50 nm, 99.95%), Cu^0 (40-60 nm, 99%), CuO (40 nm, > 99%), and SiO_2 (10-20 nm, 99.5%) were purchased from Sigma-Aldrich (St. Louis, MO); Fe^0 (46-60 nm, 99.9%), Fe_2O_3 (40 nm, 99%), Mn_2O_3 (98%), and ZnO

(10-30 nm, 99.8%) were acquired from SkySpring Nanomaterials Inc. (Houston, TX); and TiO_2 (~25 nm, 99.5%) was a gift from Aerosil (Parsippany, NJ). All NPs were obtained as dry powders.

The stability of the NPs was evaluated by determining the particle size distribution (PSD) and zeta potential (ZP) according to a previous study (Garcia-Saucedo et al., 2011). All stock solutions were also prepared as previously described (Garcia-Saucedo et al., 2011). Aliquots (3 mL) of the stock solutions (2,500 mg L^{-1}) were amended into the 160 mL serum bottles containing 27 mL of 1.1x concentrated anaerobic basal medium, 1.1x concentrated basal medium with Dispex, DI water, or acidified DI water (pH 2). Afterwards, all bottles were flushed with a N_2/CO_2 (80:20, v/v) gas mixture. Subsequently, pH, PSD and ZP were measured. In order to imitate the conditions at which the toxicity assays were performed, all bottles were shaken for 24 h at 120 rpm at 30ºC. Next, the samples were allowed to settle for 30–45 min under static conditions, and samples of the supernatant were collected carefully to avoid carryover of any settled material. Samples were analyzed immediately for PSD and ZP. The PSD and ZP is shown in Table 1S (Supplementary Information). The soluble concentration of metals in the samples was only determined for those NPs that showed toxicity by filtering the samples through 25 nm membranes.

3.2.3 Sludge source

The methanogenic anaerobic granular sludge was obtained from a full-scale upward anaerobic sludge bed reactor treating brewery wastewater (Mahou, Guadalajara, Spain). The sludge was sieved to remove fine particles and excess water. The content of volatile suspended solids (VSS) was 7.92% of the wet weight. The sludge was stored at 4°C. The maximum methanogenic activity of the sludge in assays utilizing acetate and hydrogen as substrate was 317.6±29.5 and 566.7±34.8 mg CH_4-chemical oxygen demand (COD) per gram volatile suspended solids (VSS) per day, respectively.

3.2.4 Batch acetoclastic and hydrogenotrophic methanogenic activity bioassays

All bioassays were carried out using an anaerobic medium pH (7.2) containing (in mg L^{-1}): NH_4Cl (280), $NaHCO_3$ (5,000), K_2HPO_4 (250), $CaCl_2 \bullet 2H_2O$ (10), $MgCl_2 \bullet 6H_2O$ (100), $MgSO_4 \bullet 7H_2O$ (100); yeast extract (100) with 1 mL $L^{-1}$of trace elements (Karri et al., 2006). The medium of the control without NPs, assays with Dispex without NPs, assays with NPs, and assays with NPs and Dispex was composed by combining 27 mL of a 1.1× concentrated basal medium with 3 mL of DI water, 3 mL of Dispex solution (1,500 mg L^{-1}), 3 mL of NP stock (15 g L^{-1}), and 3 mL of the NPs stock (15 g L^{-1}) with Dispex (1,500 mg L^{-1}), respectively.

Firstly, inoculum (1.5 g of VSS L^{-1}) and 1.1x concentrated medium (27 mL) were added to 160 mL bottles. Subsequently, all bottles were flushed with the gas mixture N_2/CO_2 (80:20, v/v). Either sodium acetate (1 g COD L^{-1}) or hydrogen gas were used as electron donors. H_2 was supplied to a final headspace concentration of 0.5 atm of H_2/CO_2 applied as an overpressure after first flushing the assay bottles with the N_2/CO_2 gas mixture. Subsequently, all the assays were pre-incubated overnight at 30±2ºC in an orbital shaker at 120 rpm.

Following pre-incubation, 3 mL of DI water, 3 mL of Dispex stock solution (1,500 mg L^{-1}), 3 mL of NP stock (15 g L^{-1}), and 3 mL of the NPs stock with Dispex (NPs/Dispex, 10:1, w/w) were added to the control without NPs, assays with Dispex without NPs, assays with NPs, and assays with NPs and Dispex, respectively. The controls without NPs were performed in triplicate; whereas, all the treatment assays were performed in duplicate. Once NPs were added and the experimental control was prepared, all bottles were flushed with the N_2/CO_2 gas mixture and H_2/CO_2 was added when H_2 was the intended electron donor. A second substrate feeding was supplied to assays where methanogenic inhibition was observed (*i.e.,* assays with Fe^0, Cu^0, CuO, Mn_2O_3, and ZnO NPs). Acetate or H_2 were respiked as described above for the first feeding. All assays were incubated at 30±2ºC in an orbital shaker at 120 rpm.

Gas samples (100 µL) were withdrawn from the assays two or three times a day during the experiment to measure methane production until the theoretical maximum methane production was reached. The normalized methanogenic activity (NMA) was then calculated as the percentage of the ratio of maximum methane production rates in the treatment (test concentration of NP) and the control (without NPs) as shown below:

$$\mathrm{NMA}(\%) = \left(\frac{\text{Maximum } CH_4 \text{ production rate at tested NP concentration}}{\text{Maximum } CH_4 \text{ production rate of the control}}\right) 100$$

In the assays where methanogenic inhibition was observed, a second feeding of the electron donor was provided to explore the changes of toxicity as a function of the NP exposure time. NPs which caused enhanced methanogenic inhibition in the second feeding (Cu^0, CuO, and ZnO) were further evaluated in acetoclastic and hydrogenotrophic methanogenic assays exposed to different NP concentrations. These assays also included a first and second feeding of the respective substrates. The NMA was calculated for the different concentrations of NPs applied along with the inhibition concentration at which a 50% decrease in the specific methanogenic activity (IC_{50}, relative to the non-inhibited control) was observed. The IC_{50} concentration was calculated as described elsewhere (Garcia-Saucedo et al., 2011).

3.2.5 Methanogenic inhibition by soluble Cu and Zn ions

To study the effect of soluble Cu^{2+} and Zn^{2+} on methanogens, $CuCl_2$ and $ZnCl_2$ salts were used, with the experimental conditions described in section 2.4. In this case only acetate was used as the electron donor. Stock solutions containing 2,500 mg L^{-1} of Cu^{2+} or Zn^{2+} were prepared and diluted as needed to reach the desired initial concentration of metals (5, 10, 20, 25, 50, 75, 100, and 250 mg L^{-1}). The soluble metal content of the aqueous phase was monitored by collecting a sample (1.5 mL) from each bottle at the time point when the control assays approached the expected theoretical maximum methane

production. Samples were centrifuged at 13,000 rpm for 10 min and then filtered through 25-nm membranes.

3.2.6 Analytical methods

The methane content in the headspace of the serum flasks was determined by gas chromatography with flame ionization detection as previously described (Karri et al., 2006).

The concentration of the characteristic metal (Cu, Fe, Mn and Zn) in liquid samples from assays with toxic NPs (Fe^0, Cu^0, CuO, Mn_2O_3 and ZnO) was determined following acid digestion. Details of the procedures used for sample digestion and metal analysis are provided in Supplementary Information.

3.2.7 Statistical analysis

Data analysis was performed using the software Origin 8.6 (OriginLab, Northampton, MA) using a paired sample T-test.

3.3 Results

3.3.1 Screening NP toxicity to acetoclastic and hydrogenotrophic methanogenic activity

The toxicity of a series of NPs to methanogens was tested by exposing anaerobic granular sludge to 1,500 mg L^{-1} of each NP. Two different assay substrates were tested separately to assess the activity of acetoclastic and hydrogenotrophic methanogens. In the assays amended with acetate, Cu^0 NP inhibited completely the methanogenic activity; whereas Mn_2O_3- and ZnO NPs lowered the NMA by 52.4 and 53.5% compared to a control without NPs. The assays supplied with CuO- and Fe^0 NPs showed a NMA of 87 and 85%, respectively (Figure 3.1A). However, the NMA decreased over time from 87 to 63% for the assays

supplied with CuO NPs (Figure A.1.A, See Annex 1), and from 85 to 64% for the assays amended with Fe^0 NPs (Figure A.1.2B), indicating that extended exposure to these NPs could potentially lead to increased inhibition.

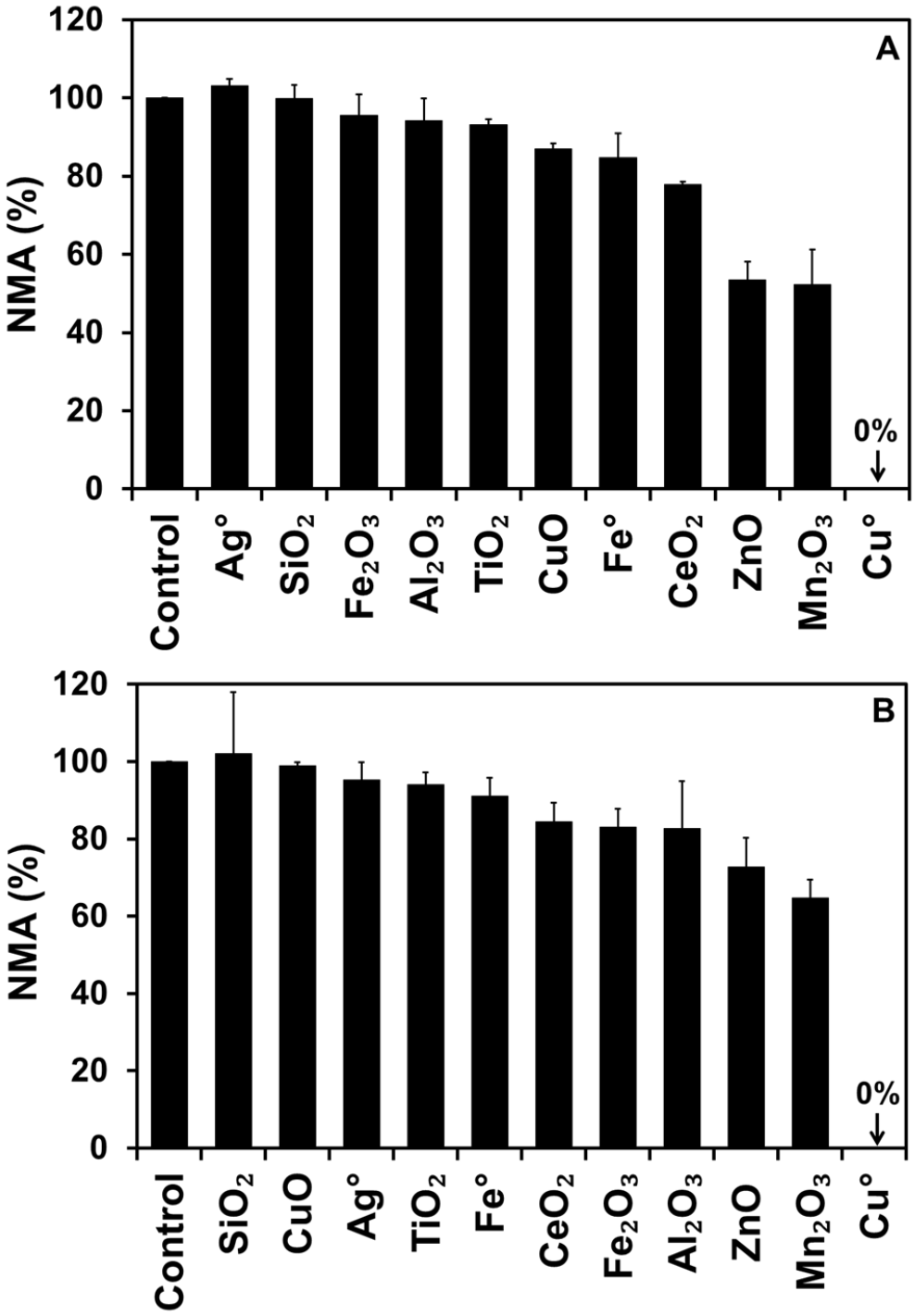

Figure 3.1 Impact of different NPs (1,500 mg L^{-1}) on the normalized specific methanogenic activity (NMA) of anaerobic sludge as determined in batch acetoclastic (A) and hydrogenotrophic (B) methanogenic assays. Results are for activities measured directly during the first feeding of the methanogenic substrates. Error bars represent the standard deviation of duplicate or triplicate assays.

In order to explore if increasing the exposure time could enhance inhibition, a second feeding of acetate was provided to the assays containing NPs of Cu^0, CuO, Fe^0, Mn_2O_3, and ZnO (Figure 3.2A). Cu^0 NP remained completely inhibitory in the second feeding. CuO, Fe^0, and ZnO NPs caused the NMA in the second feeding to decrease to 27, 56 and 0%, respectively; indicating that continued exposure indeed caused enhanced inhibition. Conversely, the treatments amended with Mn_2O_3 NPs were less inhibitory in the second feeding when the NMA was 94% suggesting full recovery of the acetoclastic methanogens.

When H_2 was used as substrate (Figure 3.1B), the results were similar to the acetoclastic assays. Cu^0 NP completely inhibited the hydrogenotrophic methanogenic activity and CuO, Fe^0 and ZnO NPs were null or only modest, corresponding to NMAs to 99, 91 and 75%; respectively. However, a trend of decreased methane production over time suggested an increase in the inhibitory effect of the CuO and ZnO NPs. Analysis of the NMA for the CuO NP supplied assays demonstrated a change over time of from 99 to 15% NMA (Figure A.1.2). A similar trend was observed in the assays amended with ZnO NPs; the NMA changed from 75% to 11%. In addition to this effect, the expected methane concentration was not reached in the presence of ZnO NPs (Figure A.1.2B). Therefore, Treatments containing Cu^0, CuO, and ZnO NPs were incubated further with a second-feeding of H_2 to confirm the presence of a toxic effect.

During the second feeding of H_2 (Figure 3.2B), the inhibition in the treatments containing CuO and ZnO NPs increased as evidenced by a major decrease in the NMA to 54 and 4%, respectively. The treatment exposed to Cu^0 NP continued to be fully inhibited in the second feeding, which corroborated a prolonged high level of Cu^0 NP toxicity. All other NPs tested and incubated under either acetoclastic or hydrogenotrophic methanogenic conditions had NMA values above 70% and did not show evidence of increasing toxicity effect over time. In each experiment, the concentration of CH_4 produced was the same or very close to the theoretical expected CH_4 production. Thus, the remaining NPs did not pose a serious inhibitory effect to methanogenesis.

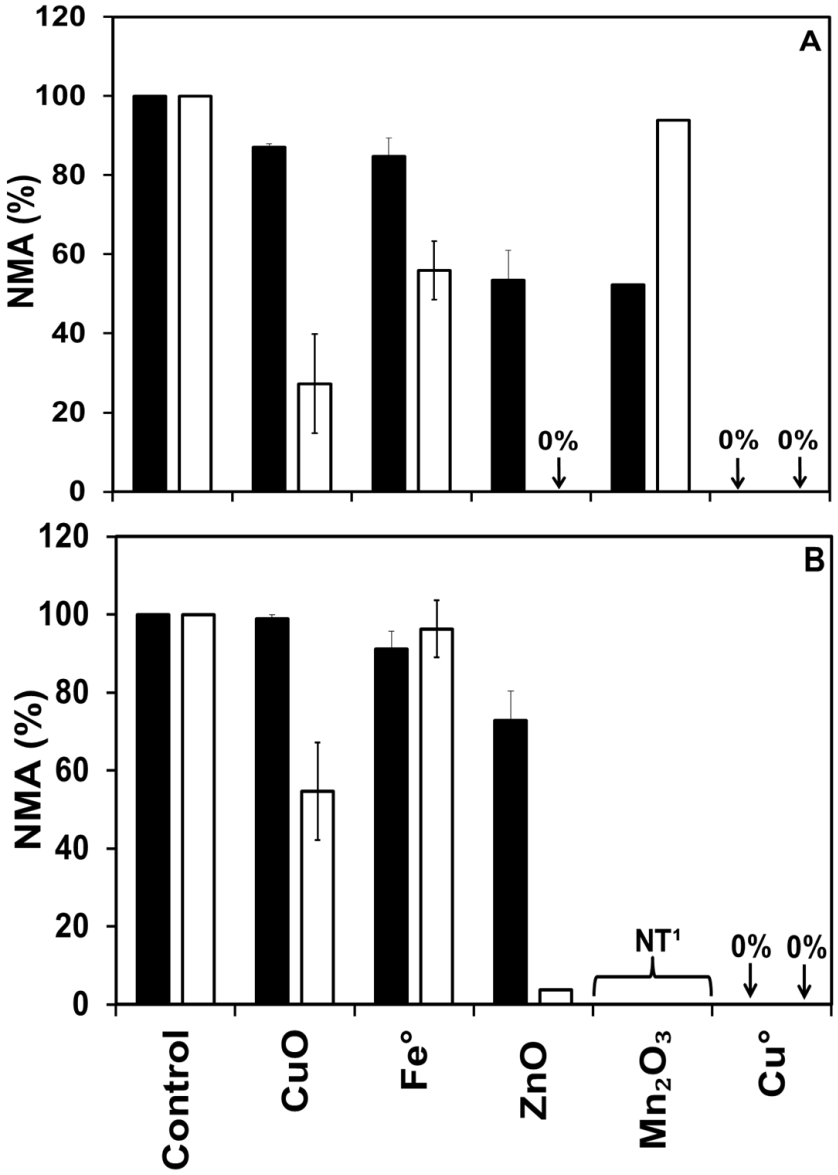

Figure 3.2 Impact of exposure time on the relative methanogenic activity (NMA) of anaerobic sludge as determined in batch acetoclastic- (A) and hydrogenotrophic (B) methanogenic assays amended with selected NPs (1,500 mg L^{-1}). NMA determined during the first feeding (filled bars) and second feeding (empty bars) of the primary substrate. Error bars (see Figure 3.1 caption). [1]NT: Not tested.

The toxic effect of NPs dispersed with Dispex, on the acetoclastic and hydrogenotrophic methanogenic activities of the anaerobic sludge was also studied. Dispex itself was found to be non-toxic to methanogens using 150 mg L^{-1} of Dispex (Table A.1.2). The presence of the Dispex (10:1, NP:Dispex mass ratio) neither

increased nor decreased the NMA of the methanogenic activity of assays exposed to 1,500 mg L^{-1} of NPs with either acetate or H_2 as substrates (Table A1.1). Further statistical analysis confirmed that the effect of Dispex was not significant (Table A2.2).

3.3.2 Inhibitory concentrations of Cu^0, CuO and ZnO NPs to methanogenic activity

Results of the second feeding of substrate showed a toxic effect of Cu^0, CuO and ZnO NPs on methanogens (Figure 3.2). Therefore, an experiment was set to determine the Cu^0, CuO, and ZnO NPs inhibitory concentrations to acetoclastic or hydrogenotrophic methanogens. The inhibitory effects of Fe^0 NPs on acetoclastic methanogens and the impact of CuO NPs on hydrogenotrophic methanogens were not further explored because the second feeding experiments showed that the IC_{50} were above 1,500 mg L^{-1} (Figure 3.2). Toxic concentrations exceeding 1,500 mg L^{-1} were out of the scope of this study. A concentration range of Cu^0 NPs was tested with acetoclastic (Figure 3.3A) and hydrogenotrophic (Figure 3.3B) methanogenic assays. The graphs show toxic responses from 50 to 250 mg Cu^0 L^{-1}. The latter concentration caused complete inhibition during the first feeding of the acetoclastic methanogenic assay, and almost complete inhibition during the second-feeding of the hydrogenotrophic methanogenic assay.

The microbial toxicity of Cu^0, as well as other Cu-based materials, has been associated with the release of Cu^{2+} ions (Chen et al., 2008; Luna-delRisco et al., 2011). For that reason, the inhibitory effect of Cu^{2+} ions to acetoclastic methanogens was evaluated (Figure 3.3C). Exposure to 25 mg Cu^{2+} L^{-1} impacted the NMA to a great extent, causing 80 to 90% inhibition, and methanogenesis was completely inhibited in assays with 50 mg Cu^{2+} L^{-1}. The level of inhibition was similar in the first and second feeding of acetate.

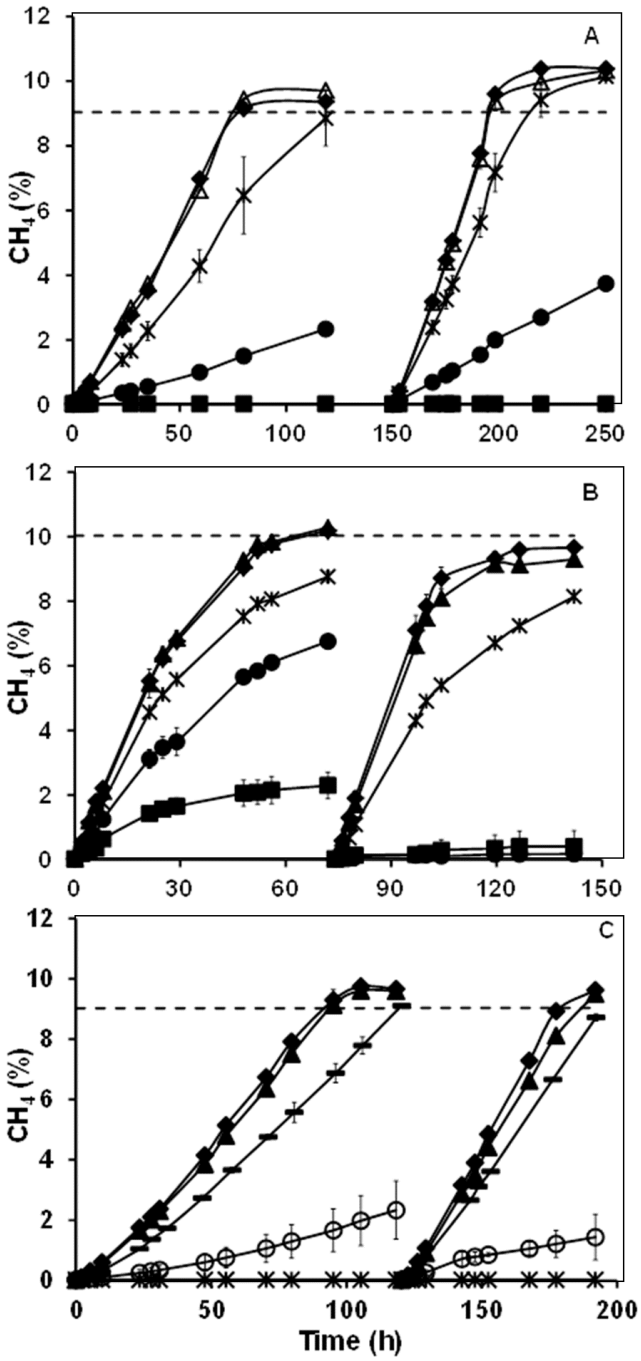

Figure 3.3 Time course of methane production in the presence of different concentrations of Cu0 NP during acetoclastic (A) or hydrogenotrophic (B) methanogenic assays with two successive substrate feedings. For comparison, acetoclastic methanogenic assays were also conducted in the presence of soluble Cu^{2+} (C). Concentrations of Cu^0 NP or Cu^{2+} added (in mg L^{-1}): 0 (◆), 5 (△), 10 (▲), 15 (–), 25 (○), 50 (✱), 100 (●), and 250 (■). Error bars (see Figure 3.1 caption).

The inhibitory effect of different concentrations of ZnO NPs on acetoclastic (Figure 3.4A) and hydrogenotrophic (Figure 3.4B) methanogenic activity was tested. Low concentrations of ZnO NPs (< 50 mg L^{-1}) did not show an impact on the methane production rate in either the first or the second substrate feeding in either assay. However, in the acetoclastic methanogenic assays, the NMA decreased from 77.0% in the first feed to 1.6% in the second feed when 100 mg ZnO L^{-1} was applied. In the treatments with 500 mg ZnO L^{-1}, the NMA was 45.9 and 0.8% for the first and second feeds, respectively. In the hydrogenotrophic culture, inhibitory responses were more pronounced at ZnO concentrations greater than 250 mg L^{-1}. In those assays, the inhibition increased significantly during the second feed, but complete inhibition was only evident at the highest concentration tested of 1,500 mg ZnO L^{-1}. For the sake of comparison, the impact of $ZnCl_2$-Zn^{2+} on acetoclastic methanogens was evaluated (Figure 3.4C). Inhibitory responses were observed at 50 mg L^{-1} added Zn^{2+} and higher. At those concentrations, the methane production in the second substrate feeding was almost completely inhibited.

When CuO NPs were tested at a range of concentrations with acetoclastic and hydrogenotrophic methanogenic assays, significant inhibition was only observed at high concentrations of CuO NP (data not shown). All the assays required 250 mg L^{-1} or more of CuO NP to lower the activity, which was only manifested in the seconding feeding. In the case of the acetate-amended assays, the NMA in the second feed for the treatments containing 250, 500 and 1,500 mg L^{-1} CuO NP was 41.4, 33.0 and 27.3%, respectively. When H_2 was supplied as a substrate, no effect was found in the first feed; while in the second feed, only the assays supplied with 250, 500, and 1,500 mg L^{-1} CuO NPs affected the methanogenic activity, decreasing the NMA to 79.9, 71.3 and 54.6%, respectively.

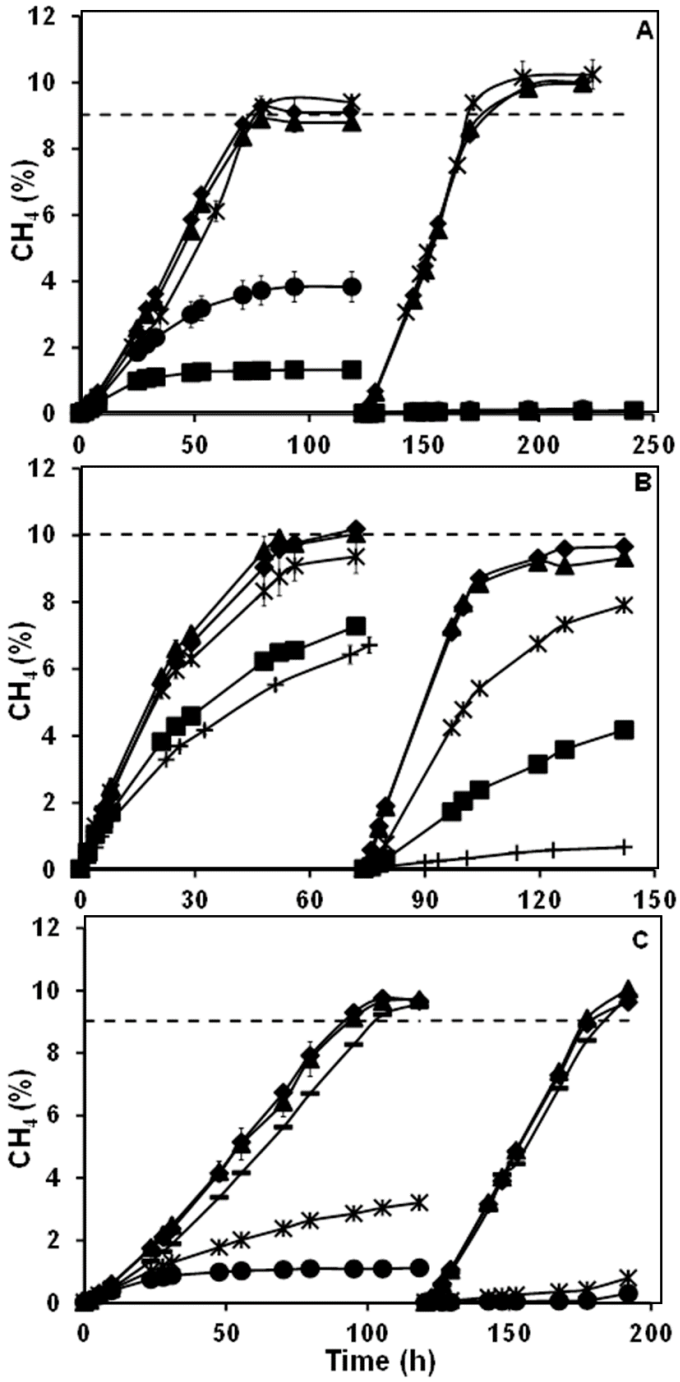

Figure 3.4 Time course of methane production in the presence of different concentrations of ZnO NPs during acetoclastic (A) or hydrogenotrophic (B) methanogenic assays with two successive substrate feedings. For comparison, acetoclastic methanogenic assays were also conducted in the presence of soluble Zn^{2+} (**C**). Concentrations of ZnO NP or Zn^{2+} added (in mg L^{-1}): 0 (◆), 10 (▲), 25(–), 50 (✱), 100 (●), 250 (□), 500 (■), and 1,500 (+). Error bars (see Figure 1 caption).

Figure 3.5 shows the NMA of the second feeding of the acetoclastic and hydrogenotrophic assays in the presence of Cu^0, CuO, and ZnO NPs. For comparison, the acetoclastic NMA values of the soluble Cu^{2+} and Zn^{2+} salts are also shown. The assays supplied with $CuCl_2$ or $ZnCl_2$ required a lower initial concentration of the metals to cause the same or greater toxic effects on the acetoclastic methanogenic activity than when the metals were added as NPs. Only 20 mg L^{-1} of $CuCl_2$-Cu was necessary to inhibit the activity by 50%, whereas 7× more CuO NP (expressed as Cu) and approximately 3× more Cu^0 NP were needed to cause the same toxicity effect. Experiments supplied with Zn followed a similar pattern. Exposure to Zn^{2+} (50 mg Zn^{2+} L^{-1}) provoked almost complete inhibition while 1.6× more ZnO NP (expressed as Zn) was required to cause a similar effect.

Figure 3.5 also provides information on the susceptibility of acetoclastic and hydrogenotrophic methanogens to the Cu- and Zn-based NPs and to their respective divalent metal ions. In the treatments supplied with CuO and ZnO NPs, the 50% inhibiting concentrations (IC_{50}) for the acetoclastic assays were estimated to be 179 mg L^{-1} of Cu (223 mg L^{-1} of CuO) and 70 mg L^{-1} of Zn (87 mg L^{-1} of ZnO), whereas in the hydrogenotrophic assays, the IC_{50} value was above 1,200 and 201 mg L^{-1} of Cu and Zn, respectively (> 1,500 and 250 mg L^{-1} for CuO and ZnO). The IC_{50} of Cu^0 NPs to the acetoclastic and hydrogenotrophic activities corresponded to 62 and 68 mg L^{-1}, respectively.

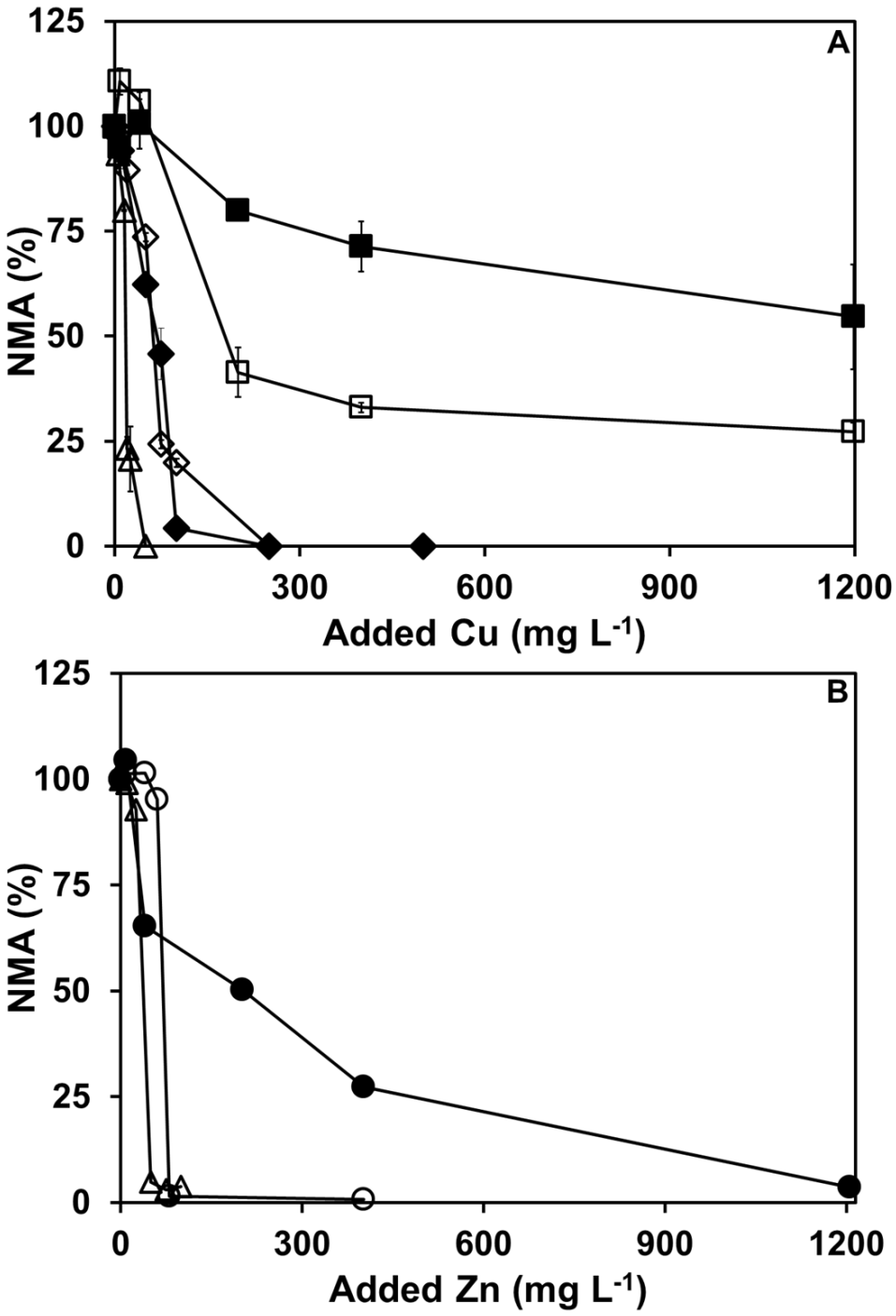

Figure 3.5 Normalized specific methanogenic activity (NMA) as a function of the initial concentration of Cu (A) as Cu^{2+} (△), as Cu^0 NP (◇, ◆), or CuO NP (□, ■) using acetate (open markers) or hydrogen (filled markers) as substrates; and NMA as function of the initial concentration of Zn (B) as Zn^{2+} (△), ZnO NP (○, ●) using acetate (open markers) hydrogen (filled markers) as substrate. Error bars (see Figure 1 caption).

3.3.3 Role of soluble species in toxicity

The final aqueous concentration of soluble species metals released from NPs may be the primary cause of metal (oxide) NP toxicity (Mu et al., 2011). Likewise, the soluble concentrations of metal salts are known to attenuate in anaerobic assay conditions similar to those used here. For example, soluble Cu^{2+} concentrations were shown to rapidly decline in methanogenic toxicity assays with anaerobic granular sludge (Karri et al., 2006). In order to corroborate that the ions released by Cu^0 and ZnO NPs were causing the toxicity to the methanogenic sludge, the final equilibrium concentrations of the ions released by the metal salts and the NPs were measured at the end of the experiments. The results indicated that at any given soluble concentration of Cu^{2+} a similar effect on the acetoclastic methanogenic activity was observed irrespective of whether the ions were released from Cu^0NP or remaining from $CuCl_2$ salt (Figure 3.6A). Figure 6.6B demonstrates a very similar pattern for Zn^{2+} in the assays spiked with $ZnCl_2$ salt and ZnO NPs. These findings suggest that the main toxicity driver was the residual soluble form of each metal.

3.3.4 Aggregation of NPs in anaerobic basal media

Aside from the solubility of the NPs, the remaining non-soluble fraction could affect the methanogenic metabolism. The level of aggregation, particle size, surface area and charge, and coating, are all expected to play an important role in NP fate and toxicity in aquatic systems (Franklin et al., 2007). As shown in Table S2, the commercial dispersant, Dispex, caused a detectable decrease in the PSD of Cu^0, CuO, Mn_2O_3, and ZnO NPs after 24 h in comparison with the treatments containing basal medium without the dispersant. This effect was most noteworthy with the Mn_2O_3 NP in which the addition of Dispex decreased its PSD by approximately 12×, whereas in the case of Cu^0, CuO and ZnO NPs, the decreases ranged only from approximately 2 to 4×.

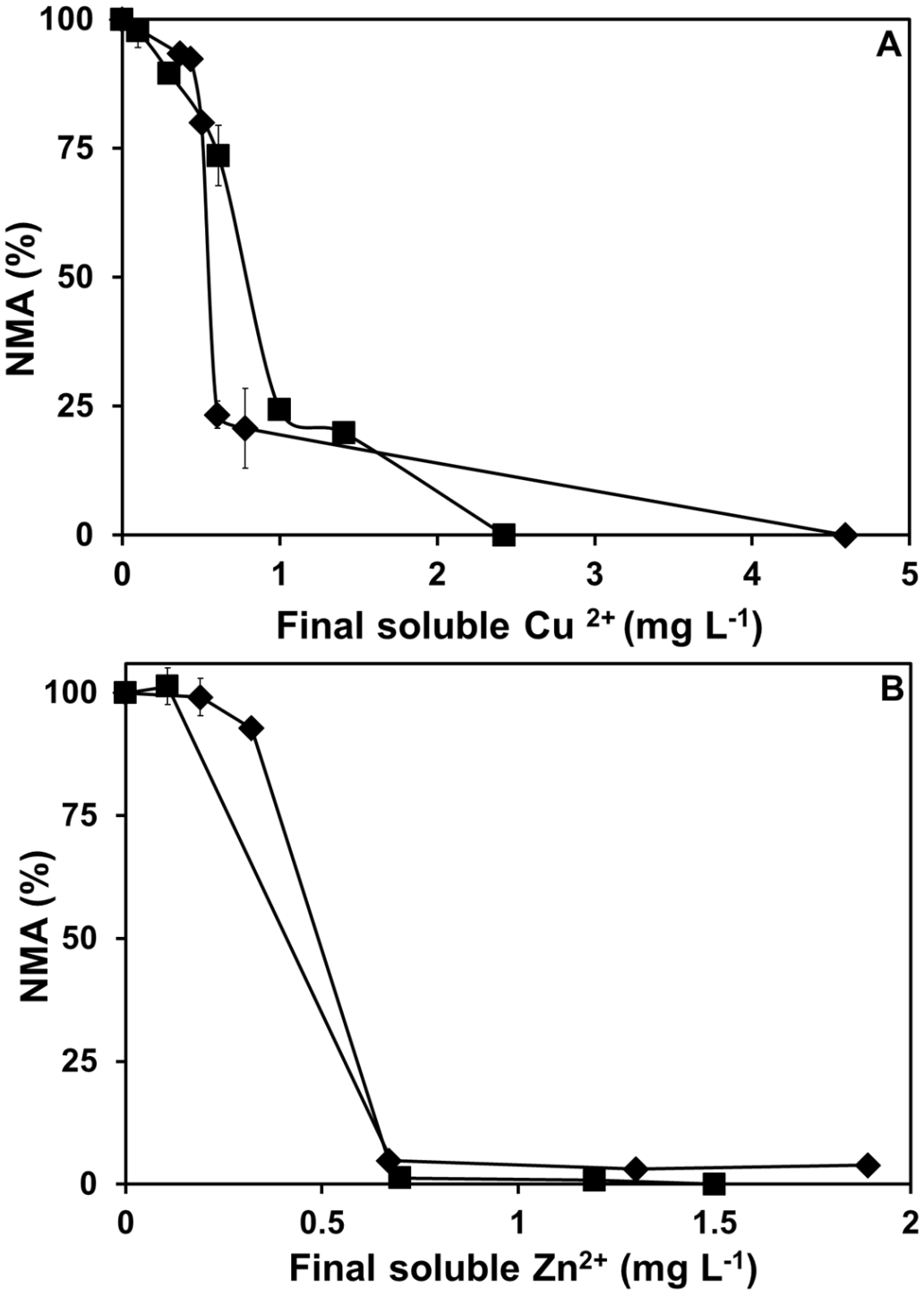

Figure 3.6 Comparison of the normalized specific methanogenic activity (NMA) as function of the equilibrium dissolved concentration of either Cu^{2+} (A) and Zn^{2+} (B) during acetoclastic methanogenic assays in experiments supplied with either chloride salts (◆) or NPs (■) as source of the metal cations. Error bars (see Figure 3.1 caption).

ZP measurements were also performed to confirm the effectiveness of Dispex as a dispersant. ZP values within the range -30 – 30 mV are commonly used as an arbitrary standard to indicate instability of the dispersion (Garcia-Saucedo et al., 2011). The addition of Dispex stabilized Cu^0, CuO, Mn_2O_3, and ZnO NP dispersions decreased the charge to less than -30 mV in all cases with the exception of the Fe_2O_3 NP dispersion where the dispersion remained unstable. The decrease of ZP was consistent with the measurements in which the PSD was also reduced, indicating an increase of the stability of the NP dispersion.

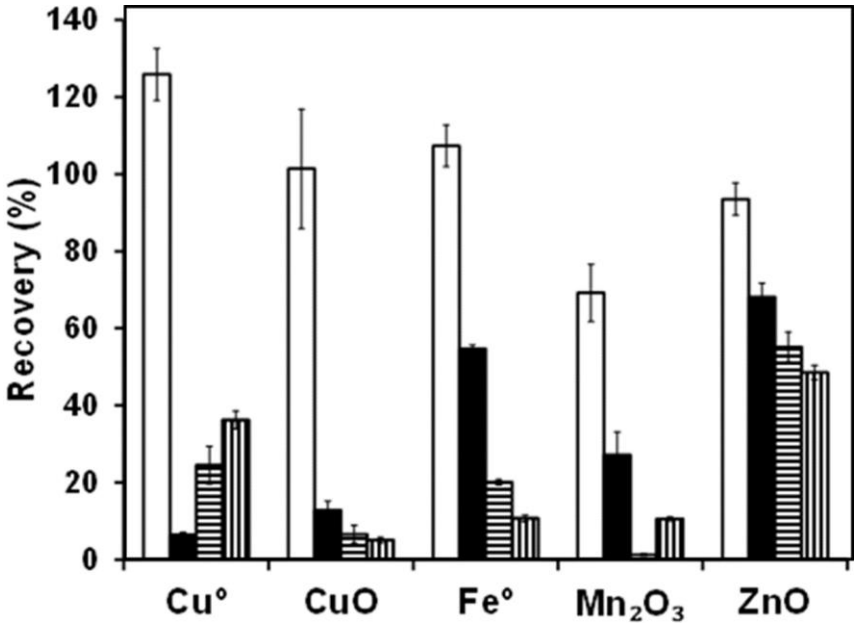

Figure 3.7 Effect of dispersant addition (NPs/Dispex, 10:1, w/w) on the concentration of different NPs in DI water and basal medium following 24 h of incubation (30°C, 110 rpm). NPs (250 mg L^{-1}) dispersed in acidic water (□), DI water (■), basal medium (horizontally striped bars), and basal medium with dispersant (vertically striped bars). The initial pH of the acidic water, DI water, basal medium, and basal medium with dispersant was 2.0, 5.7, 7.3 and 7.4, respectively.

The best indication of NP dispersion stability is to measure the concentration of NPs in the supernatant of the suspension after 24 h of settling. As shown in Figure 3.7, the stabilizing effect of the dispersant on Mn_2O_3 and Cu^0 NPs was confirmed by a higher concentration of these metals in the supernatant when Dispex was added. Despite the evidence that the dispersant increased the stability of

the toxic NPs tested here, there was no substantial evidence that these factors increased or decreased the toxicity of the NPs towards the methanogens.

3.4 Discussion

3.4.1 Main findings

The inhibitory impact of a series of inorganic NPs supplied at 1,500 mg L^{-1} on the acetoclastic and hydrogenotrophic methanogenic cultures was tested. Only Cu^0 and ZnO NPs caused high levels of inhibition to both the acetoclastic and hydrogenotrophic methanogenic activity. Additionally, CuO NP caused high toxicity to acetoclastic methanogens. The methanogens were tolerant to high concentrations of all other tested NPs. The IC_{50} values were determined for the most toxic NPs. The estimated IC_{50} values for the acetoclastic methanogens were 62, 87, and 223 mg L^{-1} for Cu^0, ZnO, and CuO NPs, respectively. While the estimated IC_{50} values for the hydrogenotrophic methanogens were 68, 250, and > 1,500 mg L^{-1}, respectively.

The toxicity effect of divalent Cu and Zn salts to the acetoclastic culture was also studied. The estimated IC_{50} values were 18 and 37 mg L^{-1} for added Cu^{2+} and Zn^{2+}, respectively. These values indicated a higher toxicity compared to initial Cu and Zn concentrations from added NPs. However, the methanogenic activity was found to be highly correlated with the equilibrium concentration of free soluble metal in the assay bottles regardless of whether the source of the ions was from NPs or salts (Figure 3.6). These results suggest that toxicity was due to the freely soluble metal.

3.4.2 Comparison to previous data

The potential inhibitory effect of CuO and ZnO NPs on methanogenic activity has previously been tested. The results have shown that different methanogenic cultures have been completely inhibited using 38 mg CuO NP L^{-1}, and severely affected by exposure of up to 200 mg ZnO NP L^{-1} (Luna-delRisco et al., 2011; Mu & Chen, 2011; Mu et al., 2012). The effect of Ag^0, Al_2O_3, SiO_2, and TiO_2 NPs on anaerobic digestion has been also been investigated and, similar to the finding in this study, no toxic effects on the methanogenic activity were observed (Garcia et al., 2012; Mu et al., 2012; Yang et al., 2012a).

Contrasting our results, other studies have found toxicity using Ag^0 and Ce_2O_3 NPs (Garcia et al., 2012; Yang et al., 2012b). Although Ag NPs are toxic to many microorganisms, this nanomaterial appears to be less inhibitory to anaerobic methanogens. Agreeing with the results of our study, two recent publications reported that relatively high concentrations of nano-Ag (40-43 mg/L) did not cause methanogenic inhibition (Garcia et al., 2012; Yang et al., 2012a). Oxysulfidation and sulfidation of Ag NPs in anaerobic environments has been shown to promote precipitation of Ag NPs as AgS, a non-toxic form of Ag (Choi et al., 2009). Therefore, the level of sulfide present in the various studies should be expected to have a considerable impact on the inhibitory potential of the Ag NPs. Conversely, Garcia (Garcia et al., 2012) observed that Ce_2O_3 NPs severely affected mesophilic and thermophilic methanogens which could potentially be explained by the different speciation of Ce (Ce_2O_3 versus CeO_2 applied in this study).

3.4.3 Mechanisms

NP solubilization has been suggested as one of the important mechanisms resulting in toxicity to microorganisms (Auffan et al., 2009; Liu et al., 2011). The toxicity of ZnO- and CuO NPs to methanogens has been previously associated with their solubility (Liu et al., 2011; Luna-delRisco et al., 2011; Mu et al.,

2011; Mu et al., 2012). ZnO NPs were found to inhibit a methanogenic culture due to the release of toxic Zn^{2+} ions, whereas the lack of toxicity of Al_2O_3-, SiO_2-, and TiO_2 NPs was attributed to their poor solubility (Mu et al., 2011). Even though a rapid attenuation of the soluble metal occurs in anaerobic media due to OH^-, CO_3^{2-} or S^{2-} precipitation, only a very small residual soluble concentration is necessary to cause methanogenic inhibition (Karri et al., 2006; Lombi et al., 2012).

The considerable decrease in the final soluble metal concentration observed in assays amended with Cu and Zn salts is likely due to the formation and precipitation of the corresponding metal-carbonate ligands (log K_{s0} $CuCO_3$= -9.63; log K_{s0} $ZnCO_3 \bullet H_2O$= -10.26) or metal-sulfide ligands (log K_{s0} CuS= -35.96; log K_{s0} ZnS = -21.97) (Benjamin, 2002). Despite the very low concentration of dissolved metals remaining in solution at the end of the second feeding (< 5 mg L^{-1}), the assays were completely inhibited. Moreover, the residual final concentration of soluble metal released by either the corrosion or dissolution of NPs or remaining after attenuation of metal salts indicated that similar quantities of dissolved metal ions caused an almost equal inhibition of methanogenic activity (Figure 3.6). Therefore, the findings of this study suggest that release of toxic metal species by NP-dissolution was the principal mechanism of methanogenic inhibition caused by Cu^0, CuO, and ZnO NPs.

In the case of Mn_2O_3, a reversible toxic effect was observed. While the NPs caused methanogenic inhibition during the first feeding, no inhibition was observed when a second feeding of acetate was provided. Mn_2O_3 is a strong oxidant and a source of reactive oxygen species (Luna-Velasco et al., 2011) which could explain the initial toxicity observed in methanogenic assays with Mn_2O_3 NPs. The experimental conditions in the methanogenic bioassays provide a highly reducing environment; therefore, it is likely that rapid reaction of Mn_2O_3 occurred leading to the formation of non-toxic Mn^{+2} species which may have passivated the NP surface following formation of insoluble precipitates with carbonate or sulfide

ions present in the medium. Formation of insoluble $MnCO_3$ and MnS salts when manganese oxides are reduced in anaerobic environments is well established (Lee et al., 2011b)

3.5 Conclusions

The findings of this research revealed that Cu^0 and ZnO NPs are highly inhibitory to acetoclastic and hydrogenotrophic methanogens with IC_{50} values of 62 to 250 mg L^{-1}. CuO NP also inhibited acetoclastic methanogens (IC_{50} = 223 mg L^{-1}) but not H_2-utilizing methanogens. The inhibitory impact of the Cu- and Zn-based NPs increased considerably with time, even after 80 h of exposure. In contrast, methanogens were not inhibited when exposed to high concentrations (1,500 mg L^{-1}) of Ag^0, Al_2O_3, Ce_2O_3, Mn_2O_3, Fe^0, Fe_2O_3, SiO_2, and TiO_2 NPs, suggesting that anaerobic treatment processes could tolerate high concentrations of these types of NPs. The results obtained indicated that the methanogenic inhibition of Cu^0, CuO and ZnO NPs is mainly due to the release of toxic divalent Cu and Zn ions caused by corrosion and dissolution of the NPs.

3.6 Acknowledgments

This work was supported by the Semiconductor ResearchCorporation (SRC)/Sematech Engineering Research Center for Environmentally Benign Semiconductor Manufacturing. Gonzalez-Estrella was partly funded by CONACyT.

CHAPTER IV- ELEMENTAL COPPER NANOPARTICLE TOXICITY TO DIFFERENT TROPHIC GROUPS INVOLVED IN ANAEROBIC WASTEWATER TREATMENT PROCESSES

Jorge Gonzalez-Estrella[a]*; Daniel Puyol[a]; Sara Gallagher[a]; Reyes Sierra-Alvarez[a]; Jim A. Field[a]

[a]Department of Chemical and Environmental Engineering, University of Arizona,

P.O. Box 210011, Tucson, AZ 85721, USA

*Corresponding author: Jorge Gonzalez-Estrella

Department of Chemical and Environmental Engineering

The University of Arizona,

P.O. Box 21011, Tucson, AZ 85721, United States

Phone: +1-520-621 6162

E-mail: jorgegonzaleze@email.arizona.edu

Abstract

Elemental copper nanoparticles (Cu^0 NPs) are potentially inhibitory materials to the different key microbial trophic groups involved in biological waste water treatment processes. Cu-based NPs are toxic to methanogens at low concentrations. However, very little is known about the toxic effect of Cu^0 NPs on other microbial groups involved in either upper trophic levels of anaerobic digestion or anaerobic nitrogen removal processes. This study evaluated Cu^0 NP toxicity to glucose fermentation, syntrophic propionic oxidation, methanogenesis, denitrification and anaerobic ammonium oxidation (anammox). Batch experiments were supplemented with Cu^0 NPs and $CuCl_2$ to evaluate Cu toxicity. Substrate consumption was measured in glucose fermentation and syntrophic propionic oxidation assays, whereas CH_4 and N_2 production was monitored in methanogenic and nitrogen removal assays, respectively. Inhibition constants (K_i) were calculated with the information obtained from the experiments. Results showed that anammox and glucose fermentation were the least and most inhibited processes with K_i values of 0.324 and 0.004 mM of added Cu^0 NPs, respectively. Similar K_i values were obtained as function of the residual soluble Cu irrespective of whether the soluble Cu originated from Cu^0 NP or $CuCl_2$ for each microbial trophic group tested. Further analyses revealed that the K_i as a function of the residual soluble Cu concentration was <0.003 mM with the exception of the *Ki* obtained for the anammox (0.076 mM Cu). These results indicated that the ions released by Cu^0 NPs were the most likely cause of the toxicity. The results taken as a whole indicate that Cu^0 NPs are toxic in different extents to all the biological processes studied. Therefore, Cu^0 NP can potentially be an important inhibitor of anaerobic wastewater treatment processes that rely in these trophic groups. The evidence suggests that corrosion and dissolution of Cu^0 NP to soluble Cu^{2+} is the mechanism of responsible for the inhibitory

Keywords: Glucose fermentation, Syntrophic propionate oxidation, Methanogenesis, Denitrification, Anammox , Inhibition, Nanomaterials, Inhibition constants

4.1 Introduction

Engineered nanoparticles (NPs) are manufactured materials with at least one dimension ≤ 100 nm. NPs are widely applied in several industrial processes and consumer products (Auffan et al., 2009). Copper-based NPs are applied in several products such as wood preservative, catalyst, printable electronics, semiconductors or antimicrobials among others (Wang et al., 2013). Elemental copper (Cu^0) and copper oxide nanoparticles (CuO and Cu_2O) are the most common types of Cu NPs used in technological applications (Wang et al., 2013). Cu-based NPs are also generated as a byproduct of chemical mechanical polishing in the semiconductor industry (Golden et al., 2000). Consequently, NPs are very likely to be discharged to domestic wastewater treatment plants after usage, namely activated sludge processes and other biological operations (Brar et al., 2010).

Accumulation of NPs in the sludge of wastewater treatment plants has recently been found to be a serious issue. Studies showed that NPs commonly applied to commercial products such as Ag^0, TiO_2, and ZnO accumulate in the sludge biosolids of both pilot and full scale activated sludge treatment plants (Kiser et al., 2010; Kiser et al., 2009; Ma et al., 2013a). These findings raise the concern that other commonly applied NPs such as Cu-based NPs will have a similar fate. Thus, potential inhibitory effects due to this accumulation can consequently be magnified during treatment of concentrated waste streams such as anaerobic sludge digestion or the liquors from dewatering of digested sludge.

Recent studies showed that Cu-based NPs are toxic to methanogens (Gonzalez-Estrella et al., 2013; Otero-González et al., 2014b)which are key microorganisms in anaerobic stabilization of waste sludge due to their role in converting acetate and hydrogen into methane. However, very little research has been performed regarding the toxic effect of Cu-based NPs to other anaerobic trophic groups of the anaerobic digestion process or those involved in N-removal. Therefore, this study evaluated the toxic

effect of Cu^0 NPs on four anaerobic trophic groups. These included glucose fermentation and syntrophic propionate oxidation (SPO) involved in the anaerobic digestion of carbonaceous substrates as well as denitrification and anaerobic ammonia oxidation (anammox) which are anaerobic trophic groups important for N-removal.

4.2 Material and Methods

4.2.1 Chemicals

Cu^0-NPs (40-60 nm, 99%) were purchased from Sky-Spring Nanomaterials Inc. (Houston, TX) $CuCl_2 \bullet H_2O$ (99%), sodium acetate (99.9%) and propionic acid (>99.4) were acquired from Sigma Aldrich (St. Louis, MO, USA). D-Glucose was bought from Fisher Scientific (Waltham, MA, USA). N_2/CO_2 (80/20, v/v) gas mix and CH_4 standard gas (99%) were acquired from Air Liquid America (Plumstedsville, PA, USA).

4.2.2 NP dispersions and metal solutions

Cu^0-NP stock dispersions were sonicated (DEX® 130, 130 Watts, 20 kHz, Newtown, CT) at 70% amplitude for 5 min. Cu^0-NP stability in anaerobic media has been previously described (Gonzalez-Estrella et al., 2013). $CuCl_2$ solutions were prepared by dissolving them in 0.01 M HCl.

4.2.3 Anaerobic sludge and anammox sludge

The anaerobic granular sludge used for glucose fermentation, SPO and denitrification assays was obtained from a full-scale upflow anaerobic sludge bed reactor treating brewery wastewater (Mahou,

Guadalajara, Spain). The sludge was stored at 4 °C. Volatile suspended solids (VSS) were 7.0 % of the wet weight. Granular anammox biomass (2.4 ± 0.6 mm) was obtained from a lab-scale expanded granular sludge bed reactor (EGSB) with a VSS content of 0.81 grams of volatile solids per gram of total solids (TSS), and had a specific anammox activity of 280.8 mg N2-N g^{-1} VSS d^{-1}.

4.2.4 Culture media

Glucose fermentation and SPO assays were performed in an anaerobic medium at pH 7.2 containing (mg L^{-1}): NH_4Cl (280), $NaHCO_3$ (3,000), K_2HPO_4 (250), $CaCl_2 \cdot 2H_2O$ (10), $MgCl_2 \cdot 6H_2O$ (183); and yeast extract (100) with 1 mL L^{-1} of trace elements. Denitrification bioassays were performed in a basal medium containing (mg L^{-1}): K_2HPO_4 (250); $(NH_4)HCO_3$ (417); $NaHCO_3$ (2680); and yeast extract (10) with 1 mL L^{-1} of trace elements. Finally, the basal medium for the anammox experiments contained (mg L^{-1}): $NaH_2PO_4 \cdot H_2O$ (57.5), $CaCl_2 \cdot 2H_2O$ (100), $MgSO_4 \cdot 7H_2O$ (200), $NaHCO_3$ (2,500), and 1 mL L^{-1} of two trace element solutions. Trace element solutions for the glucose, fermentation, SPO, and denitrification contained (mg L^{-1}): H_3BO_3 (50), $FeCl_2 \cdot$ 4H2O (2000), ZnCl2 (50), $MnCl_2 \cdot 4H_2O$ (50),$(NH_4)_6Mo_7O_{24} \cdot 4H_2O$ (50), $AlCl_3 \cdot 6H_2O$ (90), $CoCl_2 \cdot 6H_2O$ (2000), $NiCl_2 \cdot 6H_2O$ (50), $CuCl_2 \cdot 2H_2O$ (30), $NaSeO_3 \cdot 5H_2O$ (100), EDTA (1000), resazurin (200) and 36% HCl (1 mL L^{-1}). Anammox basal medium was supplied with two trace element solutions. The first trace element solution contained (in mg L^{-1}): $FeSO_4$ (5000) and ethylene diamine-tetra acetic acid (EDTA) (5000). And the second trace element solution contained (in mg L^{-1}): EDTA (1500); $ZnSO_4 \cdot 7H_2O$ (430); $CoCl_2 \cdot 6H_2O$ (240); $MnCl_2$ (629); $CuSO_4 \cdot 5H_2O$ (250); $Na_2MoO_4 \cdot 2H_2O$ (220); $NiCl_2 \cdot 6H_2O$ (190); $Na_2SeO_4 \cdot 10H_2O$ (210); H_3BO_3 (14); $NaWO_4 \cdot 2H_2O$ (50).

4.2.5 Bioassays experimental set-up

Table 4.1 describes the specific sludge concentration, pre-incubation time, electron-donor/acceptor, and range of concentration of each bioassay performed. The experiments were

performed by first adding inoculum and basal medium to 160 mL serum bottles. Subsequently, all bottles were flushed with N_2/CO_2 or He/ CO_2 (80:20, v/v) for the experiments producing either CH_4 or N_2, respectively. Subsequently, all the assays with the exception of anammox bioassays were provided with a first spike of COD as electron donor and an acceptor. Next, the bottles were pre-incubated at 30 ± 2 °C in an orbital shaker at 115 rpm. Anammox sludge was previously activated in an EGSB reactor. Then, another amendment of electron donor and acceptor (if needed) and the Cu^0 NP stock dispersion, metal stock solution, or deionized water was added to the corresponding experiments. Assays were again pre-incubated overnight at 30 ± 2 °C in an orbital shaker at 115 rpm. Liquid samples (1 or 1.5 mL) were taken to measure glucose and propionate consumption and gas samples (100 µL) were taken to track CH_4 and N_2 production during the incubation. Anammox assays were provided with a second spike of electron donor and acceptor to observe more clearly the toxic effect of Cu on the microorganisms. Finally a 1.5 mL liquid sample was taken to analyze the residual metal concentration.

Table 4.1 Summary of experimental conditions

Biological process	Sludge concentration (g VSS L^{-1})	Pre-incubation (h)	Electron donor (mg L^{-1})	Electron acceptor (mg L^{-1})	Cu^0 (mM)	$CuCl_2$ (mM)
Glucose fermentation/ methanogenesis	1.5	10-12	Glucose (471) for pre-incubation and (471) for incubation		0-0.315	0-.629
SPO/propionate methanogenesis	1.5	10-12	Propionate (330) for pre-incubation and (330) for incubation		0-0.629	0-0.315
Denitrification	1.5	72	Acetate (280) for pre-incubation and (280) for incubation	Nitrate (390) for pre-incubation and (390) for incubation	0-.629	0-.629
Anammox	0.675	EGSB	Ammonium (24)[a] and (48)[b]	Nitrite (82)[a] and (164)[b]	0-0.236	0-0.944

[a]First spike; [b]Second spike of electron-donor/acceptor

4.2.6 Analytical methods

Methane was quantified by gas chromatography with flame ionization detection (Hewlett Packard 5890 Series II). VFAs were measured by gas chromatography (7890A GC System, Agilent Technologies, Santa Clara, CA, USA) using a fused silica Stabilwax®-DA column (30 m x 530 µm x 0.25 µm; (Restek, State College, PA, USA) and a flame ionization detector. Details of the analysis are described in Otero-González et al. (2014b). Glucose samples (1.5 mL) were centrifuged for 10 min at 13000 rpm, next (0.5 mL) of the supernatant was transferred into a test tube containing 0.5 mL of 5% (v/v) phenol and 2.5 mL of concentrated sulfuric acid was added. The reaction was allowed to undergo for 20 min and subsequently, the concentration of glucose in the bioassays was determined by measuring the color intensity of the sample at 490 nm. N_2 was analyzed using a Hewlett Packard 5890 Series II gas chromatograph fitted with a Carboxen 1010 Plot column (30 m × 0.32 mm) and a thermal conductivity detector. Soluble Cu was measured by inductively coupled plasma-optical emission spectroscopy (ICP-OES Optima 2100 DV, Perkin–Elmer TM, Shelton, CT). The wavelength used for ICP-OES analysis of Cu was 324.754 nm.

4.2.7 Data processing

4.2.7.1 Data handling

Specific activities (SA) were calculated as the maximum specific rate using linear regression of four or more consecutive points that represented at least 50% of either substrate consumption or expected gas production. The whole slope was considered in assays that showed almost or complete inhibition. The normalized activity (NA) was calculated as follows:

$$NA(\%) = \left(\frac{SA_t}{SA_c} \right) \cdot 100 \qquad [1]$$

where SA_t and SA_c are the specific activities of the treatment and control experiments, respectively. The inhibitory effect on the NA was quantified as follows:

$$NA = NA_{\max} \cdot \frac{1}{1+\left(\frac{I}{K_i}\right)^n} \quad [2]$$

where NA_{max} is the maximum NA (%), I and K_i are the inhibitor concentration and inhibition constant, respectively (mM), and n is the inhibition order (dimensionless) (Puyol et al., 2012).

4.3 Results

4.3.1 Effect of Cu^0 NP and $CuCl_2$ on anaerobic digestion cultures

4.3.1.1 Effect on glucose consumption during fermentation

The inhibition effect Cu^0 NPs and $CuCl_2$ on glucose fermentation by anaerobic granular sludge was explored in batch experiments. Figures 4.1A and 4.1B show the time course of glucose with different concentrations of Cu^0 NPs and $CuCl_2$. Cu^0 NPs and $CuCl_2$ were inhibitory to glucose fermentation. Cu^0 NPs affected glucose consumption at concentrations as low as 0.040 mM. At concentrations from 0.079 to 0.315 mM Cu^0 NP, the glucose fermentation rate decreased from 5 to 95%, respectively (Fig 1A). Similarly, the inhibitory effect of $CuCl_2$ was observable with concentrations as low as 0.016 mM. Concentrations from 0.079 to 0.629 mM $CuCl_2$ decreased the rate from 70 to almost 100%, respectively (Figure 4.1B). Thus, the consumption of glucose was severely inhibited by both sources of Cu. The toxic effect of Cu in the conversion of the glucose fermentation products to methane was also investigated.

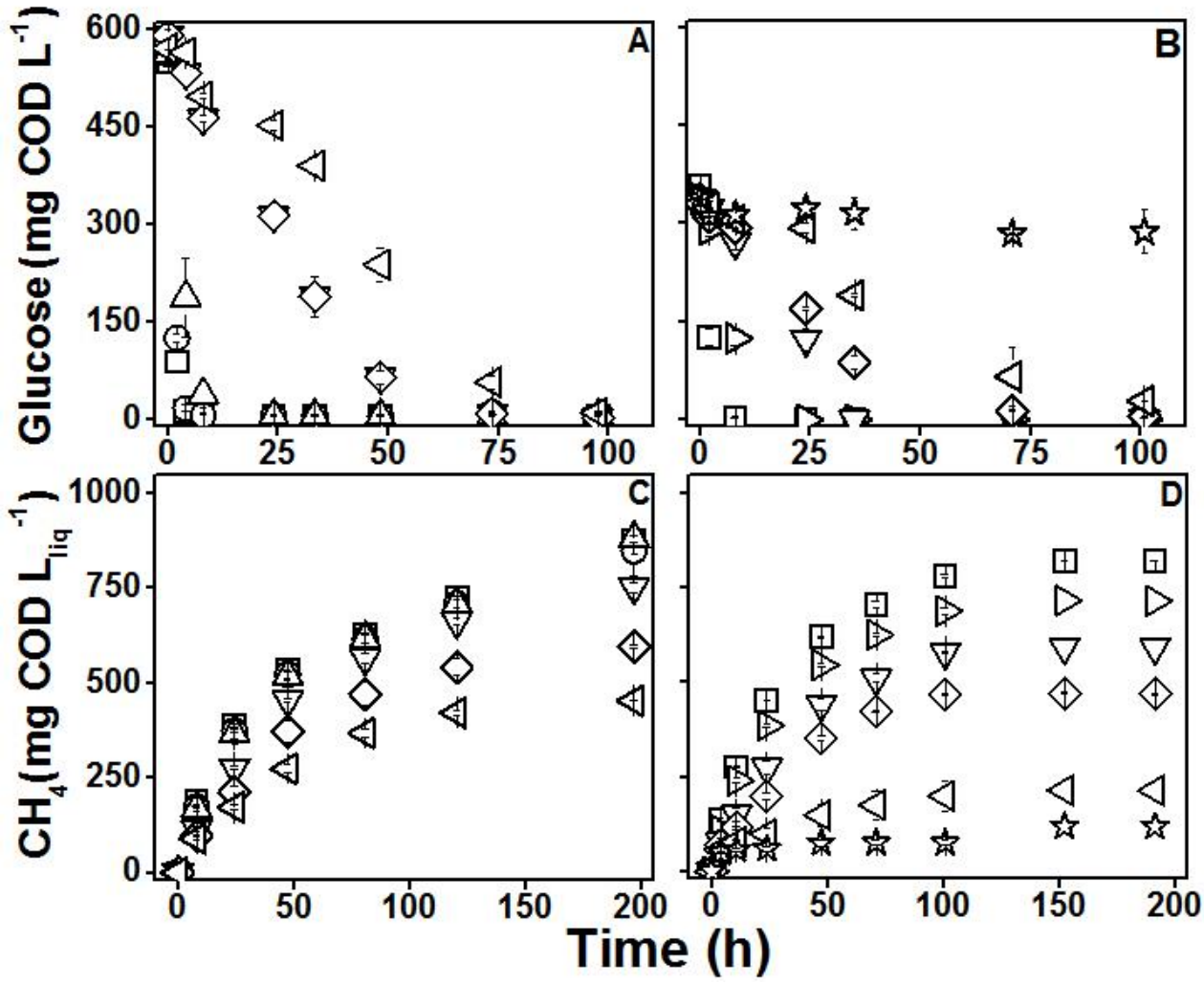

Figure 4.1 Time course of glucose and methane concentration at different concentrations (mM) of Cu^0 NP (A and C) and C uCl_2 (B and D): 0 (□), 0.008 (○), 0.016 (▷), 0.040(△), 0.079 (▽), 0.157 (◇), 0.315 (◁), and 0.629 (✯).

4.3.1.2 Effect on glucose conversion to methane during fermentation

The time course of methane produced from assays in the assays containing Cu^0 NP and $CuCl_2$ is shown in Figure 4.1C and 4.1D, respectively. Methanogenesis from glucose fermentation was distinctly limited at different supplied concentrations of Cu^0 NP and $CuCl_2$. Figure 4.1C shows that the addition of ≥0.157 mM Cu^0 NPs caused inhibition of methane production. Concentrations ≥0.157 mM Cu^0 NP slowed

the conversion of the fermentation products to methane and eventually caused the methane production to become halted after 120 h (Figure 4.1C). Inhibition of methane production was observable at 0.079 mM of $CuCl_2$ and severe inhibition was found at >0.315 mM $CuCl_2$. In all cases, methane production stopped after 100 h when >0.079 mM $CuCl_2$ was supplied to the experiments (Figure 4.1D). The results indicated that both forms of Cu caused inhibition of glucose bioconversion to methane. A COD balance was performed to analyze the effect of Cu on the anaerobic digestion of glucose.

4.3.1.3 COD balance during glucose fermentation

The experiments supplied with glucose provided information on the accumulation and consumption of intermediate compounds formed during the anaerobic degradation of glucose. The changes in concentration of these compounds can be analyzed by a COD balance performed at different times of the incubation. Figures 4.2A-B show the COD balance of the experiments supplied with Cu^0 NP after 8 and 200 h of incubation, respectively. The COD balance also takes into account the methane produced in the pre-incubation without Cu^0 NPs referred as Pre. Inc. Methane in the chart. After 8 h, the largest impact of Cu^0 NP glucose conversion was the direct inhibition of glucose consumption. At concentrations <0.079 mM, there was a small increase in butyrate, methane and low concentrations of acetate after 8 hours. Concentrations ≥0.079 mM Cu^0 NP resulted in accumulation of glucose with only minor conversion to methane and butyrate in the same time frame. After 200 h, essentially all glucose was converted in all of the Cu^0 NP treatments. The COD balance at Cu^0 NP concentrations ≤0.079 mM could be completely closed based on the methane produced. However, at concentrations ≥0.157 mM, accumulation of butyrate was evident and about 25% of the COD remained unidentified. Unidentified COD in controls and other assays could potentially indicate the presence of early intermediates (e.g lactic acid, ethanol, extracellular polysaccharides, etc.) not detected with the standard VFA protocol. Interestingly, negligible acetate or H_{2g} accumulation was found in the inhibited assays. These observations

confirmed that Cu^0 NPs inhibited the anaerobic digestion of glucose to methane. A similar analysis was performed with the assays supplied with $CuCl_2$.

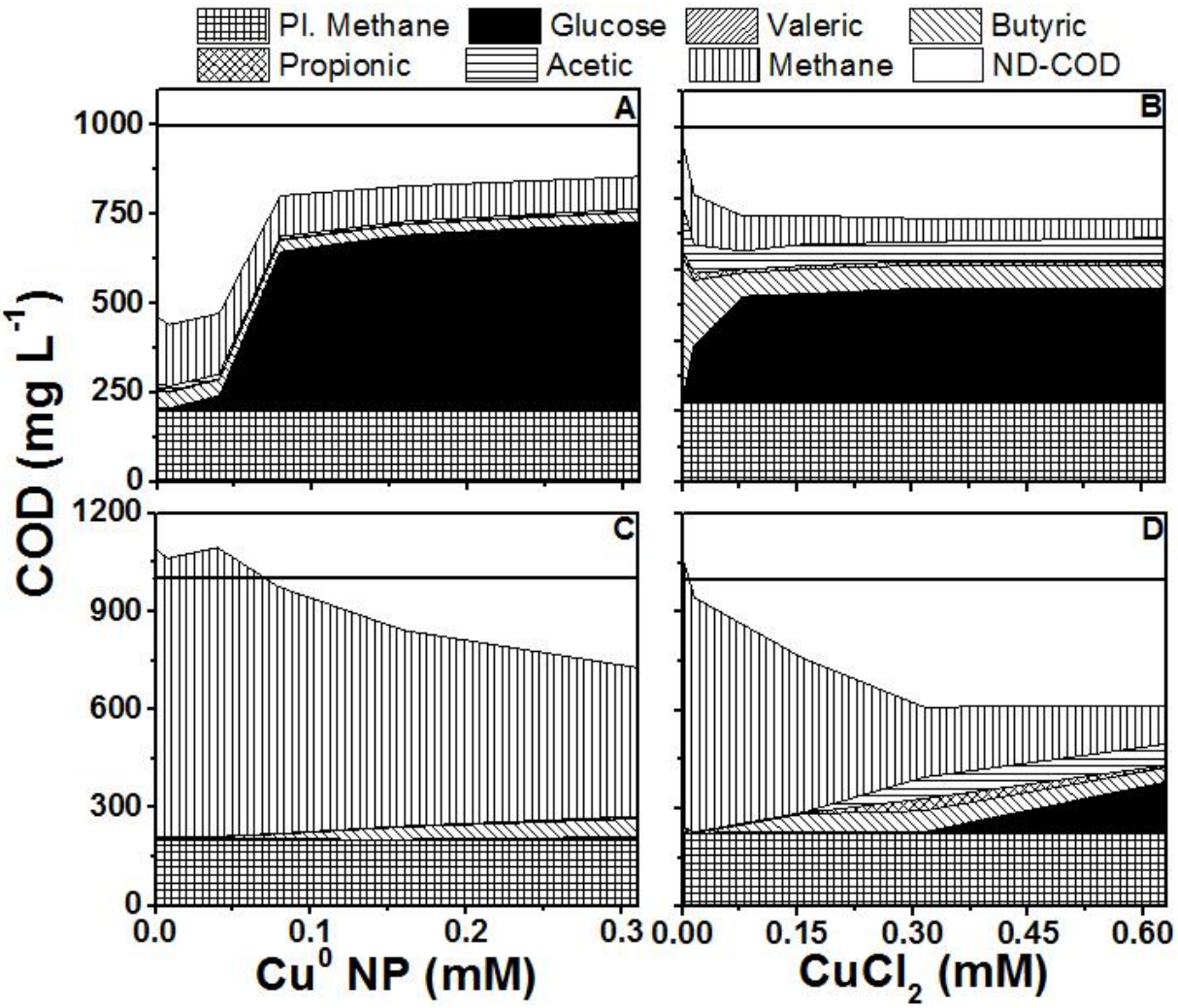

Figure 4.2 COD balance of the experiments amended with distinct concentrations of Cu^0 NP (A-C) and $CuCl_2$ (B-D) after glucose was consumed by the control (A-B) and final time (C-D). Pre-incubation methane (Pre.Inc. Methane) represents the production of methane in the activation period. ND-COD represents the non-detected COD intermediaries calculated as the theoretical total.

Figure 4.2C-D shows the COD balance of the assays amended with $CuCl_2$ after 6 and 200 h of incubation, respectively. After 6h, the inhibition of glucose consumption is evident at all concentrations of $CuCl_2$. On the other hand, the glucose was almost completely consumed to butyrate, acetate, and

methane in the control without $CuCl_2$ (Figure 4.2C). At concentrations ≥ 0.079 mM $CuCl_2$, approximately half of the COD remaining after the pre-incubation remained as unconsumed glucose. Additionally, methane, butyrate and acetate were evident but at lower proportions of the COD than in the control. All of the treatments with added $CuCl_2$ had higher unidentified COD fractions. The COD balance after 200 h of incubation (Figure 4.2D) provides evidence of full transformation of all substrates to methane in the control and accumulation of butyrate, propionate and acetate, as well as unidentified COD, in the inhibited assays. At concentrations of ≥0.315 mM $CuCl_2$, the inhibition of glucose consumption is so severe that residual glucose is still present even after 200 h. In all treatments, negligible acetate and no H_{2g} was found in all treatments after 200 h of incubation. Further investigations evaluated syntrophic acetogenesis by supplying propionate as an electron donor in the presence and absence of different Cu^0 NP and $CuCl_2$ concentrations.

4.3.1.4 Effect on propionate consumption during SPO

The time course of propionate consumption supplied either with Cu^0 or $CuCl_2$ is shown in Figure 4.3A and 4.3B, respectively. The SPO was inhibited by Cu^0 NPs and $CuCl_2$. Cu^0 NP was inhibitory to propionate oxidation when ≥0.079 mM Cu^0 NPs were supplied. Concentrations from 0.079 to 0.629 mM Cu^0 NP decreased the propionate oxidation rate from 35 to 85%, respectively (Figure 4.3A). Likewise, $CuCl_2$ was inhibitory to propionate oxidation with a concentration as low as 0.079 mM. $CuCl_2$ decreased the propionate oxidation rate from 55 to 90% when concentrations from 0.079 to 0.315 mM $CuCl_2$ were amended (Figure 4.3B). The results of the experiments demonstrate a high level of inhibition of propionate consumption when either source of Cu was supplied. Additionally, the transformation of the propionate to methane was studied.

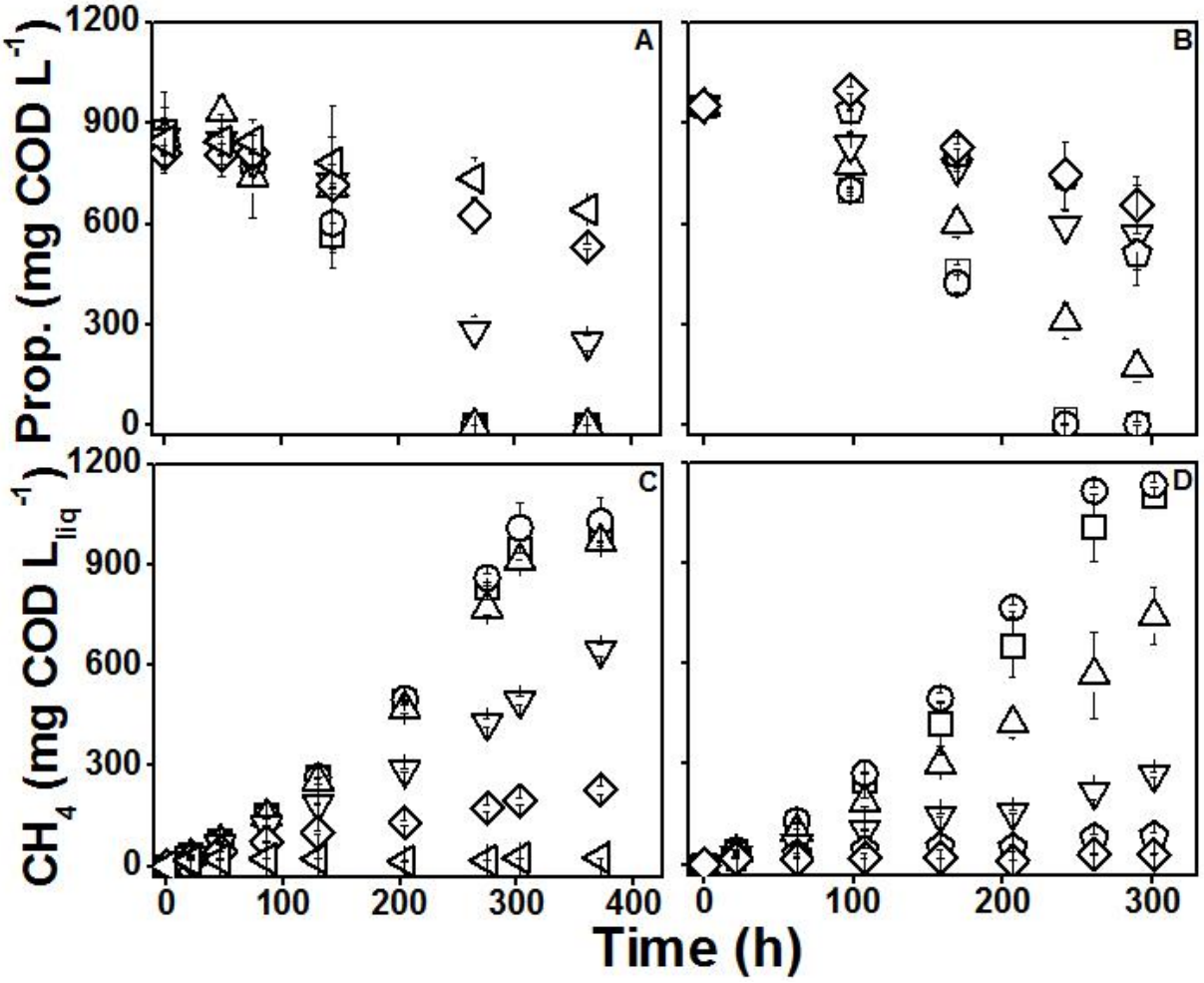

Figure 4.3 Time course of propionate consumption and methane production in experiments supplied at different concentrations (mM) of Cu^0 NP (A and C) and $CuCl_2$ (B and D): 0 (□), 0.016 (○), 0.079(△), 0.157(▽),0.236 (□), 0.315 (◇), and 0.629 (◁).

4.3.1.5 Effect on Methanogenesis during SPO

Figure 4.3C and 4.3D show the production of methane from propionate in treatments amended with Cu^0 NP and $CuCl_2$. Methane formation from propionate oxidation products was also inhibited by Cu^0 NP and $CuCl_2$. Experiments supplied with Cu^0 NPs revealed that methanogenesis was inhibited when ≥0.157 mM Cu^0 NPs was supplied (Figure 4.3C). Similarly, $CuCl_2$ decreased the methane production when ≥0.079 mM $CuCl_2$ was used (Figure 4.3D). Thus, Cu^0 NP and $CuCl_2$ were inhibitory to methanogenesis from

propionate oxidation products. A COD balance was performed for a further analysis of Cu^0 and $CuCl_2$ inhibition to propionate oxidation and methanogenesis.

4.3.1.6 Effect on COD balance of SPO

Figure 4.4A shows the COD balance of propionate acidogenesis and methanogenesis after 360 h of incubation in the propionate oxidation experiments amended with Cu^0 NPs. The period of 360 h was sufficient for propionate to be fully converted to methane in the control and low concentrations of Cu^0 NPs up to 0.079 mM. However, at concentrations ≥0.157 mM Cu^0 NPs, the residual propionate and the fraction of methane greatly increased and decreased, respectively. Up to 20% of the COD was not accounted for at the higher concentrations of Cu^0 NPs. Thus, Cu^0 NP toxicity resulted in both the inhibition of propionate consumption as well as methanogenesis. A parallel analysis was performed with the assays supplied with $CuCl_2$.

Figure 4.4B shows the COD balance after 360 hours of incubation with different concentrations of $CuCl_2$. The results showed that 360 h were sufficient time to completely convert propionate to methane in the control and the assays supplied with 0.015 mM $CuCl_2$. At concentrations of ≥0.079 mM an increases of residual propionate paralleled a significant decrease in methane produced. Likewise, a similar fraction of unaccounted COD and decreased methane production was found in inhibited assays with the highest $CuCl_2$ treatments. These results confirm that SPO was also highly inhibited by $CuCl_2$.

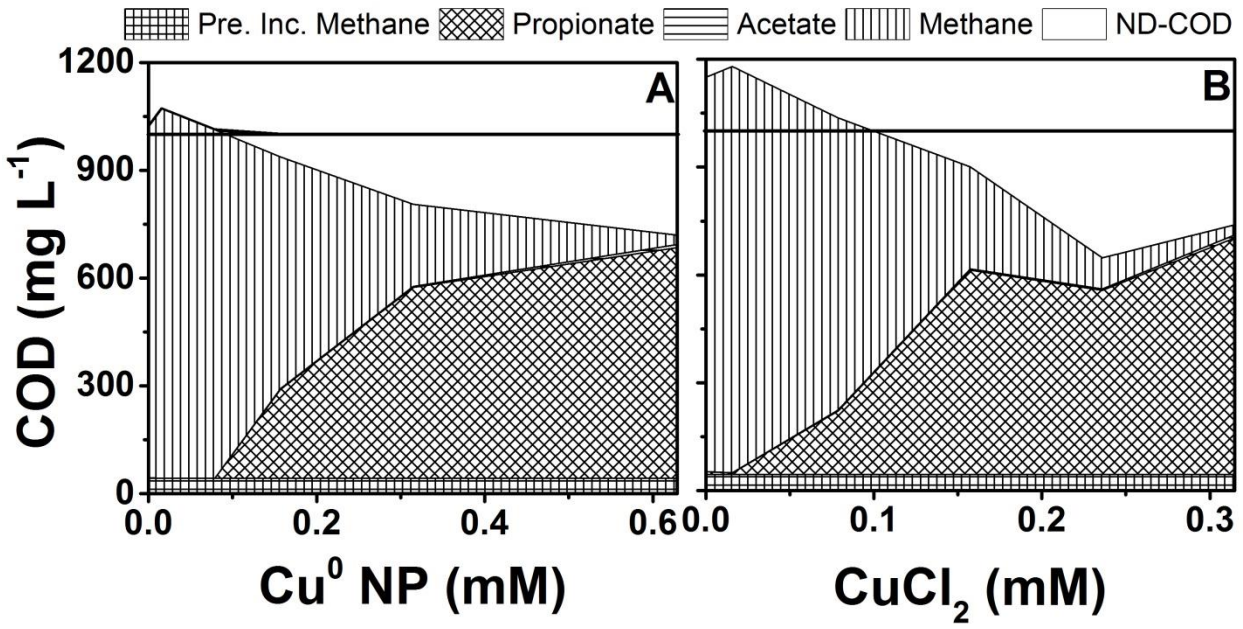

Figure 4.4 COD balance at the final time (370 h) for Cu^0 NP (A) and (300 h) for $CuCl_2$ (B). Pre-incubation methane (Pre. Inc. Methane) represents the production of methane in the activation period. ND-COD represents the non-detected COD intermediaries calculated as the theoretical total COD minus the sum of the COD from the detected intermediates.

4.3.2 Toxicity effect of Cu^0 NPs and $CuCl_2$ on nitrogen-utilizing microorganisms

4.3.2.1 Inhibition of anaerobic ammonium oxidizing (anammox) consortium

The inhibitory effect Cu^0 and $CuCl_2$ on an anaerobic ammonium oxidizing (anammox) consortium was explored in a series of batch experiments. The batch experiments were incubated for two feedings in order to observe more clearly the toxicity effects. Figures 4.5A and 4.5B show the time course of N_2 production in the second feeding of substrate as a response to the exposure to different concentrations of Cu^0 NP or $CuCl_2$, respectively. Cu^0 NPs and $CuCl_2$ decreased the maximum rate of N_2 production as the concentration of Cu increased. The lowest concentration of Cu^0 NPs supplied (0.157 mM Cu^0 NP) had a slightly inhibitory effect; however, 0.315 and 0.944 decreased the maximum rate up to 18 and 84%, respectively. Additionally, the highest concentration caused an incomplete conversion of the substrates as evidenced by the total amount of N_2 produced compared to the amount produced by the control. The

lower concentrations of $CuCl_2$ tested (0.079) did not severely affect the anammox consortium. However, 0.118 and 0.236 mM decreased the N_2 production rate by 36 and 99%, respectively. Thus, the addition of highest concentration of $CuCl_2$ resulted in an almost complete blockage of the N_2-production. Therefore, Cu^0 NPs and $CuCl_2$ were found to be inhibitory to anammox bacteria. The effect of Cu^0 and $CuCl_2$ on N_2 production by a denitrifying culture was also investigated.

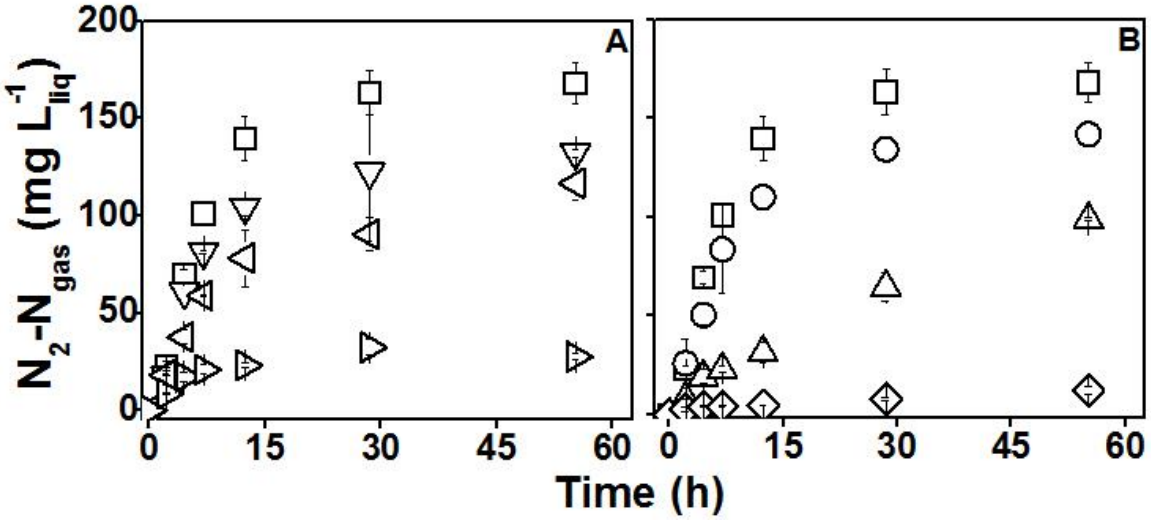

Figure 4.5 Time course of N_2 production by an anammox consortium in assays amended with different concentrations (mM) Cu^0 NP (A) and $CuCl_2$ (B): 0 (□), 0.079 (○), 0.118(△), 0.157(▽), 0.236 (◇), 0.315 (◁) and 0.94 (▷).

4.3.2.2 Toxicity effect of Cu^0 NPs and $CuCl_2$ on denitrification

Figure 4.6 shows the time course of N_2 production by a denitrifying culture as function of a range of concentrations of Cu^0 NPs and $CuCl_2$. Cu^0 NPs and $CuCl_2$ were inhibitory to the denitrifying culture at concentrations ≥0.079 mM. For both copper compounds, the lowest concentration applied of 0.016 mM caused no effect on denitrification. The production N_2 rate was decreased from 11 to 97% when concentrations from 0.079 to 0.63 mM Cu^0 NP were applied. The two highest concentration of Cu^0 NPs applied caused an almost complete blockage of the conversion of NO_3^- to N_2 (Figure 4.6A). The maximum N_2 production rate was inhibited from 11 to 97% with concentrations from 0.079 to 0.315 mM $CuCl_2$,

respectively. Additionally higher concentration completely halted the N_2 production (Figure 4.6B). Thus, these results revealed that Cu^0 NPs and $CuCl_2$ were highly inhibitory to denitrification.

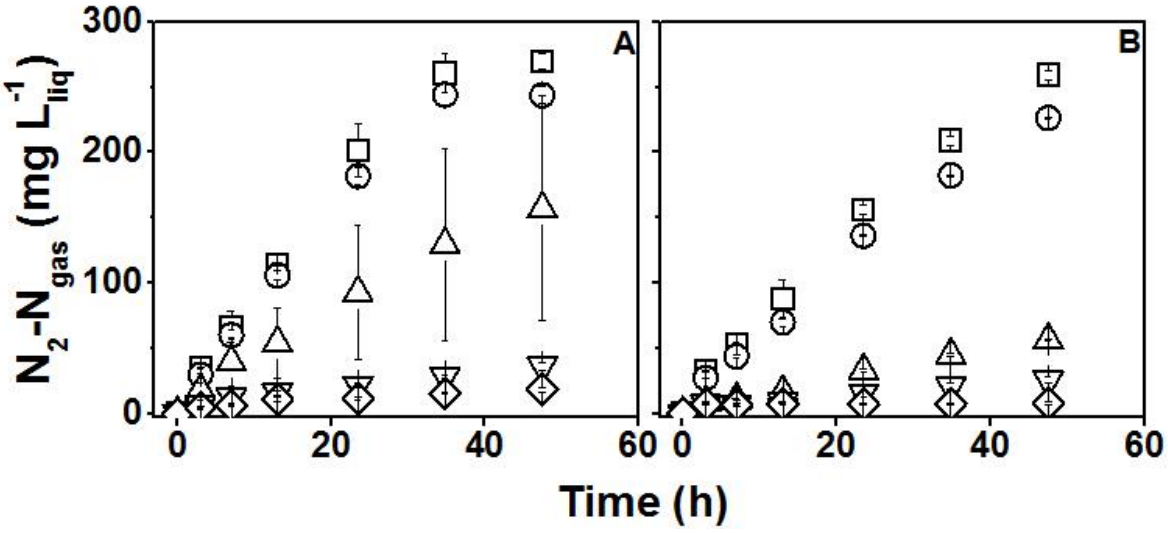

Figure 4.6 Time course of N_2 production by a denitrifying culture in assays amended with different concentrations (mM) of Cu^0 NP (A) and $CuCl_2$ (B): 0 (□), 0.016 (○), 0.079(△), 0.157(▽), and 0.315 (◇).

4.3.3 Ki for the different anaerobic trophic groups

K_i were calculated from the experiments exploring the inhibitory effect of Cu^0 NP and $CuCl_2$ on different microbial cultures. Figure 4.7A shows the inhibition constants calculated as function of added Cu^0 and $CuCl_2$. The calculated K_i demonstrate a higher toxicity of $CuCl_2$ than Cu^0 NP to all microbial cultures with the exception of methanogenesis from glucose fermentation which showed similar K_i values. The K_i of the experiments amended with Cu^0 NP illustrate that anammox was more tolerant than the other processes to Cu^0 NP, whereas glucose fermentation was the most sensitive as evidence by the lower K_i value for Cu^0 NP. The K_i obtained from the experiments supplied with $CuCl_2$ indicated less inhibition of methanogenesis from glucose fermentation compared to the other cultures. Conversely, glucose consumption (during glucose fermentation) was the most inhibited microbial process evidenced by the lowest *Ki* with respect to added $CuCl_2$. For the remainder of the cultures, the K_i values were similar with respect to added copper either as NP or salt. Overall results revealed that K_i as a function of added Cu^0 NP

vary from 0.05 to 0.33 mM, whereas the K_i obtained from $CuCl_2$ range from 0.004 to 0.12 mM. The K_i values were also calculated as a function of the residual soluble Cu in all experiments.

Figure 4.7B shows the calculated K_i as a function of the residual soluble Cu for all the microbial cultures studied. The general trend revealed very similar values of K_i for each culture as a function of the soluble concentration irrespective of whether the source was Cu^0 NP or $CuCl_2$. The range of concentrations of the K_i for almost all cultures varied from 0.001 to 0.008 Cu mM. Anammox formed an important exception with a much larger K_i than the other cultures with respect to soluble Cu. Overall the results indicated that very low soluble Cu concentrations inhibited the microorganisms in a similar manner. Therefore the ions released by Cu^0 NP and residual ions from $CuCl_2$ are very toxic for all the microbial cultures explored.

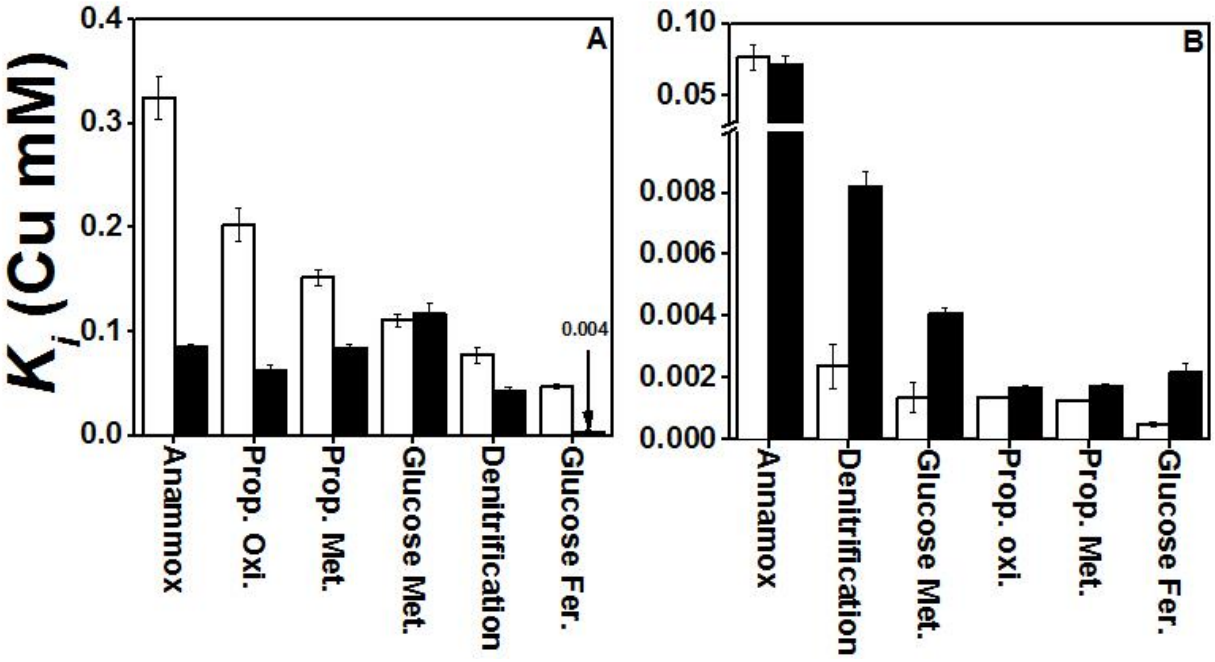

Figure 4.7 Inhibition constants as function of added Cu (A) and residual soluble Cu (B) of experiments supplied with Cu^0 NP (Empty bars) and $CuCl_2$ (Filled bars)

4.4 Discussion

4.4.1 Main findings

This study showed that Cu^0 NPs are toxic to anaerobic microbial cultures of wastewater treatment processes. The inhibitory effect of added Cu^0 NPs was somewhat less compared to Cu of added $CuCl_2$ salt. The similar order of magnitude of the inhibition response observed in all microbial cultures as a function of the residual soluble Cu indicated that the soluble ions released from Cu^0 NPs or remaining from added $CuCl_2$ were responsible for the inhibition. Similar K_i values with respect to soluble Cu were obtained for the two sources of Cu in each culture. Of all the trophic groups explored, anammox and methanogenesis from glucose were the least affected processes by Cu^0 NPs and $CuCl_2$, respectively. On the other hand, glucose fermentation was the most inhibited process by both types of Cu. The COD balance indicated that the inhibition affects all the processes involved in the fermentation of glucose and SPO as evidenced by the accumulation of substrate, intermediates (including unaccounted COD) and incomplete conversion of the intermediates to methane.

4.4.2 Comparison to other studies on the Cu-based NP inhibition of anaerobic microbial processes involved in wastewater treatment

Anaerobic digestion involves the conversion of complex molecules to methane in which several trophic groups are responsible for specific phases of the process. Cu-based and other NPs are known to inhibit anaerobic digestion (Garcia et al., 2012; Luna-delRisco et al., 2011; Mu et al., 2011); however, very little research has been performed applying model substrates such as acetate, hydrogen or volatile fatty acids (VFA) (Gonzalez-Estrella et al., 2013; Otero-González et al., 2014b). The application of model substrates provides a better understanding of the metabolic steps of anaerobic digestion that are being inhibited. In this study, glucose and propionate were supplied as substrates for anaerobic digestion.

Glucose fermentation and SPO assays showed accumulation of VFAs, some unaccounted COD and incomplete conversion of intermediates to methane when either Cu^0-NPs or $CuCl_2$ salt were amended. Otero-González et al. (2014) used a mixture of VFA as substrates (acetate, propionate, and butyrate) to feed an anaerobic reactor, and their findings showed propionate and acetate accumulation and incomplete conversion to methane due to CuO toxicity as well. This indicates that Cu^0 toxicity to anaerobic digestion is the result of the inhibition of the different microbial trophic groups involved in the anaerobic digestion process. Generally, methanogens are considered more sensitive to metal toxicity than glucose fermenters (Chen et al., 2008). However, this contrasts the results of the present study in which glucose fermenters were found to be considerably more sensitive to Cu than propionate oxidizers and methanogens.

Likewise, $CuCl_2$ has been described as toxic metal for denitrification and anammox processes; however, no research has been performed regarding Cu^0 NP toxicity to either anammox or denitrification microbial cultures. Recently, Li et al. (2014) found that $CuCl_2$ was the strongest inhibitor to anammox (IC_{50}=0.07 mM) among other heavy metals tested and highlighted the importance of the soluble concentration of each metal tested. Denitrifying microorganisms were also previously reported to be strongly inhibited at very low concentrations of $CuCl_2$ (Ochoa-Herrera et al., 2011). These findings coincide with our results indicating that concentration of <0.3 and <0.1 mM of total $CuCl_2$ are enough to inhibit by 50% the activity of anammox and denitrification processes, respectively. Recent studies have found low to moderate toxicity of Ce and Ag NPs to denitrifying microorganisms of soil ecosystems (Allison R., 2012; Dahle & Arai, 2014). Cu is one of the strongest inhibitors of microbial activity (Karlsson et al., 2015), therefore it is logical that a stronger inhibition effect of Cu^0 NPs on denitrification was found here.

4.4.3 Cu^0 NPs inhibitory mechanism on anaerobic microbial processes of wastewater treatment.

Toxicity of Cu-based NPs has been associated with the release of Cu soluble ions by the NPs which ultimately cause the inhibition effect (Gonzalez-Estrella et al., 2013; Luna-delRisco et al., 2011). This study correlates the *K*i with respect to soluble Cu regardless of whether it is released from Cu^0 NPs or it is the residual soluble Cu remaining in solution after addition of $CuCl_2$ through t. The K_i values obtained indicate that residual soluble Cu concentration correspond to inhibition based on the similarity of K_i values obtained cultures with CuCl2 or Cu^0 NP. The dissolution of Cu^0 into soluble ions in anaerobic conditions is the result of the reaction of protons with copper causing corrosion and therefore liberation of Cu ions into the liquid (Ollila, 2013). Thus, the anaerobic conditions provided in the experiments facilitated the releasing of soluble ions that consequently affected the microorganisms.

Even though the soluble ions are toxic to the microorganisms, the formation of CuxCOx or CuxPOx is hypothesized to be a major removal mechanism of soluble ions in this research; $Cu(OH)_2$, $Cu_2(OH)_2CO_3$, $CuCO_3$ and $Cu(PO_4)_2$ $(H_2O)_3$ have solubility products (log K_{s0}) of -19.36, -20.38, -33.18, -9.36, and -35.12, respectively (Benjamin, 2002). Therefore, low soluble concentrations of Cu were found in this research due to the presence of ligands such as carbonates and phosphates. Overall, all assays showed low soluble concentrations at the final time of the experiment <0.05 mM with the exception of the anammox assays (Supporting Information, Figure A.2.1). Therefore, the evidence indicates that low soluble concentrations of Cu are very toxic to the biological processes studied in the present work.

Anammox assays appeared to be more resistant to Cu^0 NP toxicity due to a greater tolerance of higher soluble concentrations than all the other bioassays. The complexation of Cu into a soluble but non bioavailable molecule may explain this behavior. For instance, a 19-fold higher concentration of EDTA in the anammox medium increased the soluble concentration of Cu in medium but potentially decreased its

bioavailability. EDTA is well-known chelating agent applied for remediation of soils polluted with cationic heavy metals such as Cu, Cd, Pb, and Zn by forming soluble and stable and non-biodegradable complexes (Dermont et al., 2008). This suggests that EDTA may have played a role increasing the resistance of anammox to Cu^0 NP toxicity by decreasing the soluble Cu bioavailability. A change in the speciation of the soluble form will probably affect the Cu toxicity mechanism.

Cu toxicity is typically associated with the binding of Cu ions with thiol and other groups on protein structures causing a disruption of the enzyme functionality (Chen et al., 2008). Novel mechanisms of Cu toxicity suggest that Cu replaces the iron-sulfur cluster of isopropylmalate dehydratase enzyme in the absence of oxygen (Solioz et al., 2010) which may account for a very important mechanism in anaerobic conditions. Additionally, Cu is known to be uptaken by the unspecific inorganic transporter (CorA) that carries Mg in Archaea (Nies, 1999), which includes methanogens. Thus, Cu^0 may have affected the enzymatic functionality of the various trophic groups responsible for a complete anaerobic digestion of glucose and propionate. Cu is also an important component of the enzymes of anammox bacteria such as nitrate reductase and nitrate oxidoreductase (Kartal et al., 2011) but an excessive concentration may be toxic. Also, Cu is utilized by several enzymes such as nitrite and nitrous reductases involved in denitrification (Zumft & Körner, 1997), thus its import into cells may occur relatively easily.

4.5 Conclusions

Cu^0 NPs cause toxicity to various anaerobic trophic groups involved in anaerobic digestion and N-removal processes with K_i values ranging from 0.004 to 0.324 mM of added Cu^0 NP. The main mechanism of toxicity of Cu^0 NP is associated with the release of dissolved Cu as evidenced by the similar toxicity response of Cu from Cu^0 NPs and $CuCl_2$ when correlated to the residual

soluble Cu. Anammox and glucose fermentation groups were the least and most sensitive processes to Cu^0 NPs inhibition, respectively. The results taken as whole reveal that Cu^0 NPs are inhibitors of various trophic groups in anaerobic processes; therefore, Cu^0 NPs represent a concern if they become concentrated in certain waste streams such as excess an activated sludge or sludge liquors.

4.6 Acknowledgments

This work was supported by the Semiconductor ResearchCorporation (SRC)/Sematech Engineering Research Center for Environmentally Benign Semiconductor Manufacturing. Gonzalez-Estrella was partly funded by CONACyT.

CHAPTER V ROLE OF BIOGENIC SULFIDE IN ATTENUATING ZINC OXIDE AND COPPER NANOPARTICLE TOXICITY TO METHANOGENESIS

Jorge Gonzalez-Estrella*, Daniel Puyol, Reyes Sierra-Alvarez, James A. Field

Department of Chemical and Environmental Engineering, University of Arizona,

P.O. Box 210011, Tucson, AZ 85721, USA

*Corresponding author: Jorge Gonzalez-Estrella

Department of Chemical and Environmental Engineering
The University of Arizona,
P.O. Box 21011, Tucson, AZ 85721, United States
Phone: +1-520-621 6162
E-mail: jorgegonzaleze@email.arizona.edu

Abstract

Soluble ions released by zinc oxide (ZnO) and copper (Cu^0) nanoparticles (NPs) have been associated with toxicity to methanogens. This study evaluated the role of biogenic sulfide in attenuating ZnO and Cu^0 NP toxicity to methanogens. Short- and long-term batch experiments were conducted to explore ZnO and Cu^0 NPs toxicity to acetoclastic methanogens in sulfate-containing (0.4 mM) and sulfate-free conditions. ZnO and Cu^0 were respectively 14 and 7-fold less toxic in sulfate-containing than in sulfate-free assays as indicated by inhibitory constants (K_i). The K_i with respect to residual soluble metal indicated that soluble metal was well correlated with toxicity irrespective of the metal ion source or presence of biogenic sulfide. Long-term assays indicated that ZnO and Cu^0 NPs caused different effects on methanogens. ZnO NPs without protection of sulfide caused a chronic effect, whereas Cu^0 NPs caused an acute effect and recovered. This study confirms that biogenic sulfide effectively attenuates ZnO and Cu^0 NPs toxicity to methanogens by the formation of metal sulfides.

Key words: Elemental copper and zinc oxide nanoparticles, anaerobic digestion, sulfate-reduction, inhibition.

5.1 Introduction

Engineered nanoparticles (NPs) are manufactured materials with at least one dimension between 1-100 nm (Brar et al., 2010). NPs are widely applied due to their unique properties provided by their small size. In the near future, the production of NPs is expected to increase (Westerhoff et al., 2013). Zinc oxide (ZnO-NPs) and copper (Cu^0-NPs) NPs are used in several consumer products and industrial processes (Luna-delRisco et al., 2011).

ZnO-NPs are used in personal care products, food additives, pigments and biosensors, whereas Cu^0-NPs are by-products in semiconductor manufacturing and are applied in inks and electronics (Brar et al., 2010). The large-scale application of NPs has raised concerns about their fate and impact on the environment. A recent study demonstrated that NPs in urban or industrial sewage are retained in activated sludge (Westerhoff et al., 2013).

Waste sludge produced by activated sludge is commonly stabilized by anaerobic digestion, which depends on methanogens to transform organic matter to methane (Metcalf et al., 2003). NPs retained by activated sludge may accumulate in the anaerobic digestion process. Such accumulation could affect methanogenesis (Mu & Chen, 2011). ZnO- and Cu^0-NP toxicity to methanogens has been reported in several studies. These studies concluded that metal cations released by NPs are correlated with the toxic effect (Gonzalez-Estrella et al., 2013; Luna-delRisco et al., 2011; Mu et al., 2011). Biogenic sulfide can attenuate Zn^{2+} and Cu^{2+} toxicity to methanogens forming non-toxic ZnS and CuS precipitates (Jin et al., 1998; Lawrence & McCarty, 1965; Zayed & Winter, 2000). Therefore, ZnO- and Cu^0-NP toxicity may be prevented by biogenic sulfide. This study investigated the role of sulfate-reduction in attenuating ZnO- and Cu^0-NP toxicity to acetoclastic methanogens.

5.2 Material and Methods

5.2.1 Chemicals

Cu^0-NPs (40-60 nm, 99%) were purchased from Sky-Spring Nanomaterials Inc. (Houston, TX) ZnO-NPs (100 nm, 99%), $CuCl_2 \bullet H_2O$ (99%), $ZnCl_2$ (98%) and sodium acetate (99.9%) were acquired from Sigma Aldrich (St. Louis, MO, USA). N_2/CO_2 (80/20, v/v) gas mix and CH_4 standard gas (99%) were acquired from Air Liquid America (Plumstedsville, PA, USA).

5.2.2 NP dispersions and metal solutions

ZnO- and Cu^0-NP stock dispersions were sonicated (DEX® 130, 130 Watts, 20 kHz, Newtown, CT) at 70% amplitude for 5 min. ZnO- and Cu^0-NP stability in anaerobic media has been previously described (Gonzalez-Estrella et al., 2013). $CuCl_2$ and $ZnCl_2$ solutions were prepared by dissolving them in 0.01 M HCl. The range of concentrations was 0.008 to 1.18 mM.

5.2.3 Anaerobic sludge

Anaerobic granular sludge was obtained from a full-scale upflow anaerobic sludge bed reactor treating brewery wastewater (Mahou, Guadalajara, Spain). The sludge was stored at 4 °C. Volatile suspended solids (VSS) were 7.92% of the wet weight. The maximum acetoclastic methanogenic activity determined was 95 ± 9 mg CH_4-COD g^{-1} VSS d^{-1}.

5.2.4 Methanogenic inhibition bioassays

Sulfate-containing and sulfate-free assays were performed in an anaerobic medium at pH (7.2) containing (mg L^{-1}): NH_4Cl (280), $NaHCO_3$ (3,000), K_2HPO_4 (250), $CaCl_2 \bullet 2H_2O$ (10), $MgCl_2 \bullet 6H_2O$ (100),

$MgSO_4 \bullet 7H_2O$ (100); and yeast extract (100) with 1 mL L^{-1} of trace elements. Sulfate-free experiments contained 183 mg L^{-1} $MgCl_2 \bullet 6H_2O$ instead of $MgSO_4 \bullet 7H_2O$.

The experiments were performed by adding inoculum (1.5 g of VSS L^{-1}) and 1.1x concentrated medium (45 mL) to 160 mL bottles. Subsequently, all bottles were flushed with N_2/CO_2 (80:20, v/v). Sodium acetate (1 g COD L^{-1}) was used as the electron-donor. Assays were pre-incubated overnight at 30 ± 2 °C in an orbital shaker at 115 rpm. Next, 5 mL of the NP stock dispersion, metal stock solution, or deionized water was added to the corresponding experiments. All bottles were reflushed with N_2/CO_2 then incubated at 30 ± 2 °C in an orbital shaker at 115 rpm. Methane samples (100 µL) were taken from the headspace several times during incubation. A second (short-term assays) or four (long-term assays) additional feedings of acetate were supplied to the bottles after the control reached the expected methane concentration. Long-term assays were rinsed out with Milliq water after the fifth acetate amendment to investigate the recovery of methanogens in a basal medium free of inhibitors.

5.2.5 Sulfate-reduction inhibition bioassays

These assays explored Zn and Cu (NPs and salt) toxicity to sulfate reduction in sulfate-containing basal medium. Sulfate was monitored by taking liquid samples (0.5 or 1 mL) from the supernatant. Samples were centrifuged at 13,000 rpm and frozen at -10°C.

5.2.6 Analytical methods

Methane was quantified by gas chromatography, soluble metals by inductively coupled plasma-optical emission spectroscopy and sulfate by suppressed conductivity ion chromatography. The analysis details are described in Supporting Information section S4.

5.2.7 Data Processing

Specific methanogenic activities (SMA) were calculated as the maximum specific methanogenic rate using linear regression for each three consecutive points. The normalized methanogenic activity (NMA) was calculated as follows:

$$NMA(\%) = \left(\frac{SMA_t}{SMA_c} \right) \cdot 100 \qquad [5.1]$$

where SMA_t and SMA_c are the specific methanogenic activities of the treatment and control experiments, respectively. The inhibitory effect on the NMA was quantified as follows:

$$NMA = NMA_{\max} \cdot \frac{1}{1 + \left(\frac{I}{K_i} \right)^n} \qquad [5.2]$$

where NMA_{max} is the maximum NMA (%), I and K_i are the inhibitor concentration and inhibition constant, respectively (mM), and n is the inhibition order (dimensionless) (Puyol et al., 2012). The inhibition order relates the steepness of the inhibition response to the dose curve as described in Supporting Information section A.3.1.

Long-term Cu and Zn (salts and NPs) toxicity to methanogenesis was analyzed by calculating the apparent growth rate of methanogens at different Cu and Zn concentrations. The experimental data was fitted to the following equation:

$$MA = \mu_{app} \cdot S_{consumed} + MA_o \quad [5.3]$$

where *MA* represents the instantaneous volumetric methanogenic activity (mg COD L^{-1} d^{-1}), MA_0 represents *MA* at t_0, μ_{app} is the apparent specific growth rate (d^{-1}), and $S_{consumed}$ is the cumulative substrate consumed (mg COD L^{-1}). Eq. [5.3] assumes that viable cells have a given activity (μ_{app}/Y) and loss of activity is caused by cell death (verification of this assumption provided in SI). The volumetric activity has been assumed to be proportional to biomass concentration, so that an increment in the methanogenic activity can be directly related to an increment in biomass concentration. When cell death exceeds growth, μ_{app} becomes negative. The derivation of Eq. [5.3] is described in Supporting Information section S2.

Theoretical sulfide production was calculated assuming that a mole of sulfate consumed produces a mole of sulfide. Endogenous decay of the biomass was measured. Therefore, sulfide production is defined throughout the manuscript as the theoretical sulfide produced by sulfate reduction and sulfide production from endogenous decay. Details of the software used for modeling are described in Supporting Information section S3.

5.3 Results

5.3.1 Role of sulfide in Zn toxicity to acetoclastic methanogenesis

The effect of sulfide on the attenuation of ZnO NP and $ZnCl_2$ inhibition to methanogens was investigated. Zn added as ZnO or $ZnCl_2$ was less toxic to acetoclastic methanogens in assays with sulfate-containing compared to sulfate-free medium (Figure 5.1). Methanogenesis was inhibited when >0.02 mM ZnO or $ZnCl_2$ were added in sulfate-free conditions, whereas sulfate-containing assays required >0.5 mM and >0.4

mM ZnO and $ZnCl_2$ to initiate inhibition, respectively (Figure 5.1A-B). Both observations agreed with the amount of endogenous sulfide produced in sulfate-free conditions (0.02 mM S^{2-}) and with the theoretical maximum biogenic sulfide production in sulfate-containing conditions (0.43 mM S^{2-}) each represented as dashed-dotted vertical lines (Figure 5.1A-B). Finally, the experiment indicates that ZnO and $ZnCl_2$ in presence or absence of biogenic sulfide have a similar inhibitory effect on methanogens (Figure A.3.2, see Annex A.3). Therefore, the results strongly suggest that ZnO and $ZnCl_2$ affect methanogenesis in a similar fashion in sulfate-free or sulfate-containing conditions.

Additionally, the estimated K_i corroborated the role of S^{2-} on attenuation of ZnO and $ZnCl_2$ toxicity. The K_i for ZnO and $ZnCl_2$ in sulfate-containing conditions were 13.6 and 12.0-fold higher (less toxic) than the K_i in the corresponding sulfate-free conditions (Table 5.1). Zn additions did not severely inhibit sulfate-reducers as evidenced by the full conversion of sulfate to sulfide (Figure A.3.3). Overall, these results provided conclusive evidence that biogenic sulfide decreased the toxicity of ZnO NP to methanogenesis. The soluble concentration of Zn was analyzed to confirm the role of biogenic sulfide in lowering the metal ion equilibrium concentration in the attenuation of methanogenic toxicity.

The soluble Zn ion concentration was dependent upon the presence or absence of sulfide. Sulfate-free conditions required less ZnO or $ZnCl_2$ than sulfate-containing conditions to achieve a given concentration of soluble Zn (Figure 5.1C-D). The region of the graph where the molar concentration of added metal NPs or salts is less than the biogenic sulfide concentration is referred to as the sulfide buffer-zone. Within this zone, the final soluble Zn concentration in sulfate-containing assays was around half the concentration found in sulfate-free assays at similar added Zn concentrations.

Table 5.1 Inhibition constant values and goodness of fitting of the experimental data to Eq. 5.1

Material	Basal Medium	K_i (mM)	R^2	n
Added NP or salt				
Cu^0	SO_4^{2-}-containing	0.750 ± 0.01	0.97	6.0 ± 0.07
Cu^0	SO_4^{2-}-free	0.109 ± 0.006	0.99	2.2 ± 0.2
$CuCl_2$	SO_4^{2-}-containing	0.295 ± 0.005	0.99	7.6 ± 0.7
$CuCl_2$	SO_4^{2-}-free	0.066 ± 0.003	0.99	2.3 ± 0.2
ZnO	SO_4^{2-}-containing	0.558 ± 0.002	0.98	33.9 ± 8.2
ZnO	SO_4^{2-}-free	0.041 ± 0.002	0.99	2.0 ± 0.2
$ZnCl_2$	SO_4^{2-}-containing	0.600 ± 0.01	0.96	11.5 ± 2.1
$ZnCl_2$	SO_4^{2-}-free	0.050 ± 0.004	0.97	2.2 ± 0.4
Residual Soluble Metal Concentration from NP or salt				
Cu^0	SO_4^{2-}-containing	0.061 ± 0.01	0.97	4.3 ± 0.8
Cu^0	SO_4^{2-}-free	0.018 ± 0.006	0.99	5.5 ± 1.2
$CuCl_2$	SO_4^{2-}-containing	0.012 ± 0.005	0.99	5.7± 0.7
$CuCl_2$	SO_4^{2-}-free	0.014 ± 0.003	0.99	4.6 ± 0.4
ZnO	SO_4^{2-}-containing	0.011 ± 0.002	0.98	41.0 ± 12
ZnO	SO_4^{2-}-free	0.010 ± 0.001	0.99	21.3 ± 2.6
$ZnCl_2$	SO_4^{2-}-containing	0.008 ± 0.001	0.96	5.6 ± 1.2
$ZnCl_2$	SO_4^{2-}-free	0.005 ± 0.004	0.97	4.8 ± 2.1

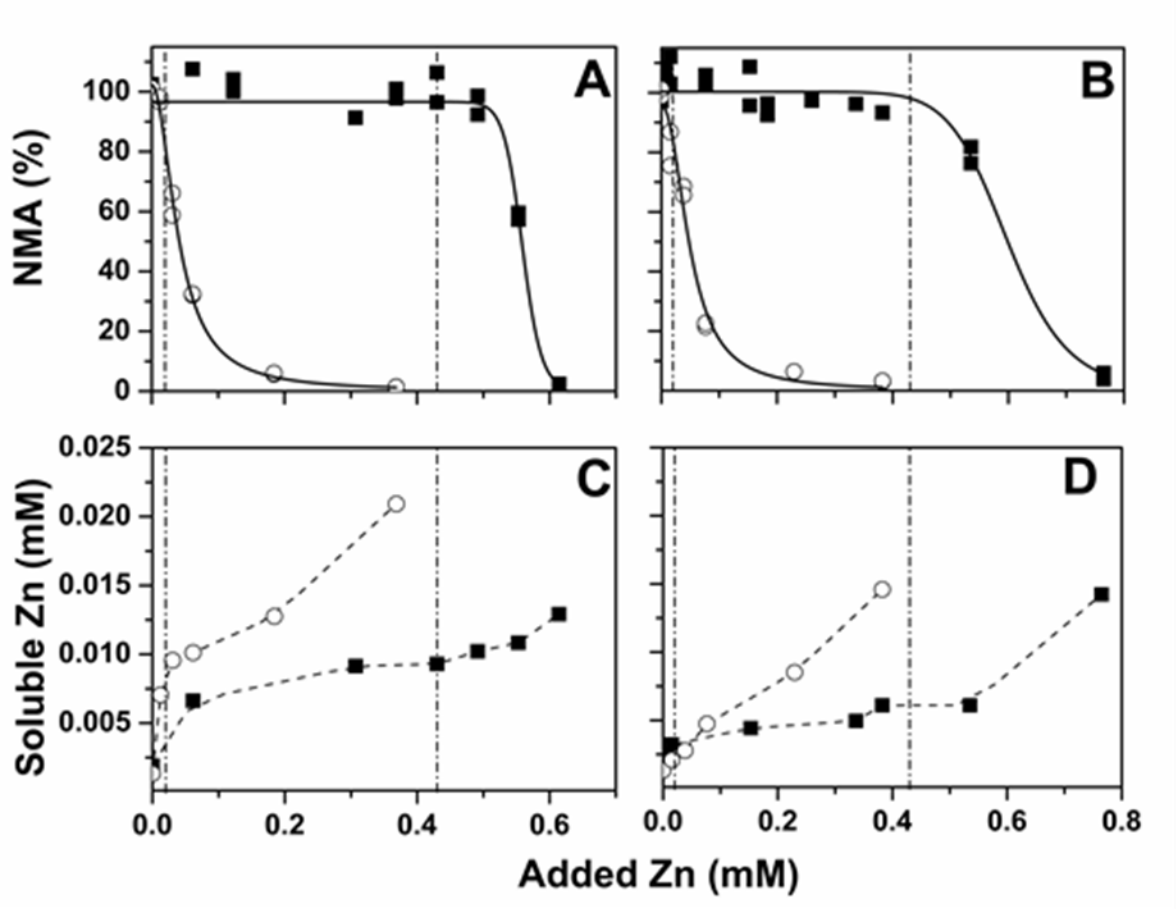

Figure 5.1. Effect of added Zn as ZnO-NP (A) and $ZnCl_2$ (B) on the normalized acetoclastic methanogenic activity in sulfate-containing (■) and sulfate-free (○) conditions and measured soluble Zn at the start of second acetate feeding relative to the initial ZnO-NP (C) and $ZnCl_2$ (D). Continuous lines are fittings to Eq. 5.1. Dash-dot vertical lines represent the endogenous sulfide production in the sulfate-free assays and the theoretical maximum sulfide from the sulfate-containing assays.

Additionally, toxicity became evident at soluble Zn concentrations higher than 0.01 and 0.005 mM in ZnO and $ZnCl_2$ experiments, respectively, which corresponded to the limit of the sulfide buffer-zone. The soluble Zn concentration data indicated that biogenic sulfide controlled the amount of freely soluble Zn and as a result also the inhibitory effect of Zn ions on acetoclastic methanogens. A similar set of

experiments were performed applying Cu^0-NPs and $CuCl_2$ in sulfate-free and sulfate-containing conditions.

5.3.2 Role of sulfide in Cu toxicity to acetoclastic methanogenesis

Biogenic sulfide decreased Cu^0-NP and $CuCl_2$ toxicity to methanogens (Figure 5.2). Cu became inhibitory when $\geq$0.02 mM Cu^0-NPs or $CuCl_2$ was added in sulfate-free experiments. In sulfate-containing assays, Cu was inhibitory when >0.2 mM Cu was added as Cu^0-NPs or $CuCl_2$. The initial Cu concentration causing inhibition agreed with the amount of endogenous biogenic sulfide produced in sulfate-free conditions (0.02 mM S^{2-}) and with the concentration of biogenic sulfide produced in sulfate-containing conditions depending on the extent to which Cu affected sulfate-reduction (Figure 5.2A-B). Likewise, the estimated K_i confirmed that biogenic sulfide decreased toxicity. The K_i in sulfate-containing conditions for Cu^0-NPs and $CuCl_2$ was 6.9 and 4.5 -fold higher than the K_i in the corresponding sulfate-free conditions (Table 1). These observations confirmed that biogenic sulfide attenuated Cu^0-NP toxicity to methanogenesis. Additionally, the soluble concentration of Cu was measured in sulfate-free and sulfate-containing experiments.

The soluble concentration of Cu in assays supplied with either Cu^0-NPs or $CuCl_2$ was dependent upon the presence or absence of biogenic sulfide. Assays with sulfate-containing medium required greater addition of Cu^0-NP and $CuCl_2$ to reach a soluble Cu concentration comparable to that reached in the sulfate-free assays (Figure 5.2C-D). The final soluble Cu concentration in the sulfide buffered-zone was about 50% lower in sulfate-containing compared to sulfate-free assays at comparable added Cu concentrations. Methanogenic activity decreased in all cases once a concentration of 0.01 mM of soluble Cu was reached. Likewise, all experiments exhibited a substantial increase of soluble Cu, released either from Cu^0-NPs or $CuCl_2$, once the concentration of added Cu started to inhibit the sulfide production process (Figure 5.2E-F). These observations confirmed that soluble copper, despite its source, was

controlled by the concentration of biogenic sulfide produced. An experiment evaluating Cu toxicity to biogenic sulfide production was performed to provide more insight.

$CuCl_2$ and to a lesser extent Cu^0-NPs had an inhibitory effect on the sulfate reduction activity as shown by the calculated sulfide production. The sulfate consumption efficiency at increasing Cu concentrations confirmed toxicity of Cu to sulfate-reduction within the concentration range applied (Figure 5.2E-F). $CuCl_2$ inhibited sulfate consumption more than Cu^0-NPs. Thus, the effect of sulfate in the medium on the attenuation of $CuCl_2$ toxicity was clearly less effective than for the attenuation of Cu^0-NP toxicity. Consequently, the methanogenic activity decreased before the theoretical maximum sulfide production was reached in the case of $CuCl_2$. Therefore, Cu toxicity to methanogenesis also depended on Cu inhibition to sulfate reduction.

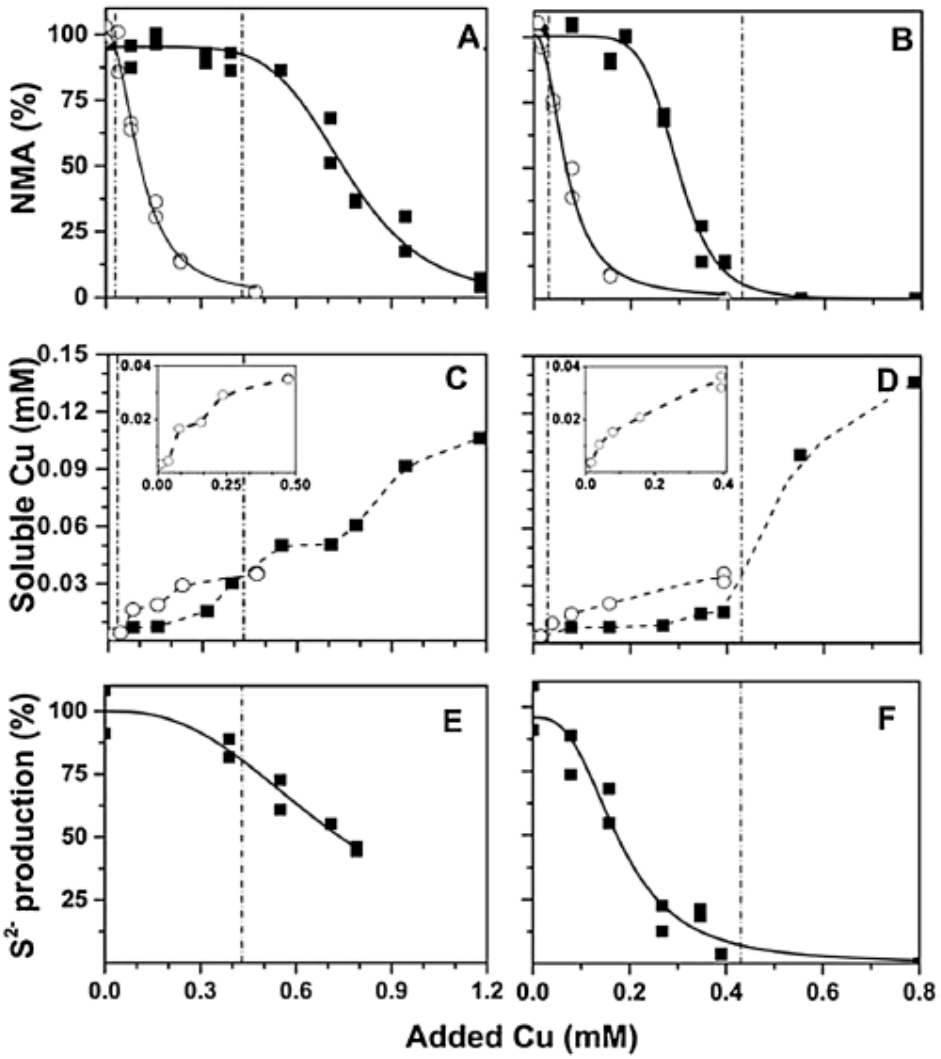

Figure 5.2 Effect of Cu^0-NP (A) and $CuCl_2$ (B) on the normalized acetoclastic methanogenic activity in sulfate-containing (■) and sulfate-free (○) conditions, measured soluble Cu at the start of second acetate feeding relative to the initial Cu^0-NP (C) and $CuCl_2$ (D), and effect of Cu^0-NP (E) and $CuCl_2$ (F) on the biogenic sulfide production. Continuous lines are fittings to Eq. 5.1. Dash-dot vertical lines represent the theoretical endogenous sulfide from the sulfate-free assays and the theoretical maximum sulfide from the sulfate-containing assays. Inserted boxes on panels C and D are zooms of soluble Cu concentrations from sulfate-free assays.

5.3.3 Effect of the soluble Zn and Cu on the methanogenic activity

An analysis of methanogenic activity as a function of the residual soluble Zn was conducted. Figure 5.3 shows the NMA as a function of the residual soluble concentration of the assays amended with ZnO-NPs and ZnCl2 in sulfate-containing and sulfate-free conditions. The inhibitory response of the methanogenic activity was predominantly related to the residual soluble Zn concentration irrespective of the Zn source or sulfate addition (Figure 5.3A-B). There was a minor exception for the assay amended with $ZnCl_2$ performed in sulfate-free conditions which had a slightly higher toxic response based on the residual soluble concentrations (Figure 5.3B). The assays amended with ZnO-NPs and $ZnCl_2$ in sulfate-free and sulfate-containing conditions showed very similar K_i when the kinetic parameter was obtained using the residual soluble Zn (Table 5.1).

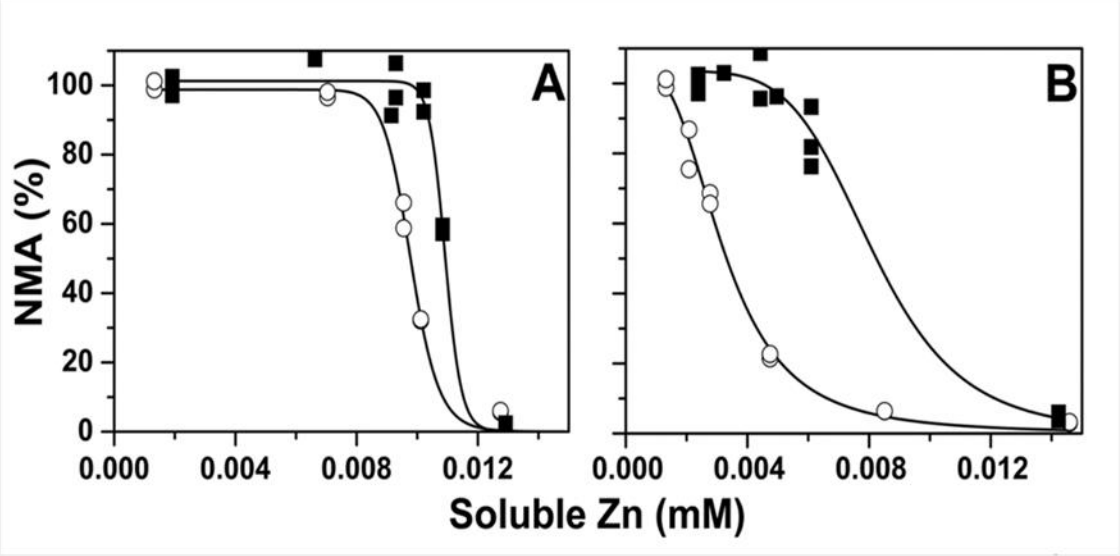

Figure 5.3 Effect of the soluble Zn concentration at the end of the first feed released from ZnO-NPs (A) or remaining in solution from $ZnCl_2$ (B) on the normalized methanogenic activity of the second feeding in the sulfate-containing (■) and sulfate-free (○) conditions. Continuous lines are fittings to Eq. 5.1.

Figure 5.4 shows the NMA as function of the residual soluble concentration of the assays amended with Cu^0-NPs and $CuCl_2$ in sulfate-containing and sulfate-free conditions. Likewise, Cu toxicity to methanogens in most of the explored cases was associated with similar residual soluble Cu^{2+} concentrations, irrespective of Cu source (Figure. 5.4A-B). There was one outlier for the assay amended with Cu^0-NPs in sulfate-containing conditions (Figure 5.4A) which appeared to have a lower inhibitory effect in relation to residual soluble Cu^{2+}. The calculated K_i ranged from 0.012 to 0.018 mM of soluble Cu with the exception of the outlier K_i of 0.061 mM (Table 5.1).

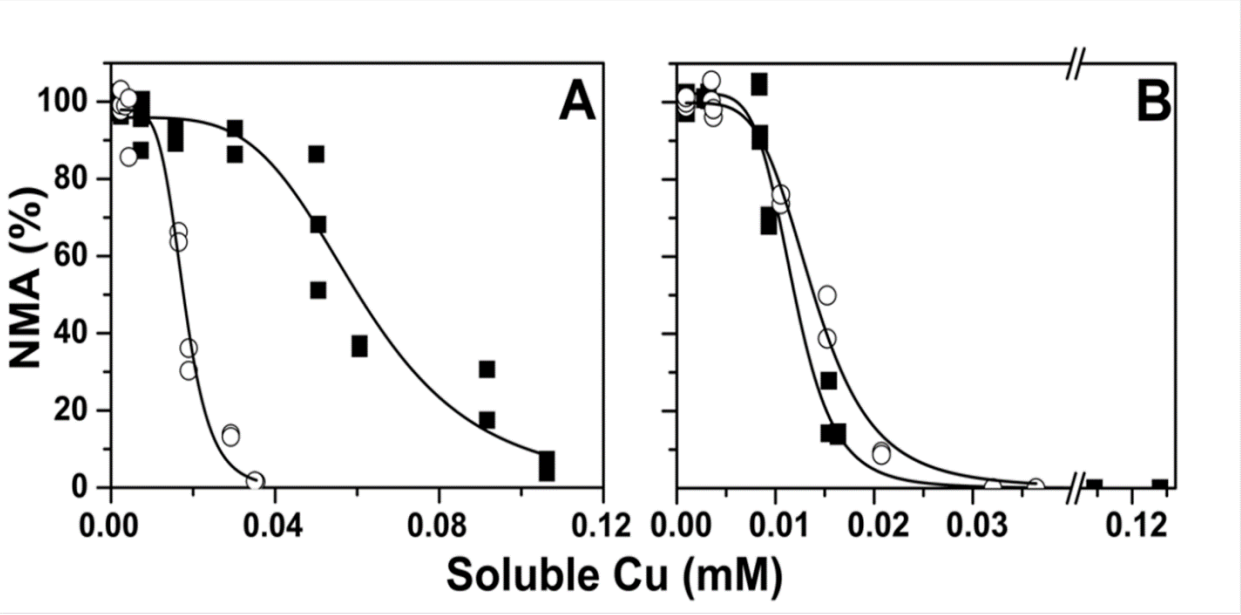

Figure 5.4 Effect of the soluble Cu concentration at the end of the first feed released by Cu^0-NPs (A) or remaining in solution from $CuCl_2$ (B) on the normalized methanogenic activity of the second feeding in the sulfate-containing (■) and sulfate-free (○) conditions. Continuous lines are fittings to Eq. 5.1.

5.3.4 Long-term exposure to ZnO- and Cu^0-NPs

ZnO- and Cu^0-NP inhibition to acetoclastic methanogens was evaluated in a series of repeated feedings to investigate their long-term effect in sulfate-containing assay conditions on methanogenesis. Figure 5.5 shows the time course of methane production at selected concentrations of ZnO-NPs and $ZnCl_2$.

The treatments supplied with >0.494 mM of ZnO-NPs and $ZnCl_2$ were highly inhibitory for methanogenesis. However, at lower concentrations (≤0.382 Zn mM), methanogenesis readily occurred (Figures 5.5A and 5.5B). Zn toxicity was stoichiometrically attenuated by 0.43 mM of biogenic sulfide as long as $\leq$ 0.43 Zn mM were supplied. The ZnS precipitates formed during the attenuation did not harm the methanogens. The highest tested concentrations of ZnO-NPs and $ZnCl_2$ (>0.43 Zn mM) gradually decreased methanogenesis until a total inhibition was reached. During these assays, the soluble Zn^{2+} concentrations observed at the end of the first feeding remained relatively constant until the last feeding (Figure 4S). A similar experiment was performed with Cu^0-NPs and $CuCl_2$.

Figure 5.5 shows the time course of methane production as function of different Cu^0-NP and $CuCl_2$ concentrations applied in sulfate-containing conditions. Low concentrations (<0.32 Cu mM) remained harmless to the methanogens after 5 feedings of acetate as evidenced by similar methane production-rates compared to the control. Conversely, mid-to-high concentrations decreased methane production during the first feeding ($\geq$ 0.39 Cu mM). However, after five feedings of acetate, the assays amended with the higher concentrations of Cu^0-NP showed a progressive recovery of methanogenesis relative to the first feeding. However, methanogenesis was completely inhibited through the multiple feedings by the highest concentration of $CuCl_2$. Additionally, mid concentrations of $CuCl_2$ were inhibitory in the buffer zone in the first feeding as a result of partial inhibition of the sulfate-reducing bacteria; however, methanogenic activity recovered over time. These findings suggest that CuS precipitate formed at low-to-mid concentrations did not harm the acetoclastic methanogens over multiple feedings. Finally, the concentration of soluble Cu dropped from the first to last feeding (Figure A.3.5). The information obtained from the long-term experiments was later used to calculate kinetic parameters according to Eq. 5.3.

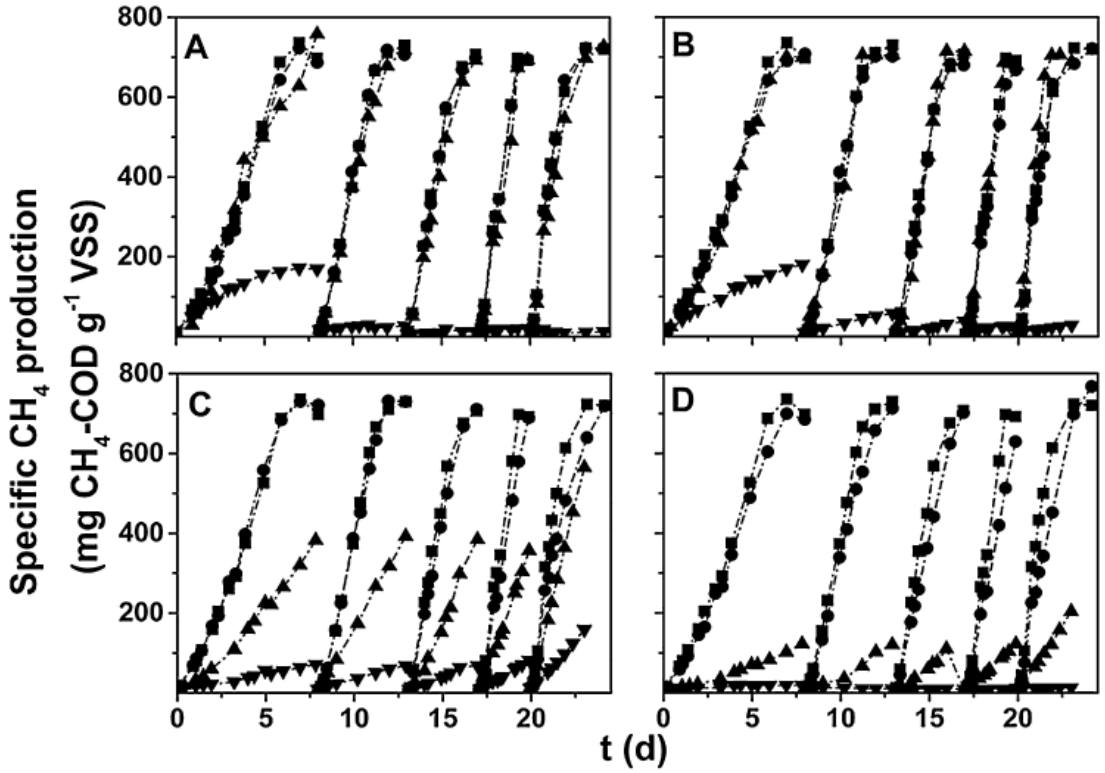

Figure 5.5 Long-term exposure of acetoclastic methanogens to ZnO-NPs (A), $ZnCl_2$ (B), Cu^0-NPs (C), and $CuCl_2$ (D) in sulfate-containing conditions. Added concentrations (mM Zn or Cu in A, B, C and D, respectively): 0 (■); 0.099, 0.153, 0.315, 0.157 (●); 0.247, 0.382, 0.787, 0.393 (▲); 0.494, 0.765, 1.180, 0.787 (▼). The standard deviation of each measurement was <5% during the whole experiment (Data not shown)

Figure 5.6 shows the calculated initial methanogenic activity (MA_o) and apparent growth rate (μ_{app}) of the assays amended with ZnO-NPs and $ZnCl_2$. Lower concentrations of Zn had a negligible inhibitory effect on MA_o, whereas the highest concentrations of ZnO-NPs and $ZnCl_2$ decreased the MA_o approximately 3-fold compared to the control (Figure 5.6A-B). The μ_{app} was not affected by supplying lower concentrations (≤0.382 mM) of Zn (within the sulfide buffer zone). Conversely, the highest concentrations of ZnO-NP and $ZnCl_2$ (outside the buffer zone) stopped the growth and caused cell death as evidenced by the negative value of μ_{app} (Figure 5.6A-B). In order to verify cell death had taken place over the prolonged exposures, the sludge was rinsed to remove Zn from the basal medium to measure the remaining methanogenic activity of the sludge (Figure A.3.6). The lost activity was not immediately

recovered by rinsing, confirming that the activity loss was due to cell inactivation. The results taken as a whole agree with toxicity attenuation by sulfide. Very little negative effect on activity (MA_o) or growth (μ_{app}) was observed at concentrations below the theoretical amount of sulfide present in the system, while a drastic decrease in the values of both kinetic parameters was observed when Zn concentrations were in excess of the biogenic sulfide. The same kinetic analysis was made for the Cu amended assays.

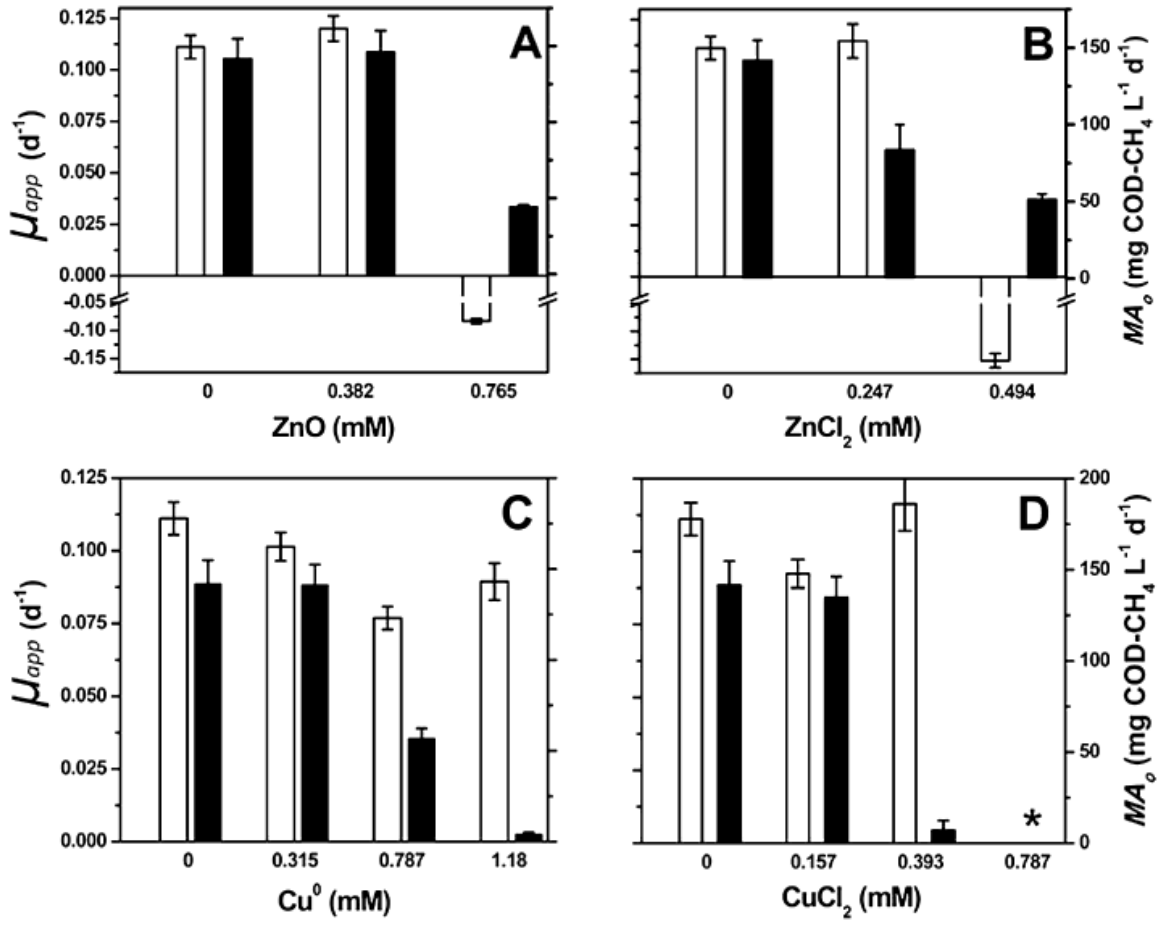

Figure 5.6 Specific apparent growth rate ($\mu_{max\text{-}app}$) (non-filled bars) and initial methanogenic activity (MA_o) (black filled bars) of the assays supplied with ZnO-NPs (A), $ZnCl_2$ (B), Cu^0-NPs (C), and $CuCl_2$ (D).

Figure 5.6 shows MA_o and μ_{app} for the assays amended with Cu^0-NPs and $CuCl_2$. Growth of methanogens occurred in all tested concentrations with the exception of the highest $CuCl_2$ concentration (0.787 mM). MA_0 decreased at the highest tested concentrations of Cu^0-NPs (>0.315mM Cu) and of $CuCl_2$ ($\geq$0.39 mM) (Figure 5.6C-D). In three out of four cases, growth of methanogens was evident even after noteworthy inhibition of the MA_0, suggesting attenuation of Cu inhibition over time, including conditions where Cu was in excess of biogenic sulfide. This enabled regrowth of methanogens as evidenced by the progressive recovery in activity over time. (Figure 5.5C and Figure 5.6C).

5.4 Discussion

5.4.1 Main findings

Biogenic sulfide attenuated ZnO- and Cu^0-NPs toxicity to acetoclastic methanogens. The results indicate that biogenic sulfide produced by sulfate-reduction decreased toxicity of ZnO-NPs by 14-fold, whereas the toxicity of Cu^0-NPs was decreased by approximately 7-fold. Zn toxicity was stoichiometrically attenuated by the theoretical biogenic sulfide expected from added sulfate. Conversely, Cu toxicity was only attenuated in part since inhibition of the sulfate reducing bacteria prevented full conversion of added sulfate to sulfide. Release of metal ions in sulfate-free conditions resulted in methanogenic inhibition. A kinetic analysis, based on the residual soluble Zn and Cu concentration as the active inhibitor confirmed that the soluble ions were well-correlated with toxicity. Long-term experiments indicated that concentrations of ZnO-NPs in excess of the theoretical sulfide are more toxic over the long- versus short-term, whereas Cu^0-NPs in excess of sulfide exhibited more toxicity in short-term assays, but recovered after extended incubations due to regrowth of methanogens facilitated by prolonged loss of soluble Cu concentration by other ligands in addition to sulfide.

5.4.2 Attenuation of metal toxicity by sulfide

Toxicity of Zn and Cu salts to methanogens is well-documented (Chen et al., 2008). Biogenic sulfide produced by sulfate-reduction has been applied to precipitate soluble toxic ions. Lawrence and McCarty (1965) decreased Zn and Cu toxicity to methanogens by the formation of biogenic sulfide from $ZnSO_4$ and $CuSO_4$. Additionally, direct application of Na_2S prevented the toxicity effect of $ZnCl_2$ or $CuCl_2$ and restored to some extent the activity of an inhibited methanogenic culture.(Jin et al., 1998; Zayed & Winter, 2000) Thus, direct addition of either sulfide or biogenic sulfide provided effective attenuation of heavy metal toxicity.

The results of our study indicated Cu inhibition of sulfate reduction which decreased the attenuation capacity, resulting in methanogenic inhibition at concentrations within the theoretical sulfide buffered zone (<0.43 mM). Other studies have found Zn and Cu toxicity to different cultures of sulfate-reducing bacteria (Karri et al., 2006; Sani et al., 2001; Utgikar et al., 2003). Thus, attenuation of metal toxicity by biogenic sulfide also depends on metal toxicity sulfate-reducers.

5.4.3 Mechanisms of NPs toxicity attenuation

Recent studies found that ZnO- and Cu^0-NPs were more toxic to methanogens than their bulk particle analogues (Luna-delRisco et al., 2011) and suggested soluble ions released by NPs as the toxicity mechanism (Gonzalez-Estrella et al., 2013; Mu et al., 2011). Recently sulfide was applied to attenuate up to 80% of Ag NP toxicity to nitrifying organisms due to the formation of Ag_2S precipitates (Choi et al., 2009). Our study demonstrated that conditions favoring biogenic sulfide formation attenuated ZnO- and Cu^0-NP toxicity to methanogens.

In our study, biogenic sulfide was the result of sulfate reduction by endogenous substrates as electron-donors. Acetate, the main substrate of the methanogenic activity assays, did not stimulate biogenic sulfide formation, while H_2 did (Figure A.3.4). Acetate can be a suitable electron-donor for sulfate-reducers, but only after long periods of microbial enrichment when utilizing methanogenic biofilms (Omil et al., 1998). There is evidence that endogenous biomass decay of granular sludge provided electron-donors for hexavalent uranium bioreduction (Tapia-Rodriguez et al., 2010). Thus, it conceivably can also support sulfate-reduction.

Precipitation of Zn and Cu as ZnS and CuS is a probable attenuation mechanism. Dissolution and corrosion of ZnO and Cu^0 is likely in anaerobic conditions; ZnO-NPs release Zn^{2+} ions mainly by dissolution (Lombi et al., 2012; Mu et al., 2011), whereas Cu^0 corrodes in presence of H^+ into Cu^{2+} (Ollila, 2013). Another possible attenuation mechanism that stops the release of ions by the formation of a metal-sulfide layer on the surface of NPs is passivation (Ma et al., 2013a). Sulfidation led to the decrease of solubility, change on surface charge and aggregation of ZnO and Ag^0 NPs. Recently, Ma et al. (Ma et al., 2013b) demonstrated that ZnO NP rapidly dissolved into Zn^{2+} soluble. Their findings confirmed that ZnO NPs dissolve in anaerobic conditions in a circumneutral pH. They also witnessed that sulfide effectively decreased the soluble fraction of Zn^{2+} as we have observed in the present study. They hypothesize that these changes could affect the fate and toxicity of ZnO NPs. Lombi et al. (2012) suggested that ZnO-NPs were rapidly dissolved and subsequently transformed by precipitation/complexation reactions into ZnS or thiol ligands (modeled by cysteine). Their results showed that 80% of the Zn from NPs was transformed to ZnS after 10 days of anaerobic digestion. Therefore, in our study the formation of low soluble ZnS and CuS (log Ks_0 = -21.9 for ZnS and log Ks_0 = -35.96 for CuS (Benjamin, 2002)) in the liquid media or on the surface of the NPs in sulfate-containing conditions decreased the bioavailability of the toxic soluble ions, whereas sulfate-free assays allowed higher concentrations of toxic metal ions. If true, ZnO- and Cu^0-NP toxicity should be highly correlated with freely soluble metal ions in the media, irrespective of their origin.

Also secondary minerals formed from corrosion/dissolution of NP such as metal carbonates or hydroxides formed may be more bioavailable than sulfides and this too may have a role in the toxicity outcome.

The *Ki* obtained from the kinetic evaluation of inhibition as a function of the soluble metal was very similar in value regardless of the source being ZnO-NP or $ZnCl_2$ either in sulfate-containing or free conditions. This was also true in the case of Cu in three out of four conditions. The *Ki* using residual soluble Zn or Cu as the inhibitors in tested conditions overall show more similarity between each other than if the same comparison is made with *Ki* obtained from the Zn or Cu added (Table 1). The similarities found between *Ki* of the assays using the residual soluble metal suggest that the soluble ions are the likely responsible agents for the toxicity to methanogens either in sulfate-containing or sulfate-free conditions. The behavior of outlier may be explained by difference in bioavailability of the residual solids such as passivated ZnO and Cu^0 NP surfaces. These reactions can result in different flux of ions released from the NP surface (Ma et al., 2013b). The inhibition order "*n*" also provides important insight into attenuation caused by sulfide.

Inhibition order becomes larger when the toxic response is steeper, providing a "cliff-like" shape in response curves. When evaluating sulfate-containing experiments plotted as a function of added metal concentration, Zn experiments provide graphs with steep cliff-like characteristics (*n* = 11.5 to 33.9) precisely as the concentration of Zn exceeds the sulfide buffer-capacity. These *n* values are up to 5.5-times higher than the experiments with Cu, which have curves shaped like "slopes" rather than "cliffs". The reason for the difference is that sulfate reduction was inhibited by Cu such that the actual level of sulfide buffering was an array of concentrations depending on the Cu concentration added. In such a scenario, there is no sharp point where the metal concentration exceeds sulfide. In graphs plotting activity as a function of the residual soluble metal concentration, cliff-like characteristics (*n* = 21.3 to 41.0) are also

evident from Zn in both sulfate-containing and sulfate-free experiments with ZnO-NPs. These findings suggest that Zn toxicity is tolerated up to a threshold determined by the sulfide buffer zone.

Long-term experiments provided important information about Zn and Cu toxicity as each distinctly affected the methanogens. Such differences may be explained by ZnO- and Cu^0-NP interactions with the liquid media and with the anaerobic sludge. Although Lombi et al. (Lombi et al., 2012) demonstrated that ZnO-NPs were rapidly transformed to ZnS, if sulfide was limiting, a fraction of the nanoparticles could accumulate in the sludge as ZnO-NPs, which consequently could allow the release of high localized toxic ion concentrations. A recent study that explored long time exposure of sludge to ZnO-NPs observed accumulation of ZnO-NPs in the sludge by scanning electron microscopy. This accumulation provided a constant source of Zn ions for the sludge that gradually inhibited the methanogens (Mu & Chen, 2011). Additionally, the results obtained by Otero-Gonzalez et al. (Otero-González et al., 2014a) demonstrated that long-term exposure to low concentrations of ZnO-NPs (0.005 mM) gradually inhibited acetoclastic methanogens. These results confirm the progressive inhibitory effect of Zn on methanogens.

Once Zn is in direct contact with the methanogen, it can potentially enter the cell by the unspecific inorganic transporter (CorA) that carries Mg in Archea organisms (Nies, 1999), or can be bound by a protein responsible for Mn uptake (McDevitt et al., 2011). Zn ions could interfere with the transmembrane electrochemical proton gradient, a driver for ATP synthesis (Lee et al., 2011a). Furthermore, some heavy metals can bind with thiol groups, part of the structure of coenzyme M (HS-CoM) and coenzyme B (HS-CoB) whih play a critical role in the last steps of methanogenesis (Deppenmeier, 2002; Nies, 1999). Therefore, prolonged contact with ZnO-NPs and $ZnCl_2$ may have allowed chronic toxicity by several mechanisms that gradually caused severe toxicity to methanogens.

Conversely, assays amended with Cu^0-NP in excess of sulfide more strongly affected methanogens in the short-term; however, methanogenic activity recovered over time due to cell regrowth. Cu toxicity is typically caused by the production of hydroperoxide radicals and interactions with the cell membrane (Nies, 1999). However, this mechaninism may be less important in anaerobic conditions. Cu^{2+} could also be taken up by CorA (Nies, 1999); nonetheless, Cu^{2+} is less likely to be sorbed as strongly as Zn^{2+} by sludge (Wang et al., 2003). These differing interactions were evidenced by the decrease of soluble of Cu and constant soluble Zn over the course of five feedings of acetate (Figure A.3.5). Thus, Cu^{2+} may have progressively precipitated as hydroxides, carbonates, and/or phosphates such as $Cu(OH)_2$, $Cu_2(OH)_2CO_3$, $CuCO_3$ or $Cu(PO_4)_2$ $(H_2O)_3$ with solubility products log K_{s0} of -19.36, -20.38, -33.18, -9.36,-35.12, respectively (Benjamin, 2002).

Long-term experiments provided kinetic information regarding ZnO- and Cu^0-NP toxicity to methanogens. Growth constants of non-inhibited acetoclastic methanogens agreed with values reported in the literature for *Methanosaete* (0.05-0.192 d^{-1}) (Conklin et al., 2006; Dezeeuw, 1985). Likewise, the assays amended with Cu^0-NPs that were initially highly inhibitory sustained regrowth of methanogens once soluble copper was attenuated. The growth constants during regrowth are also similar to those reported *Methanosaete* values, which supports a mechanism of growth recovery of methanogens. Finally, long-term exposure experiments demonstrated that biogenic sulfide protected methanogenesis against Zn and Cu toxicity, which evidenced that metal sulfides were stable and non-inhibitory for methanogens over time.

5.5 Conclusions

Biogenic sulfides are an effective attenuator of ZnO- and Cu^0-NP toxicity to acetoclastic methanogens. Residual soluble metal ions are strongly correlated with the toxicity independent of their source (NP or salt) in the presence or absence of sulfide. Since Zn is less toxic to sulfate-reducers than methanogens; Zn toxicity can be stoichiometrically attenuated by sulfate. Conversely, Cu inhibits sulfate-reducers; thus, methanogens can be only partially protected due to less than stoichiometric biogenic sulfide production. Metal sulfides remain stable over time; consequently, the effect of biogenic sulfide on preventing ZnO- and Cu^0-NP methanogenic toxicity was sustainable over time. A prolonged exposure of ZnO-NPs and $ZnCl_2$ in excess of biogenic sulfide caused cell death. Conversely, Cu^0-NPs and $CuCl_2$ caused immediate acute toxicity, but methanogens recovered after prolonged loss of soluble Cu under most conditions as evidenced by regrowth rates comparable to the control and in the range expected for *Methanosaete*. The results taken as a whole establish that biogenic sulfide can be successfully used as a strategy to decrease the toxicity caused by ZnO- and Cu^0-NPs.

5.6 Acknowledgments

This work was supported by the Semiconductor Research Corporation (SRC)/Sematech Engineering Research Center for Environmentally Benign Semiconductor Manufacturing. Gonzalez-Estrella was partly funded by CONACyT.

CHAPTER VI- IRON SULFIDE ATTENUATES THE METHANOGENIC TOXICITY OF ELEMENTAL COPPER AND ZINC OXIDE NANOPARTICLES AND THEIR SOLUBLE METAL ION ANALOGS

Jorge Gonzalez-Estrella[a]*, Sara Gallagher[a], Reyes Sierra-Alvarez[a], Jim A. Field[a]

[a]Department of Chemical and Environmental Engineering, University of Arizona,

P.O. Box 210011, Tucson, AZ 85721, USA

*Corresponding author: Jorge Gonzalez-Estrella

Department of Chemical and Environmental Engineering

The University of Arizona,

P.O. Box 21011, Tucson, AZ 85721, United States

Phone: +1-520-621 6162

E-mail: jorgegonzaleze@email.arizona.edu

Abstract

Elemental copper (Cu^0) and zinc oxide (ZnO) nanoparticles (NPs) are strong inhibitors of methanogens, which are microorganisms that play a key role during the stabilization and degradation of bio-solids in anaerobic digesters. The toxicity caused by Cu^0 and ZnO NPs to methanogens has been associated with the release of soluble ions from these NPs. Iron sulfide (FeS) plays a key role controlling the concentration of heavy metals in aquatic sediments through displacement of the Fe from FeS which consequently results in the formation of low solubility heavy metal sulfides. As a consequence, FeS also controls the toxicity caused by heavy metals in these environments. Therefore, if the toxicity of Cu^0 and ZnO NPs is caused by the release of soluble ions, then FeS would be expected to attenuate the toxicity of these ions to methanogens. This work studied the role of FeS in attenuating the methanogenic toxicity of Cu^0 and ZnO NPs and their soluble salt analogs. Fine (FeS-f, 25-75 μm) and coarse (FeS-c, 500-1200 μm) preparations of FeS were synthetized and their toxicity attenuating capacity was tested in the presence of highly inhibitory concentrations of $CuCl_2$, $ZnCl_2$ Cu^0 and ZnO NPs. FeS-f attenuated methanogenic toxicity better than FeS-c. The results revealed that 2.5× less FeS-f than FeS-c was required to recover the methanogenic activity to 50%. The results also indicated that a molar ratio FeS-f/Cu^0, FeS-f/ZnO, FeS-f/Zn Cl_2, and FeS-f/$CuCl_2$ of 3, 3, 6, and 12 respectively, was necessary to provide a high recovery of methanogenic activity (>75%). Displacement experiments demonstrated that $CuCl_2$ and $ZnCl_2$ partially displaced Fe from FeS. Taken collectively the results indicate that not all the sulfide in FeS was readily available to react with the soluble Cu and Zn ions which may explain the need for a large stoichiometric excesses of FeS to fully attenuate Cu and Zn toxicity. Overall, this study provides evidence that FeS attenuates the toxicity caused by Cu^0 and ZnO NPs and their soluble ion analogs to methanogens.

Keywords: Nanomaterials, Elemental copper, Zinc Oxide, Toxicity attenuation, anaerobic digestion, inhibition constants

6.1 Introduction

Engineered nanoparticles (NPs) are man-made materials with at least one dimension <100 nm. Copper-based (Cu-based) and zinc oxide (ZnO) NPs are applied in several industrial processes or commercial products. Cu-based NPs are used in products such as wood preservatives, catalysts, printable electronics, or antimicrobials (Wang et al., 2013); likewise, Cu-based NPs are the byproduct of the chemical and mechanical polishing (Golden et al., 2000). ZnO NPs are also applied in industrial processes and extensively used in consumer products such as sunscreens, cosmetics, and bottle coatings due to their ultraviolet blocking properties and visible transparency (Klaine et al., 2008).

The majority of NPs applied in consumer products are likely to be disposed into the sewer (Kim, 2014); therefore, NPs will end up in biological processes such as aerobic activated sludge of wastewater treatment plants. Studies investigating the fate of NPs in wastewater treatment have found accumulation of NPs in activated sludge (Westerhoff et al., 2013). The accumulation of NPs may have toxic effects not only to the activated sludge microorganisms, but also in the microbial cultures involved in the stabilization of the waste sludge by anaerobic digestion, such as methanogens.

Recent research has consistently shown that elemental copper (Cu^0) and ZnO NPs are toxic to methanogens (Gonzalez-Estrella et al., 2015; Gonzalez-Estrella et al., 2013; Mu et al., 2012; Otero-González et al., 2014a). Results have also indicated that the soluble ions released by NPs cause toxicity.(Luna-delRisco et al., 2011; Mu et al., 2011) Recently it was shown that biogenic sulfide (S^{2-}) produced by sulfate reduction decreased the toxic effect of Cu^0 and ZnO NPs (Gonzalez-Estrella et al., 2015). Soluble ions released from these types of NPs are hypothesized to precipitate with the sulfide. These findings establish that biogenic S^{2-} from sulfate reduction reliably attenuate Cu^0 and ZnO NP toxicity to methanogens. Other potential sources of S^{2-} present in anaerobic environments may also play a similar attenuating role.

The oxidization of organic matter in anaerobic environments provides the conditions for the bio-reduction of sulfate and Fe(III) (Morse et al., 1987) yielding S^{2-} and Fe^{2+} which react with each other to form iron sulfide (FeS) and pyrite (FeS_2) (Haaijer et al., 2012; Morse et al., 1987). FeS is a poorly soluble mineral (log K_{s0} =-16.84 (Benjamin, 2002)). FeS is subject to reactions with other metals (Besser et al., 1996). For example, if divalent metals with more affinity for S^{2-} such as cadmium, copper, lead, mercury, or zinc are present in anaerobic sediments, the Fe^{2+} of FeS can be displaced by these divalent metals forming more stable metal sulfides and releasing Fe^{2+} cations to the aqueous phase (Peng et al., 2009). For example, Cu^{2+} and Zn^{2+} have higher stability for sulfide (CuS (log K_{s0} =-35.96) and ZnS (log K_{s0} =-21.97) (Benjamin, 2002)) than FeS. Previous studies have demonstrated the immobilization of Cd, Cu, and Zn by reaction with FeS (Simpson et al., 2000). The mechanism is illustrated in Eq.1

$$FeS + Me^{2+} \rightarrow MeS + Fe^{2+} \quad [6.1]$$

where Me^{2+} are heavy metals such as Cu^{2+} or Zn^{2+}. Therefore, if the toxic Cu^{2+} and Zn^{2+} ions released by Cu^0 and ZnO nanoparticles displace the Fe^{2+} in FeS to form stable metal sulfides, Cu^0 and ZnO toxicity can be expected to be attenuated by FeS. The purpose of this work was to evaluate the attenuation of Cu^0 and ZnO toxicity to methanogens by FeS.

6.2 Material and Methods

6.2.1 Chemicals

Cu^0-NPs (40-60 nm, 99%) were purchased from Sky-Spring Nanomaterials Inc. (Houston, TX), ZnO-NPs (100 nm, 99%), $CuCl_2 \bullet H_2O$ (99%), $ZnCl_2$ (98%), sodium acetate (99.9%), and $Na_2S \cdot 9H_2O$ (>98%) were acquired from Sigma Aldrich (St. Louis, MO, USA). $FeCl_2 \cdot 4H_2O$ (>99%) was acquired from Fisher-Scientific. CH_4 standard gas (99%) was acquired from Air Liquid America (Plumstedsville, PA, USA).

6.2.2 Nanoparticle dispersions and metal solutions

ZnO- and Cu^0-NP stock dispersions were sonicated (DEX® 130, 130 Watts, 20 kHz, Newtown, CT) at 70% amplitude for 5 min. ZnO- and Cu^0-NP stability in anaerobic media has been previously described (Gonzalez-Estrella et al., 2013). Stock $CuCl_2$ and $ZnCl_2$ solutions were prepared by dissolving the salts in 0.01 M HCl.

6.2.3 FeS synthesis and characterization

FeS was synthesized by adapting a methodology previously used (Patterson et al., 1997). FeS was prepared by mixing an equimolar concentration of sodium sulfide and iron chloride ($FeCl_2$) for 10 min. Next, the suspension was centrifuged in 50 mL vials at 4000 rpm for 20 min. The supernatant was discarded and the pellet of FeS was resuspended with ~50 mL ethanol. Subsequently, the suspension was subjected twice to centrifuging (4000 rpm for 20 min) and rinsing procedure to eliminate the majority of the water. Next, the supernatant was discarded and the pellet was rapidly transferred to test tubes. The test tubes were sealed and flushed with N_2 gas until the pellet was completely dry. After drying the pellet, the product was composed of a coarse preparation of FeS particles (FeS-c). Half of the FeS-c was agitated in the test tube vigorously with a vortex mixer until the particle size was decreased to a fine preparation of FeS particles (FeS-f). The synthetized FeS preparations were kept in sealed flask with N_2 atmosphere to prevent oxidation. The particle size of FeS-c and FeS-f particles was evaluated by SEM analyses. The images of the SEM analyses of FeS-c and FeS-f are shown in Figure 6.1. The analyses indicated that FeS-c had a particle size range of 500 to 1200 μm, whereas the range FeS-f particles were 25-75 μm. It should be noted that a few coarse pieces of FeS can be observed in FeS-f as shown in Figure 6.1B. A sample of each fraction was characterized by scanning electron microscopy (SEM) and X-ray diffraction (XRD) analyses. XRD analysis revealed an amorphous composition by the lack of clear X-ray diffraction signals in the samples.

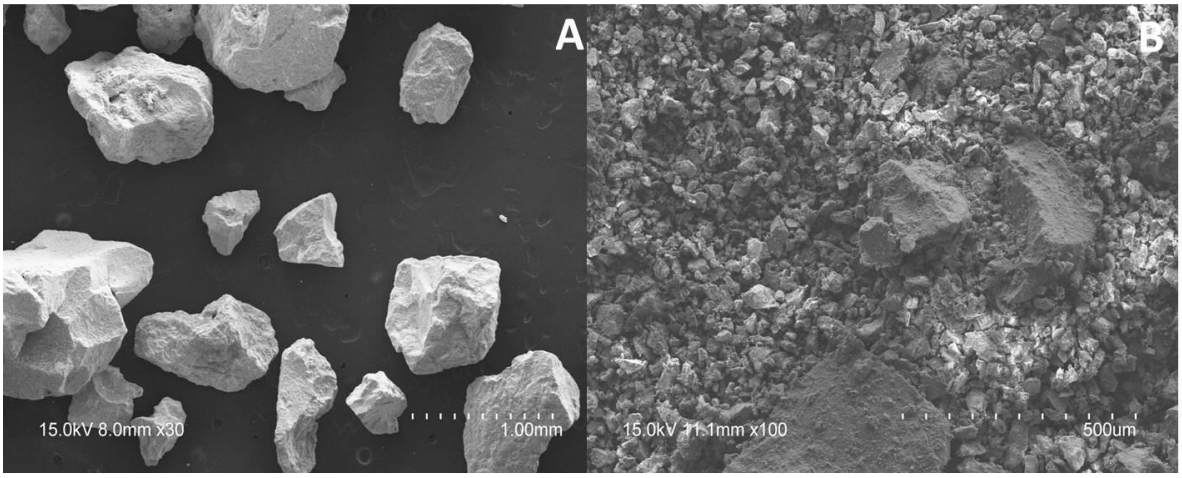

Figure 6.1 SEM analysis of FeS-c (A) and FeS-f (B). The whole scale bar represent an scale of 1.0 and 0.5 mm in panel A and B, respectively.

6.2.4 Anaerobic sludge

Anaerobic granular sludge was obtained from a full-scale upflow anaerobic sludge bed reactor treating brewery wastewater (Mahou, Guadalajara, Spain). The sludge was stored at 4 °C. Volatile suspended solids (VSS) were 7.0% of the wet weight. The maximum acetoclastic methanogenic activity determined was 280.5 $\pm$10.1 mg CH_4-COD g^{-1} VSS d^{-1}.

6.2.5 General bioassay description

Table 6.1 describes the specific sludge concentration, range of FeS concentration used, and metal salt or NP applied as an inhibitor in each bioassay performed. All experiments were performed in 160 mL serum bottles in a sulfate-free basal medium containing (mg L^{-1}): NH_4Cl (280), $NaHCO_3$ (3,000), K_2HPO_4 (250), $CaCl_2 \bullet 2H_2O$ (10), $MgCl_2 \bullet 6H_2O$ (183), and yeast extract (100) with 1 mL L^{-1} of trace elements previously described in Gonzalez-Estrella et al. (2013). All bottles were flushed with N_2/CO_2 (80:20, v/v) and incubated at 30 ± 2 °C in an orbital shaker at 115 rpm. The bioassays were provided with three feedings of sodium acetate (1 g chemical oxygen demand (COD) L^{-1} each). The second and third acetate feedings were provided after the control reached the expected methane production (1.0 g CH_4-COD

produced L^{-1} liquid). Methane samples (100 µL) were taken from the headspace several times during the incubation. All experiments included a control free of toxic metals in order to have a reference of the control specific methanogenic activity. The treatments also included a control amended with only FeS to investigate the toxic effect of FeS on the methanogenic activity.

Table 6.1 Experimental design

Experiments	Sludge concentration (g VSS L^{-1})	FeS Coarse (mM)	FeS Fine (mM)	Inhibitor (mM)
Effective 50% attenuation concentration	1.5	0.6-3.6	0.2-2.4	$CuCl_2$ and $ZnCl_2$ (0.05-0.6)
Effect on K_i values	1.5	1.8	0.6	$CuCl_2$ and $ZnCl_2$ (0.2)
NP toxicity attenuation	1.5	----	Cu^0 assays (0.24 and 0.72) ZnO assays (0.18 and 0.54)	Cu^0 NP (0.24) ZnO NP (0.18)
Effect of long-term FeS pre-exposure to NPs and salts before sludge addition	1.5	----	$CuCl_2$ and $ZnCl_2$ assays (0.6) Cu^0 assays (0.72) ZnO assays (0.54)	$CuCl_2$ and $ZnCl_2$ (0.2) Cu^0 NP (0.24) ZnO NP (0.18)
FeS displacement	----	----	1	$CuCl_2$ and $ZnCl_2$ (0.25-2.0)

Specific methanogenic activities (SMA) were calculated as the maximum specific methanogenic rate using linear regression for each four or more consecutive points that represented at least 50% of the substrate consumption. The normalized methanogenic activity (NMA) was calculated as follows:

$$NMA(\%) = \left(\frac{SA_t}{SA_c} \right) \cdot 100 \qquad [6.2]$$

where SA_t and SA_c are the specific activities of the treatment and control experiments, respectively.

The details and objectives of each bioassay performed are described below.

6.2.5.1 Attenuation of $CuCl_2$ and $ZnCl_2$ methanogenic toxicity by FeS

The experiments were performed with the objective of determining the effect of FeS on the attenuation of $CuCl_2$ and $ZnCl_2$ toxicity to methanogens. Our previous study indicated >90% loss of the methanogenic activity in a sulfate-free medium by 0.2 mM of $CuCl_2$ and $ZnCl_2$ (Gonzalez-Estrella et al., 2015). Therefore, a concentration 0.2 mM of both $CuCl_2$ and $ZnCl_2$ was selected for this experiment. The bioassays were pre-incubated overnight at the conditions described in section 6.2.5 with a range of FeS concentrations (Table 6.1). After pre-incubation, 0.2 mM of $CuCl_2$ or $ZnCl_2$ were provided to the bottles, the bottles were reflushed with the N_2/CO_2 gas mix, and CH_4 production was monitored over the course of the experiment. Finally, with that information the concentration of FeS-c and FeS-f that recovers the NMA to 50% (R-NMA_{50}) was estimated.

6.2.5.2 Impact of FeS on the inhibition constants

A series of concentrations of $CuCl_2$ and $ZnCl_2$ were provided to quantify the inhibition effect on the NMA by the calculating inhibition constant (K_i). The K_i was calculated as follows:

$$NMA = NMA_{\max} \cdot \frac{1}{1+\left(\frac{I}{K_i}\right)^n} \qquad [6.3]$$

where NMA_{max} is the maximum NMA (%), I and K_i are the inhibitor (metal) concentration and inhibition constant, respectively (mM), and n is the inhibition order (dimensionless). The interpretation of each variable has been previously described in (Gonzalez-Estrella et al., 2015).

A parallel experiment with the same concentrations of inhibitors and with the R-NMA_{50} concentration (0.8 and 0.6 mM of FeS-c and FeS-f, respectively) was performed to investigate the impact of the R-NMA_{50}

on the K_i. After overnight pre-incubation of FeS, a range of concentrations of $CuCl_2$ and $ZnCl_2$ (described in Table 6.1) were provided to the bottles.

6.2.5.3 Attenuation of NP toxicity

The experiments were performed with the objective of studying the effect of FeS-f on the attenuation of highly inhibitory concentrations of Cu^0 and ZnO NPs. Our previous study indicated >85% loss of the methanogenic activity in a sulfate-free medium by 0.18 and 0.24 mM of Cu^0 and ZnO, respectively (Gonzalez-Estrella et al., 2015). Thus, concentrations of 0.18 mM Cu^0 NPs and 0.24 mM of ZnO NP mM were selected for this experiment. The bioassays were pre-incubated overnight at the conditions with the FeS concentrations (described in Table 6.1). After pre-incubation, 0.24 and 0.18 mM of Cu^0 and ZnO NPs were provided to the bottles, respectively.

6.2.5.4 Effect of long-term FeS pre-exposure to NPs and salts before sludge addition

The experiments were carried out to determine if a long-term pre-exposure FeS-f to highly inhibitory concentrations of Cu^0 NPs, ZnO NPs, $CuCl_2$ and $ZnCl_2$ would increase the toxicity attenuation effect of FeS. For that purpose, different concentrations (Table 6.1) of Cu and Zn (NPs and salts) were pre-exposed to a concentration of FeS which corresponded to an stoichiometric ratio FeS/Me=3 for five days in the absence of sludge. After five days of exposition of the metals to FeS, the sludge and electron donor were added to initiate the assay.

6.2.6 Fe displacement mechanism

This experiment was performed to demonstrate that FeS releases Fe^{2+} cations by a displacement mechanism by soluble Cu^{2+} and Zn^{2+} cations. The assays were performed in deionized water (pH 6 adjusted with HCl) with concentrations of FeS-f, $CuCl_2$, and $ZnCl_2$ described in Table 6.1. Liquid samples (1.4 mL) were taken after 2, 24, and 120 h. The samples were filtered through a 0.4 µm filter and immediately

acidified with concentrated HNO_3. The samples were later analyzed by inductively coupled plasma optical emission spectrometry (ICP-OES) to determine the content of soluble Fe, Cu, and Zn. If the displacement mechanism were important, S^{2-}should not have been significantly released from the FeS; to ensure that this was the case, the soluble concentration of sulfide was also measured.

6.2.7 Analytical methods

Methane was quantified by gas chromatography with flame ionization detection (Hewlett Packard 5890 Series II). The GC was fitted with a Nukol fused silica capillary column (30 m length, 0.53 mm ID, Supelco, St. Louis, MO). Details of the measurement parameters are described in Karri et al. (2006). Analysis of soluble metals by inductively coupled plasma-optical emission spectroscopy (ICP-OES Optima 2100 DV, Perkin–Elmer TM, Shelton, CT). The wavelengths used for ICP-OES analysis of were 324.754, 259.940, and 206.200 for Cu, Fe and Zn, respectively. All samples were centrifuged at 13,000 rpm and filtered (0.4 µm VSWP, Millipore, Billerica, MA, USA), acidified with concentrated HNO_3 and frozen prior ICP analysis.

6.3 Results

6.3.1 FeS attenuation of methanogenic inhibition caused by $CuCl_2$ and $ZnCl_2$ salts

A range of FeS-c and FeS–f concentrations of were supplied to attenuate the methanogenic toxicity over three feedings of acetate. Figures 6.2A and 6.2C show the NMA response as a function of increasing concentrations of FeS in presence of 0.2 mM of $CuCl_2$. $CuCl_2$ decreased the NMA to <10% in the absence of FeS. However, the NMA activity was recovered by FeS-c and FeS-f over three feedings of acetate. FeS-c attenuated $CuCl_2$ toxicity by recovering the NMA to 20-100% when supplying molar ratios of FeS-c/Cu of 4.5 to 36, respectively (Figure 6.2A). Similarly, FeS-f attenuated $CuCl_2$ toxicity by recovering the NMA to 25-75% with added molar ratios (FeS-f/Cu) from 1 to 12, respectively. Neither FeS-c nor FeS-f caused

toxicity to methanogens during the 3rd feeding of acetate (Figure A.4.1). Additionally, $CuCl_2$ did not impart its full toxicity impact until the second feeding, necessitating comparisons of the NMA in the 2nd and 3rd feeding to appreciate the full scope of the FeS attenuation effect. The lowest FeS concentrations tested improved the NMA in the latter two feedings compared to the $CuCl_2$-only treatments. The attenuation effect increased in the second and third feedings of acetate when stoichiometric ratios FeS-c/Cu$\geq$9 were supplied; whereas the attenuation was more immediate with FeS-f. The concentration required to restore 50% of the NMA (R-NMA_{50}) were estimated from interpolation of the response curves in Figures 6.2A and 6.2C. The R-NMA_{50} estimated values were 1.5 and 0.6 mM for FeS-c and FeS-f, respectively. These results indicated that a lower molar ratio of FeS/Cu was required when FeS-f was added to attenuate $CuCl_2$ toxicity to methanogens compared to FeS-c. Overall, the results revealed that FeS attenuated $CuCl_2$ toxicity. An analogous experiment was carried out by supplying $ZnCl_2$ as the inhibiting metal.

Figure 6.2B and 6.2D shows the NMA as a function of increasing concentrations of FeS in presence of 0.2 mM of $ZnCl_2$. The NMA decreased to <15% when $ZnCl_2$ was added in absence of FeS. Nevertheless, FeS decreased the toxicity of $ZnCl_2$ to methanogens successfully over three feedings of acetate. FeS-c increased the NMA from 25 to 100% with added molar ratios FeS-c/Zn concentrations from 4.5 to 36 (Figure 6.2B). Likewise, Figure 6.2D shows that FeS-f attenuated $ZnCl_2$ toxicity by increasing the NMA to 23-98% with added molar ratios FeS-f/Zn 1 to 12. At concentrations less than 1 mM FeS, $ZnCl_2$ did not incur its full impact until the 3rd feeding; whereas at concentrations greater than 1 mM FeS, the full attenuation impact of $ZnCl_2$ was also not evident until the 3rd feeding. Thus the most prudent comparisons of the FeS attenuation effect of $ZnCl_2$ toxicity should be based on those of the 3rd feeding. The lowest FeS-f concentration tested (FeS-f/Zn=1) significantly improved the NMA in the 2nd and 3rd feedings compared to the $ZnCl_2$ only treatments. A similar significant effect required a much higher concentration of FeS-c (FeS/Zn=10). The estimated R-NMA_{50} for attenuating the $ZnCl_2$ methanogenic inhibition was observed to be 2.0 and 0.8 mM of FeS-c and FeS-f, respectively, which also indicated that a lower FeS/Zn was needed

when FeS-f was added to attenuate $ZnCl_2$ to the same extent (Figure 6.2B and 6.2D). Thus, these results confirmed that FeS attenuates $ZnCl_2$ toxicity effectively. Finally, after determining the R-NMA_{50} for $CuCl_2$ and $ZnCl_2$, a corresponding concentration of 1.8 and 0.6 mM of FeS-c and FeS-f was selected for further attenuation experiments since these concentrations corresponded approximately to the R-NMA_{50} values for $CuCl_2$ and $ZnCl_2$.

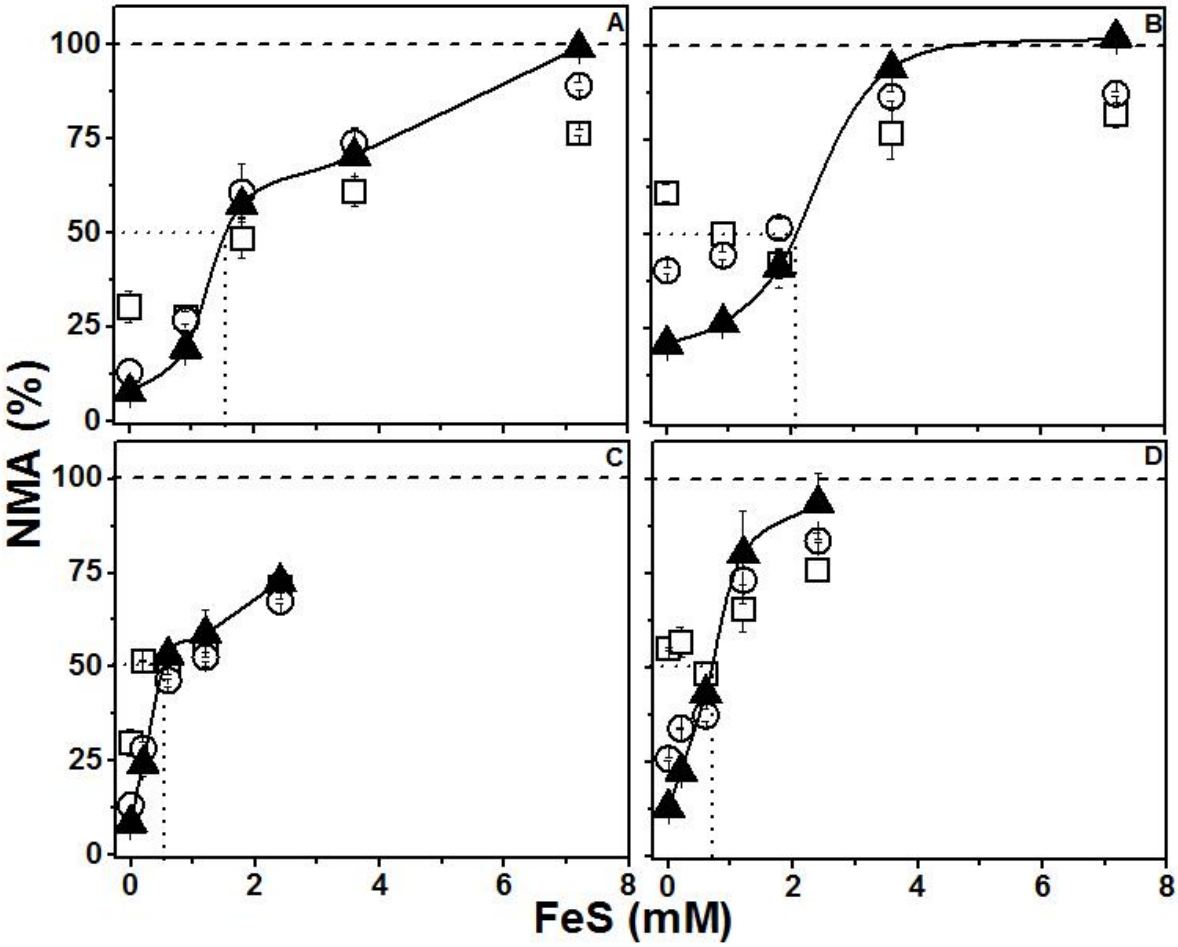

Figure 6.2 $CuCl_2$ (A and C) and $ZnCl_2$ (B and D) toxicity attenuation by coarse FeS (top panels) and fine FeS (bottom panels) in the 1st Feeding (□), 2nd feeding (○), and 3rd feeding (▲) of acetate. The solid trend line represents the response of the NMA of the third feeding, the dotted line represents the 50% toxicity attenuation concentration of FeS, and the dashed line represents the NMA activity of the control without metals or FeS.

6.3.2 Impact of FeS on the K_i

A range of increasing concentration of $CuCl_2$ and $ZnCl_2$ was supplied to evaluate the effect FeS on the K_i estimated from the third acetate feeding. Figure 3 shows the calculated K_i of $CuCl_2$ and $ZnCl_2$ in presence and absence of FeS of after three feedings of acetate. Addition of 1.8 mM FeS-c increased the K_i values of both $CuCl_2$ and $ZnCl_2$ by approximately 2-fold (Figure 6.3A). Addition of 0.6 mM of FeS-f increased the *K*i values of $CuCl_2$ and $ZnCl_2$ by 1.3 and 2.2-fold respectively (Figure 6.3B). Both observations demonstrated that the estimated R-NMA_{50} values used in these experiments have a beneficial effect by doubling the K_i value (decreasing the toxicity 2-fold) of both metal salts in almost all of the assays.

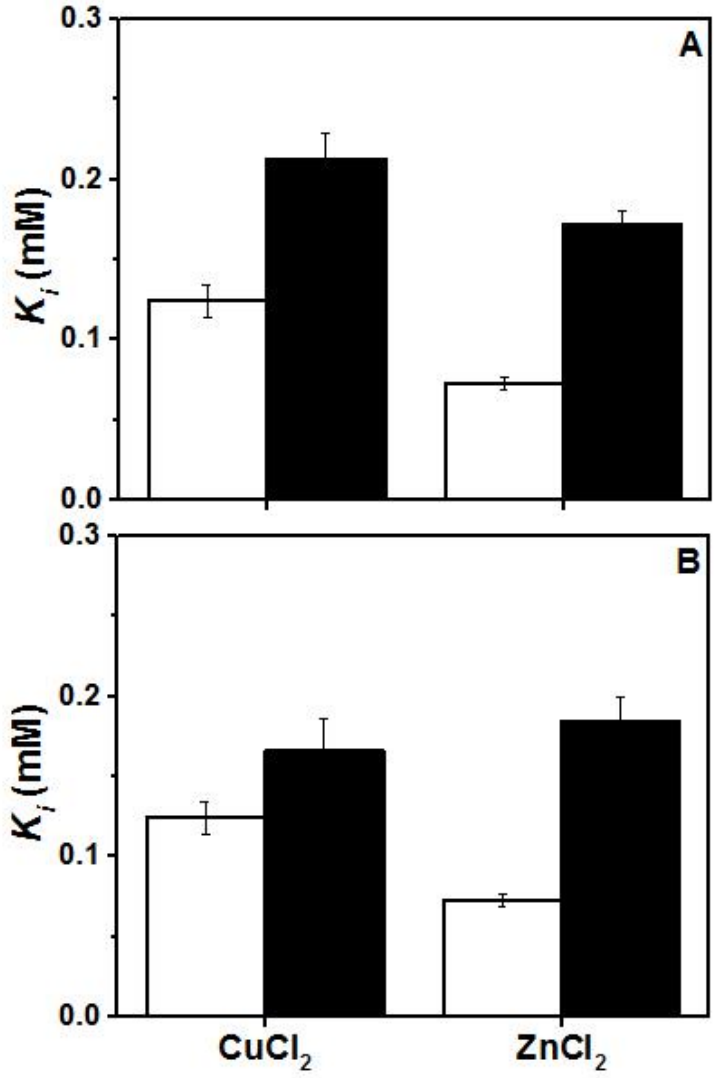

Figure 6.3 Inhibition constant values in the assays supplied with no-FeS (empty bars) and FeS (filled) after three feedings of acetate. Assays were supplied with 1.8 mM FeS-coarse (A) and 0.6 mM of FeS-fine (B)

6.3.3 Attenuation of NP toxicity

The effect of FeS-f on the attenuation of Cu^0 and ZnO NP toxicity over three feedings of acetate was also investigated. Concentrations of 0.24 mM of Cu^0 and 0.18 mM ZnO NPs in absence of FeS-f decreased the NMA after three feedings of acetate to 27 and 10%, respectively. FeS-f effectively decreased the toxic

effect of Cu^0 NPs with increasing concentrations of FeS-f (Figure 6.4A). FeS-f recovered the NMA to 63 and 80% NMA after the 3rd feeding when the FeS-f concentration was increased from 0.18 to 0.54 mM corresponding to stoichiometric values of FeS/Cu^0 of 1 to 3. The estimated R-NMA_{50} value for Cu^0 NPs was 0.12 mM of FeS-f. Likewise, Figure 6.4B shows that FeS-f attenuated ZnO NPs methanogenic toxicity by increasing the NMA to 25 and 90% NMA with addition of 0.18 and 0.54 mM FeS-f, respectively. In this case, the effect was less evident when the lowest concentration of FeS-f was supplied (FeS/ZnO=1); however, an almost full recovery was observed in the assay amended with the highest concentration of 0.58 mM of FeS-f (FeS/ZnO=3). The progressive inhibitory impact of ZnO NPs was clearly observed in the assay lacking FeS as evidenced by a NMA which decreased from approximately 50 to 10 % in the 1st to the 3rd feedings of acetate. Also at the highest FeS-f concentration, the attenuation effect of FeS towards the added ZnO NP progressively increased over the course of the three feedings. The estimated R-NMA_{50} values were 0.12 and 0.32 mM of FeS-f for the attenuation of Cu^0 and ZnO NPs, respectively. Therefore, these experimental results demonstrate that the toxic effect of Cu^0 and ZnO NPs could be successfully attenuated by providing either equimolar or excess concentrations of FeS.

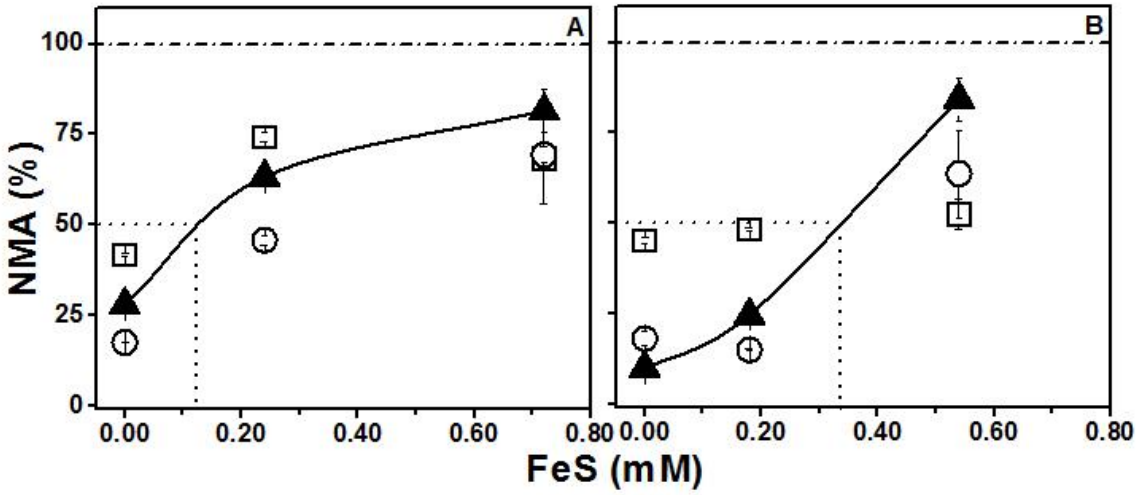

Figure 6.4 Toxicity attenuation of a high inhibitory concentration of Cu^0 (A) and ZnO NPs (B) to methanogenesis over the 1st Feeding (□), 2nd feeding (○), and 3rd feeding (▲) of acetate by an equimolar and 3X concentration of FeS-f. The solid trend line represents the response of the NMA of the third feeding, the dotted line represents the 50% toxicity attenuation concentration of FeS, and the dashed line represents the NMA activity of the control without metals or FeS. Assays were amended with 0.24 mM and 0.18 mM of Cu^0 and ZnO NPs. respectively.

6.3.3.1 Effect of long-term FeS pre-exposure to NPs and salts before sludge addition

An experiment was performed to evaluate whether a pre-exposure of FeS-f for five days to highly inhibitory concentrations of metal salts and NPs before the incubation with methanogens would increase the attenuation effect of FeS-f. Figure 6.5 shows the NMA as a function of the long-term pre-exposure and regular incubation treatment with either no FeS-f or an exposure to FeS-f provided at a molar ratio of FeS/metal = 3. The results show that the absence of pre-incubating sludge with substrate and FeS overnight resulted in a more severe toxic effect of the metals. Nonetheless, the pre-exposure to FeS-f and the metals increased the NMA to 65 and 63% in the assays amended with $CuCl_2$ and $ZnCl_2$, respectively; compared to recovery of the NMA to 50 and 40 % shown in a regular incubation in which $CuCl_2$ and $ZnCl_2$ were introduced after the sludge was incubated overnight (Figure 6.5A and 6.5C), respectively. Even though the pre-exposure of FeS-f to Cu^0 and ZnO NPs recovered the NMA to 90 and 80% (Figure 6.5B and

6.5D), the improvement in recovery compared to the regular incubation was not as obvious as in the assays supplied with salts. There was a small improvement in the NMA in the case of Cu^0 NP due to pre-exposure; however, the longer exposure of Cu^0 NPs alone to the methanogens (in absence of FeS) also increased the NMA as well.

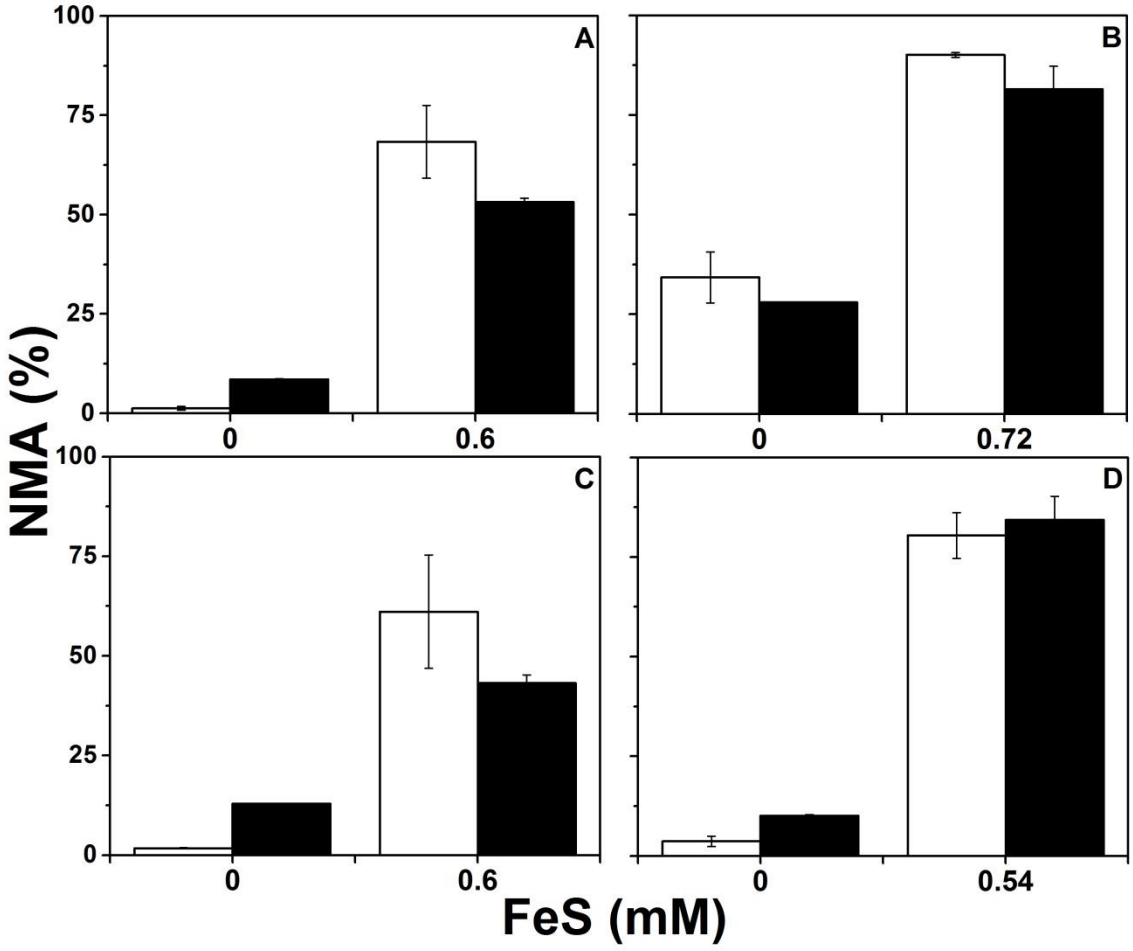

Figure 6.5 Effect of pre-exposure of FeS-f to a high inhibitory concentration of $CuCl_2$ (A), Cu^0 NPs (B), $ZnCl_2$ (C), and ZnO (D) of on the methanogenic activity after three feedings of acetate. Empty bars represent the NMA the assays pre-exposed to FeS for five days prior to initiation of assay and filled bars represent a regular incubation in which FeS the assay is initiated by addition of metals at the start of the first feeding. The NMA represents the activity after three feedings of acetate. Assays were amended with 0.24, 0.2, 0.18 and 0.2 mM of Cu^0, $CuCl_2$, ZnO NPs, and $ZnCl_2$ respectively.

6.3.4 FeS displacement mechanism

An experiment was carried out to investigate if Fe can be displaced from FeS to different extents by supplying a range of $CuCl_2$ and $ZnCl_2$ concentrations. Figure 6.6 shows the variation of the soluble concentration of Fe at different incubation times and the final concentration of soluble S^{2-} as a function of increasing concentrations of added salts in presence of 1mM of FeS. The concentration of soluble Fe^{2+} increased as a function of $CuCl_2$ concentration. The most evident increase was observed after 24 h of incubation (Figure 6.6A). The experiments supplied with $ZnCl_2$ showed a similar pattern of increasing concentration of Fe^{2+} as a function of the added $ZnCl_2$ concentration. Likewise, the most obvious increase of Fe^{2+} was observed after 24 h of incubation (Figure 6.6B).

Additionally, sulfide was measured to corroborate that no S^{2-} was released from the displacement of Fe from FeS reacted with the soluble Cu and Zn ions after 120 h of incubation. The measurements confirmed little correlation of increasing $CuCl_2$ concentrations with S^{2-} (Figure 6.6C). The assays amended with $ZnCl_2$ showed a very small increase of the concentration of S^{2-} as a function of the added $ZnCl_2$. Nevertheless, the concentration of S^{2-} found was very low (<3.5 µM) (Figure 6.6D). Overall, these findings confirm that Fe is displaced from FeS in presence of Cu^{2+} and Zn^{2+} cations.

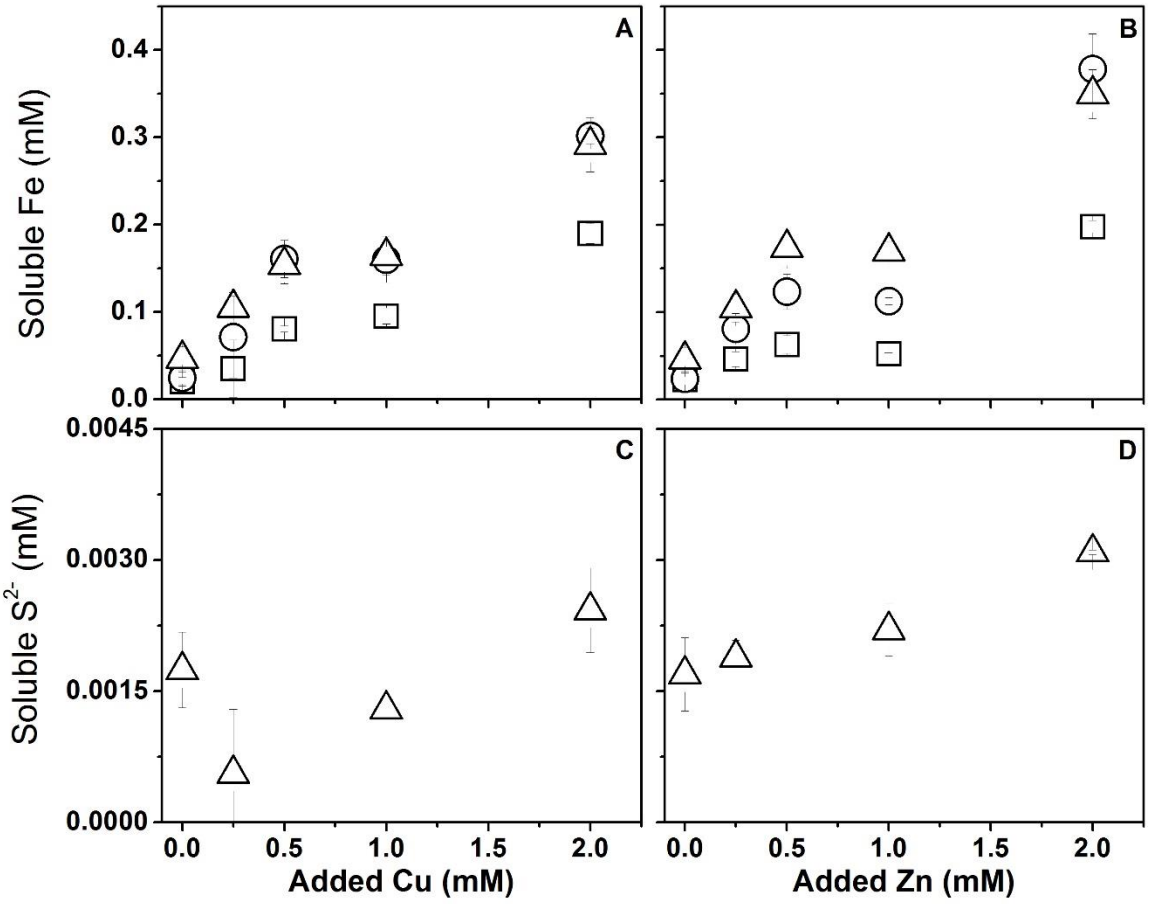

Figure 6.6 Fe and S^{2-} release as function of added $CuCl_2$ (A and C) and $ZnCl_2$ (B and D) after 2 (□), 24 (○), and 120 (△) h of incubation. Assays were performed in acidic deionized water (pH 6) with a N_2 headspace.

6.4 Discussion

6.4.1 Main findings

FeS is an effective attenuator of methanogenic toxicity caused by Cu and Zn. Attenuation occurred regardless of whether the metals were added as chloride salts or as NPs. The particle size of FeS influenced the attenuation effect since 2.5-fold less FeS-f than FeS-c was needed for the restoration of 50% of the NMA exposed to 0.2 mM of $CuCl_2$ or $ZnCl_2$. Additionally, methanogenic toxicity caused by Cu^0 and ZnO NPs was also decreased by FeS-f. Results also indicated that molar ratios of FeS-f/Cu^0, FeS-f/ZnO, FeS-f/ZnO,

FeS-f/$ZnCl_2$ and FeS-f/$CuCl_2$of 3, 3, 6, and 12 respectively, was necessary to show a high recovery of the methanogenic activity (>75%). Finally, a displacement mechanism was demonstrated by measuring progressively greater releases of Fe^{2+} in response to increasing concentrations of $CuCl_2$ or $ZnCl_2$. This demonstrated that toxic divalent metals with a greater affinity for S^{2-} could be removed from the solution by exchanging with Fe in the amorphous FeS.

6.4.2 Cu and Zn toxicity to methanogenesis and attenuation approaches.

Cu and Zn are well-known inhibitors of methanogenesis (Chen et al., 2014). The toxicity of these heavy metals has been attributed to its binding to protein structures which results in the disruption of essential enzymes of these organisms (Chen et al., 2008). Thus, if these metals are already known to be toxic to methanogens, Cu and ZnO NPs are expected to be toxic as well. Recent studies found that Cu-based (Cu^0 and CuO) and ZnO NPs are highly toxic to acetoclastic methanogens (Gonzalez-Estrella et al., 2015; Gonzalez-Estrella et al., 2013; Otero-González et al., 2014a; Otero-González et al., 2014b) . In these studies, acetoclastic methanogenic activity was inhibited by 50% in absence of sulfide with concentrations ranging from 0.17 to 0.30 mM for CuO NPs, 0.11 mM for Cu^0 MPs, and from 0.041 to 0.19 mM for ZnO NPs. Therefore, strategies to overcome this toxicity effect are necessary given the importance of methanogenesis in the digestion of waste sludge.

The methanogenic toxicity of soluble Cu and Zn salts has been successfully attenuated by precipitating these metals as CuS or ZnS. The precipitation can be achieved by generating biogenic sulfides via sulfate reduction (Lawrence & McCarty, 1965) or by directly supplying sulfide as a salt (e.g. Na_2S) (Jin et al., 1998; Zayed & Winter, 2000). A similar approach could also be considered for NPs composed of metals. There is a consensus that Cu-based and ZnO NP methanogenic toxicity is due to the release of soluble ions during dissolution and corrosion of the NPs (Gonzalez-Estrella et al., 2013; Luna-delRisco et al., 2011; Mu et al., 2011). By that same principle, biogenic sulfide effectively decreased the methanogenic toxicity caused by

Cu^0 and ZnO NPs due to precipitation of metal ions released from the NPs forming metal sulfides (Gonzalez-Estrella et al., 2015). These findings indicated a substantial decrease in toxicity as evidenced by the 7 and 14-fold increase of the K_i for Cu^0 and ZnO, respectively, in assays where biogenic sulfide was formed compared to the K_i of assays lacking biogenic sulfide. The present study agreed with the previous findings. The methanogenic toxicity of Cu^0 and ZnO NPs01 and their corresponding salts could be significantly attenuated by another important source of S^{2-}, namely FeS, commonly present in anaerobic digesters and anaerobic sediments (Gerardi, 2003; Morse et al., 1987).

6.4.3 The mechanism of FeS toxicity attenuation

FeS is commonly formed by the reaction of S^{2-} and Fe^{2+} in anaerobic environments where the oxidation of organic matter is linked to SO_4^{2-} and Fe(III) reduction generating S^{2-} and Fe^{2+} which precipitate with each other (Allen et al., 1993; Morse et al., 1987). This phenomena takes place mostly in anaerobic marine sediments where there is a high content of sulfate (Morse et al., 1987). Even though FeS is a poorly soluble mineral, the amorphous monosulfide (FeS) is considered one of the most reactive phases of sulfide in the sediments (Di Toro et al., 1992). The reactive S^{2-} fraction of FeS, commonly measured as the acid-volatile sulfide (AVS), is usually determined by adding cold acid to the solid S^{2-} fraction, distilling, and trapping the liberated H_2S (Allen et al., 1993). AVS is a key phase controlling the soluble concentration of metal cations (Ankley et al., 1994) and thus, has important implications regarding heavy metal toxicity in aquatic environments (Casas & Crecelius, 1994).

Trace metals such as Cu or Zn, with more affinity to sulfide than Fe are expected to react with sulfide and become incorporated into insoluble sulfide minerals by displacing Fe^{2+} (Simpson et al., 2000). The presence of soluble ions should displace the Fe from FeS to form CuS and ZnS according to the solubility

constants of FeS, CuS, and ZnS. If true, the displacement of Fe from FeS by either Cu^{2+} or Zn^{2+} should result in increasing concentrations of soluble Fe as the concentration of added Cu^{2+} and Zn^{2+} increases. The present study showed that the concentration of soluble Fe increased as a function of added Cu or Zn; however, in neither case was 120 h enough for the full displacement of Fe from 1mM of FeS initially added even with excess of Cu and Zn. Our findings are in agreement with Simpson et al. (2000) which also found increasing soluble Fe concentrations as a function of Zn and Cd added to a sulfidic estuarine sediments. FeS was used as well to immobilize Hg^{2+} (Han et al., 2014). The study observed 100% of Hg removal at concentrations <0.5 mM of Hg in 10 min; however, concentrations >1mM of Hg required up to 800 min to achieve the same results. Such results may be explained partially by a low availability of the sulfide (AVS) for the total metal added in the first minutes of the experiment

The AVS fraction of FeS has been successfully applied in some studies to predict the toxicity effect of Cd on benthic organisms (Di Toro et al., 1990). Their findings showed that molar ratios AVS/Me$\geq$1 effectively prevent Cd toxicity to amphipods. Di Toro et al. (1992) also found that AVS predicts Cd and Ni toxicity to freshwater and marine organisms if a ratio of AVS/Me >1 was used to prevent toxicity; all the experiments performed followed the prediction. If the same ratio of AVS/Me is applied to our experiments, assuming that the total FeS added represents AVS, the ratio of AVS/Me>1 fails to predict the toxicity to methanogens. Figure 6.7 shows the NMA response as of function of the ratio of FeS-f/Me. In the assays amended with Cu, a ratio of FeS/Cu^0 and $FeS/CuCl_2$ of 3 and 12 respectively was needed to obtain a high recovery (>75%) of the methanogenic activity (Figure 6.7A). Likewise, a ratio of FeS/ZnO and $FeS/ZnCl_2$ of 3 and 6 respectively was needed to observe a high level of recovery response (Figure 6.7B). According to the prediction, all the points displayed in the provided chart inside the diagonal lines would have shown a NMA around 100%. Therefore, in our experiments it can be assumed that not all of the total FeS added was readily available for reaction with added heavy metals (and corresponding NPs).

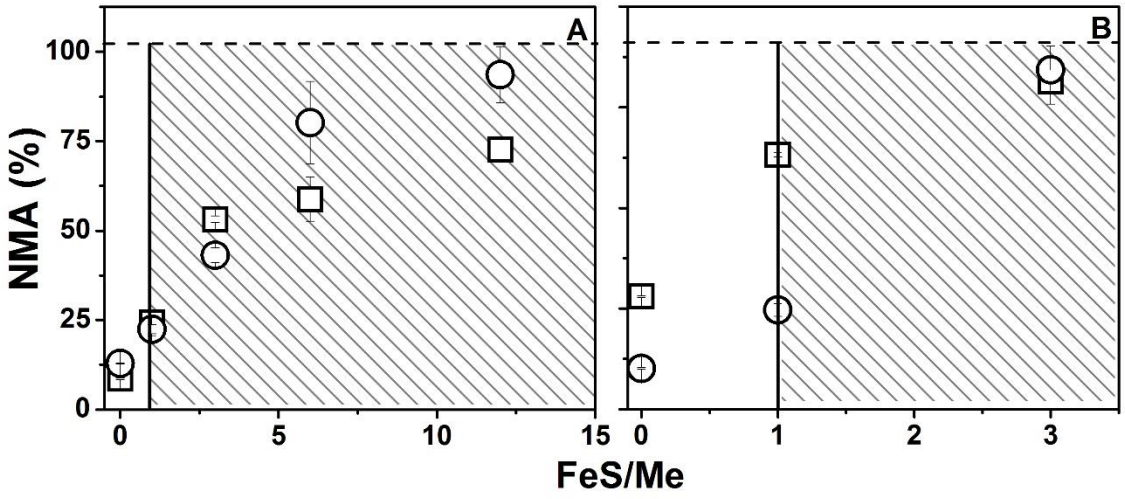

Figure 6.7 NMA after three feedings of acetate as a function of increasing molar ratios of FeS-f/Me. The symbols represent Cu (□) and Zn (○) either as chloride salts (A) or NPs (B). The diagonal lines show the theoretical area where the toxicity attenuation should approach 100%. This analysis was made with the data of the assays amended with 0.2, 0.2, 0.24 and 0.18 mM of $CuCl_2$, $ZnCl_2$, Cu^0, and ZnO NPs.

Our findings demonstrated that FeS-f improved the metal toxicity attenuation effect most likely by increasing the availability of the AVS fraction due to the increase the total surface area. The total surface area increase from FeS-c to FeS-f was~17-fold (assuming average spherical particle sizes for FeS-f and FeS-c of 50 and 850 µm, respectively and a specific gravity of 4.84 g mL^{-1}). However, the increase of attenuation of FeS-f due to its particle size was only 2.5-fold. This discrepancy maybe caused by microporosity of FeS-c which may increase the AVS availability and occurrence of coarse particles in the experiments supplied

Three major observations indicate not all the S^{2-} from FeS was available to react with the soluble metals. Firstly, a ratio FeS-f>1 was necessary to observe a clear attenuation in all of the bioassays performed in this study (Figure 6.7). Secondly, the Fe displacement experiments did not demonstrate a stoichiometric displacement based on the added heavy metals even when the heavy metals were added in excess of FeS. And thirdly, the pre-exposure did not increase to the maximum recovery even with five

days of contact of FeS with the toxic metals, only the assays amended with salts showed an increase in the recovery with respect to a regular incubation. These results strongly suggest that not all of the S^{2-} in the FeS was available to react with Cu^{2+} and Zn^{2+}. Recently, we also demonstrated that sulfate reduction provides sulfide that can readily stoichiometrically precipitate toxic metals. Therefore, the attenuation of metal toxicity by FeS is limited by the reactive S^{2-} phase of FeS.

6.5 Conclusions

FeS was found to be effective in attenuating the methanogenic toxicity caused by Cu^0 and ZnO NPs and their soluble chloride salt analogs. The attenuation effect of FeS on Cu and Zn toxicity was increased by decreasing the particle size. At least 2.5 times less FeS-f was needed to observe the same attenuation effect of FeS-c. The K_i values were doubled in almost every case by providing the R-NMA_{50} concentrations. Results also demonstrate that the Fe from FeS is displaced in the presence of Cu^{2+} and Zn^{2+} soluble cations. In order to achieve nearly complete attenuation of Cu and Zn toxicity, FeS had to be added in large stoichiometric excess, indicating that not all the sulfide was readily available for sequestering the metals. The results taken as a whole indicate that the toxicity caused by the release of Cu-based and ZnO NPs and their soluble metal analogs could be effectively attenuated by FeS.

6.6 Acknowledgments

This work was supported by the Semiconductor ResearchCorporation (SRC)/Sematech Engineering Research Center for Environmentally Benign Semiconductor Manufacturing. Gonzalez-Estrella was partly funded by CONACyT.

CHAPTER VII CONCLUSIONS

- Cu^0 and ZnO NPs cause severe toxicity to methanogens. In general, acetoclastic methanogens are more sensitive than hydrogenotrophic methanogens to the toxicity of Cu-based and ZnO NPs as evidenced by the IC_{50} values. The toxicity of any given metal was highly correlated with its final dissolved concentration in the assay irrespective of whether it was initially added as a NP or chloride salt, indicating that corrosion and dissolution of metals from NPs may have been responsible for the toxicity. This study also demonstrates high tolerance of methanogens to high concentrations of Ag^0, Al_2O_3, Ce_2O_3, Mn_2O_3, Fe^0, Fe_2O_3, SiO_2, and TiO_2 NPs, suggesting that anaerobic treatment processes could tolerate high concentrations of these types of NPs.
- Cu^0 NPs are toxic to glucose fermentation, syntrophic propionic oxidation, methanogenesis, denitrification and anammox biological processes. Glucose fermentation and anammox were the most and the least affected processes. The similarities of the K_i values calculated as a function of the residual concentrations strongly suggest that all these processes are affected by the release of soluble ions of Cu^0 NPs. Cu^0 NPs represent a possible risk for anaerobic microorganisms if they become accumulated in wastewater treatment plants.
- Biogenic sulfide decreases the methanogenic toxicity of Cu^0 and ZnO NPs. The K_i values calculated from the residual metal concentration of sulfate-free and sulfate-containing assays are very similar. This indicates that the residual soluble ions cause toxicity regardless of what the source of the metal is and regardless of whether biogenic sulfide was present or absent. ZnO NPs are less toxic to sulfate reduction, thus ZnO NP and $ZnCl_2$ toxicity to methanogens was stoichiometrically attenuated. However, Cu^0 NPs and $CuCl_2$ are toxic to sulfate reducing bacteria which impacted the effectiveness by which sulfate was reduced to sulfide and thus the attenuation of methanogenic toxicity caused by Cu^0 NP and $CuCl_2$ was not fully stoichiometric with the sulfate supplied. Long term experiments

showed that the toxicity effect of ZnO NPs and $ZnCl_2$ progressively increased over time, while the methanogens inhibited by Cu^0 NPs and $CuCl_2$ could recover from a partial toxicity unless the dose was initially lethal. Overall biogenic sulfide attenuates the toxicity caused by Cu^0 and ZnO and their salt analogs to methanogens.

- FeS is an effective attenuator of the toxicity of Cu^0 and ZnO NPs and their soluble salt analogs to methanogens. The results demonstrated that a greater attenuation can be achieved by decreasing the particle size. Less FeS-f was necessary to achieve a similar methanogenic recovery observed when a coarse FeS was supplied. The presence of Cu and Zn ion soluble ions displaced the Fe from FeS as evidenced by an increase in measurable dissolved Fe. Excess molar ratios of FeS were required to observe a high recovery (>75%) of the methanogenic activity indicating that not all the sulfide in FeS was readily available to attenuate the heavy metals. Overall strong evidence was provided that FeS attenuates the methanogenic toxicity caused by $Cu^0$and ZnO NPs and their salt analogs to methanogens, albeit that molar excesses of FeS are needed.
- Overall this research indicates that Cu-based and ZnO NPs are highly toxic to anaerobic wastewater processes. Accumulation of such NPs in wastewater treatment facilities will cause a severe inhibition of the biological anaerobic processes. The findings of the different experimental chapters strongly suggest that the toxicity of these NPs is caused by the release of soluble ions. Therefore, decreasing the concentration of soluble ions by the formation of sulfide precipitates can attenuate the severe toxic effect. This work demonstrates that the application of biogenic sulfide or FeS can effectively attenuate Cu and ZnO toxicity to anaerobic digestion.

ANNEX I: TOXICITY ASSESSMENT OF INORGANIC NANOPARTICLES TO ACETOCLASTIC AND HYDROGENOTROPHIC METHANOGENIC ACTIVITY IN ANAEROBIC GRANULAR SLUDGE

A.1.1 Materials and methods - Digestion and metal analysis

Samples containing Fe^0 and Mn_2O_3 (1 mL) were digested using 37% HCl (1 mL), and ZnO and CuO samples (1 mL) using 70% HNO_3 (10 mL). These digestions were performed at 30°C overnight at 100 rpm. Samples containing Cu^0 (1 mL) were digested with 10 mL of nitro-hydrochloric acid (HNO_3:HCl, 1:3) solution in 50 mL vials using a microwave assisted digestion system (MARS System, CEM Corp., Matthews, NC) as previously described (Garcia-Saucedo et al., 2011). Digested samples were diluted when needed with HNO_3 acid to a final concentration of 2% (v/v). Dissolved metals were measured by inductively coupled plasma-optical emission spectroscopy (ICP-OES Optima 2100 DV, Perkin–Elmer TM, Shelton, CT). The wavelengths used for ICP-OES analysis of the different elements were as follows: Cu (324.754), Fe (259.940), Mn (257.610), and Zn (206.200). The detection limit was 1 µg L^{-1} for all metals measured.

A.1.2 Nanoparticles Aggregation

The stability of the NPs was evaluated by determining the particle size distribution (PSD) and zeta potential (ZP) according to a previous study (Garcia-Saucedo et al., 2011). Table A.1 shows the average hydrodynamic diameter and zeta potential of the NPs tested.

Table A.1.1. Average hydrodynamic diameter and zeta potential of a series of NPs in the absence and presence of Dispex

NP[1]	Particle Size (nm)							
	pH 2		DI[2] water		Basal Medium		Dispex	
	t 0 h	t 24h	t 0 h	t 24h	t 0 h	t 24h	t 0 h	t 24h
Ag^0	ND[3]	ND	ND	ND	ND	171 ± 2	ND	ND
Al_2O_3	521 ± 17	338 ± 33	584 ± 147	388 ± 23	6970 ± 639	2252 ± 301	775 ± 297	287 ± 9
CeO_2	183 ± 17	167 ± 5	166 ± 9	1598 ± 5	3588 ± 126	1037 ± 178	187 ± 4	187 ± 4
Cu^0	930 ± 37	1047 ± 512	1252 ± 27	1094 ± 261	958 ± 34	648 ± 14	493 ± 1	391 ± 13
CuO	710 ± 152	765 ± 377	824 ± 86	588 ± 183	841 ± 253	1662 ± 22	475 ± 59	435 ± 73
Fe^0	737 ± 320	422 ± 300	2147 ± 106	558 ± 90	3335 ± 333	844 ± 110	3303 ± 288	1114 ± 234
Fe_2O_3	228 ± 144	2119 ± 852	151 ± 1	2041 ± 973	167 ± 8.2	139.8 ± 5	596 ± 311	138 ± 6
Mn_2O_3	586 ± 249	1119 ± 468	1419 ± 195	1208 ± 259	2340 ± 93	2416 ± 438	244 ± 5	209 ± 4
SiO_2	ND	ND	616.9 ± 95	614.0 ± 97	9472 ± 101	5811 ± 2538	3740 ± 420	5012 ± 2269
TiO_2	ND	ND	1120 ± 482	ND	1452 ± 934	ND	98 ± 3	ND
ZnO	464 ± 33	1893 ± 362	1696 ± 76	612 ± 190	1008 ± 46	1051 ± 41	718 ± 24	608 ± 9
	Zeta Potential (mV)							
Ag^0	ND	ND	ND	ND	ND	12.1 ± 1.0	ND	ND
Al_2O_3	35.3 ± 2.3	36.3 ± 1.8	45.7 ± 4.5	52.9 ± 7.0	-19.1 ± 2.0	-20.9 ± 0.4	-28.3 ± 0.5	-30.0 ± 0.8
CeO_2	37.1 ± 0.9	42.0 ± 2.1	38.5 ± 9.5	51.1 ± 4.2	-15 ± 0.3	-15.6 ± 1.9	-31.0 ± 1.5	-32.4 ± 1.1
Cu^0	4.1 ± 0.6	6.3 ± 4.0	-2.6 ± 0.4	0-5.2 ± 3.0	-14 .9 ± .9	-16.3 ± 1.8	-33.8 ± 3.6	-30.3 ± 1.1
CuO	13.8 ± 3.2	11.1 ± 3.3	-6.6 ± 13.5	-8.6 ± 3.1	-16.8 ± 0.9	-17.6 ± 2.3	-27.9 ± 1.1	-28.0 ± 2.2
Fe^0	7.3 ± 6.9	16.4 ± 14.7	-9.2 ± 0.5	2.8 ± 1.0	-16.1 ± 0.7	-13.5 ± 1.4	-34.5 ± 1.0	-12.5 ± 1.6
Fe_2O_3	34.8 ± 3.8	-16.3 ± 0.5	41.0 ± 1.7	-16.9 ± 1.0	44.6 ± 12.0	-31.75 ± 1.5	18.0 ± 14.1	-33.4 ± 1.2
Mn_2O_3	38.8 ± 1.3	35.1 ± 1.5	8.6 ± 0.7	-2.3 ± 4.0	-16.3 ± .4	-11.9 ± 2.7	-32.15 ± 2.0	-31.5 ± 2.0
SiO_2	ND	ND	-19.4 ± 9.4	-29.6 ±8.8	-24.8 ± 1.1	-24.4 ± 0.7	-25.4 ± 1.0	-24.4 ± 0.7
TiO_2	ND	ND	ND	ND	ND	-12.9 ± 1.0	ND	ND
ZnO	7.4 ± 3.7	9.0 ± 1.2	-5.5 ± 1.6	-10.4 ± 1.2	-32.8 ± 0.9	-35.1 ± 0.6	-45.6 ± 4.5	-42 ± 1.7

[1] NP: Engineered Nanoparticle
[2] DI: Deionized Water
[3] ND: Not determined

A.1.2 Effect of dispersant on NP toxicity to methanogens.

The effect of DISPEX on NP toxicity to methanogens was investigated. Table A.1.2 shows the NMA activity of assays supplied with 1500 mg L^{-1} of NP with and without DISPEX. Results showed no significant effect ($p > 0.001$) of the DISPEX on the NP toxicity to methanogens.

A.1.3. Toxic effect of CuO and Fe^0 on acetoclastic methanogenic activity

The toxic effect of CuO and Fe^0 on acetoclastic methanogenic activity was investigated. Figure A.1.1 shows the CH_4 production as a function of 1500 mg L^{-1} of CuO and Fe^0 NPs over two feedings of acetate. Results showed an increasing toxic effect of CuO NPs after two feedings of acetate. The methane production in the first feeding of the assay amended with CuO was similar than the control, whereas the CH_4 production rate dropped in more >50% in second feeding Figure A.1.1A. Conversely, the assays amended with Fe^0 did not showed an increase of the toxicity after two feedings of acetate. The methane production rate assays amended with Fe^0 only decreased <10% in both feedings. Figure A.1.1B. Overall this result demonstrated an increasing toxic effect of CuO NP on the acetoclastic methanogenic activity.

Table A.1.2. Effect of dispersant addition (150 mg Dispex mg L^{-1}) on the toxicity of different NPs (1,500 mg L^{-1}) to acetoclastic- and hydrogenotrophic methanogenic cultures.

Substrate	**Acetate**						**H_2**					
NP	**No-dispersant NMA[1](%)**	**Dispersant NMA (%)**	**T Test**	**DF[2]**	**Prob>|t| (p-value)**	**Significantly different (significance level = 0.05)**	**No-dispersant NMA (%)**	**Dispersant NMA (%)**	**T Test**	**DF**	**Prob>|t| (p-value)**	**Significantly different (significance level = 0.05)**
Control	100 ± 0	107 ± 1.3	-1.2	2	0.4	NO	100	104.6 ± 0.2	1.2	1	0.4	NO
Ag^0	103.2 ± 1.6	104 ± 0.1	-0.7	1	0.6	NO	95.3 ± 4.6	93.3 ± 1.4	0.5	1	0.7	NO
Al_2O_3	94.2 ± 5.8	95.2 ± 2.1	-0.2	1	0.9	NO	82.8 ± 12.1	96.2 ± 6.5	-1.0	1	0.5	NO
CeO_2	77.9 ± 0.6	75.1 ± 6.7	-0.30	1	0.8	NO	84.4 ± 5	92.5 ± 5	-1.2	1	0.5	NO
Cu^0	0	0	-	-	-	NO	0	0	-	-	-	NO
CuO	87 ± 1.3	90.5± 10.0	-0.58	1	0.7	NO	98.9 ± 1.0	80.1 ± 7.6	4.0	1	0.2	NO
Fe^0	84.8 ± 6.1	89.2 ± 0.4	-1.1	1	0.5	NO	91.2 ± 4.6	76.7 ± 0.6	3.93	1	0.2	NO
Fe_2O_3	95.6 ± 5.3	109.6 ± 1.8	-5.6	1	0.1	NO	83.0 ± 4.7	90.2 ± 0.8	-2.6	1	0.2	NO
Mn_2O_3	52.4 ± 8.9	52.0 ± 4.8	0.03	1	1.0	NO	64.8 ± 4.7	79.5 ± 2.5	-2.9	1	0.2	NO
SiO_2	99.9 ± 3.5	97.3± 9.0	0.3	1	0.8	NO	102.1± 15.8	100.3 ± 7.4	0.3	1	0.8	NO
TiO_2	93.2 ± 1.3	103 ± 4.9	-0.9	1	0.6	NO	94.1 ±3.1	91.7 ± 5.6	0.4	1	0.8	NO
ZnO	53.5 ± 4.7	64.5 ± 2.7	-2.1	1	0.3	NO	72.7 ± 7.6	75.2 ± 3.4	-0.3	1	0.8	NO

[1] NMA: Normalized methanogenic activity
[2] DF: Degrees of freedom

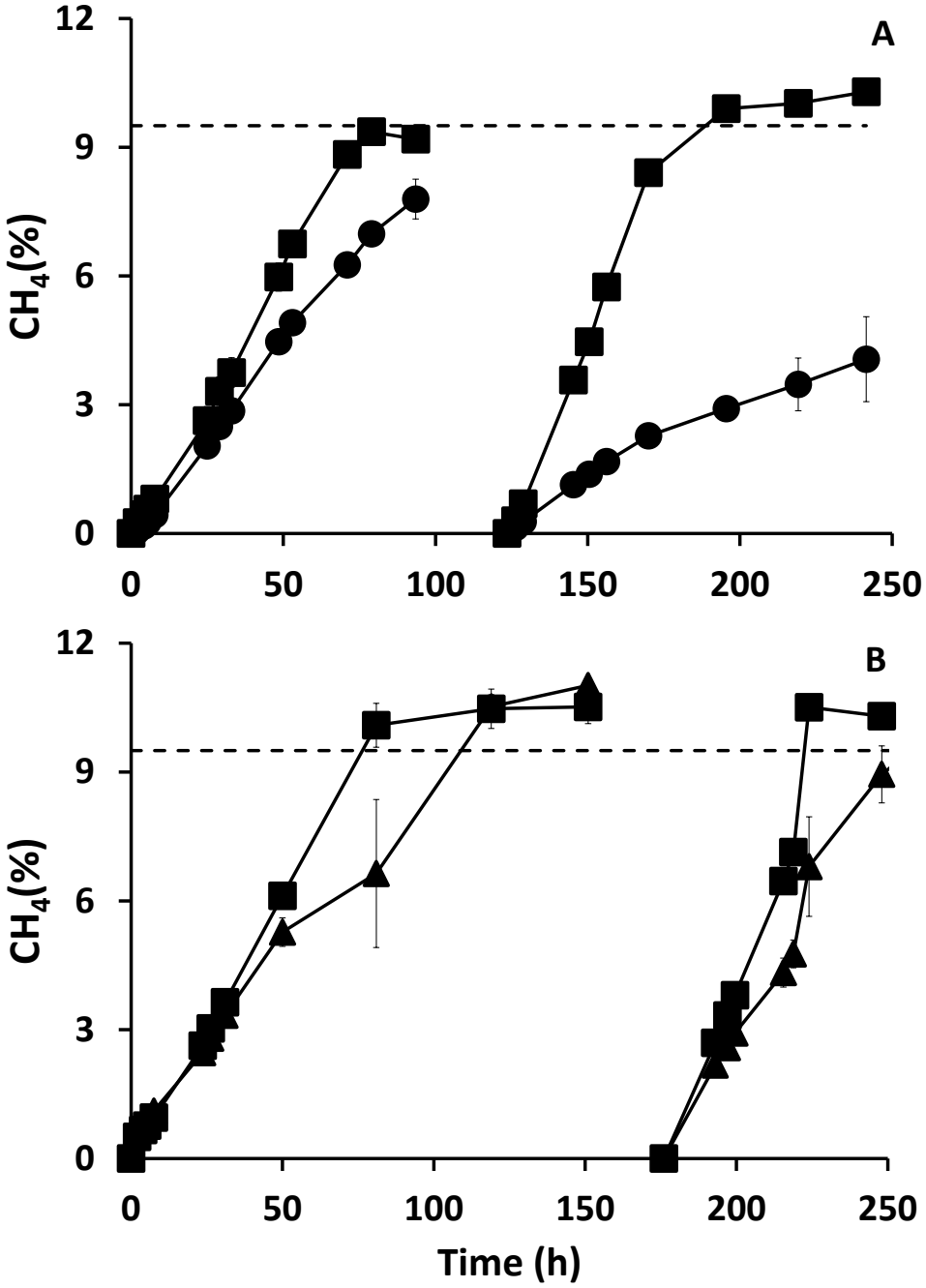

Figure A.1.1. Time course of acetoclastic methane production in the presence of 1,500 mg L^{-1} of CuO NP (**A**) or Fe^0 NP (**B**). Controls without NPs (■), assays with CuO (●), and assays with Fe^0 (▲).

A.1.3. Toxic effect of CuO and ZnO on acetoclastic methanogenic activity

The toxic effect of CuO and ZnO on hydrogenotrophic methanogenic activity was investigated. Figure A.1.2 shows the CH_4 production as a function of 1500 mg L^{-1} of CuO and ZnO NPs over two feedings of acetate. Results showed a slightly increasing toxic effect of CuO NPs after two feedings of acetate (Figure A.1.2). The methane production in the first feeding of the assay amended with CuO was almost the same of that of the control, nevertheless the CH_4 production rate dropped to around 20% in second feeding. The assays supplied with ZnO NPs showed a noticeable increase of toxicity after 24 h of incubation, which resulted an incomplete conversion of H_2 to CH_4. This highly inhibitory effect remained during the second feeding in which the CH_4 production rate was reduced by >95%. Overall this result demonstrated a low toxicity of CuO NP and a severe ZnO toxicity to hydrogenotrophic methanogens.

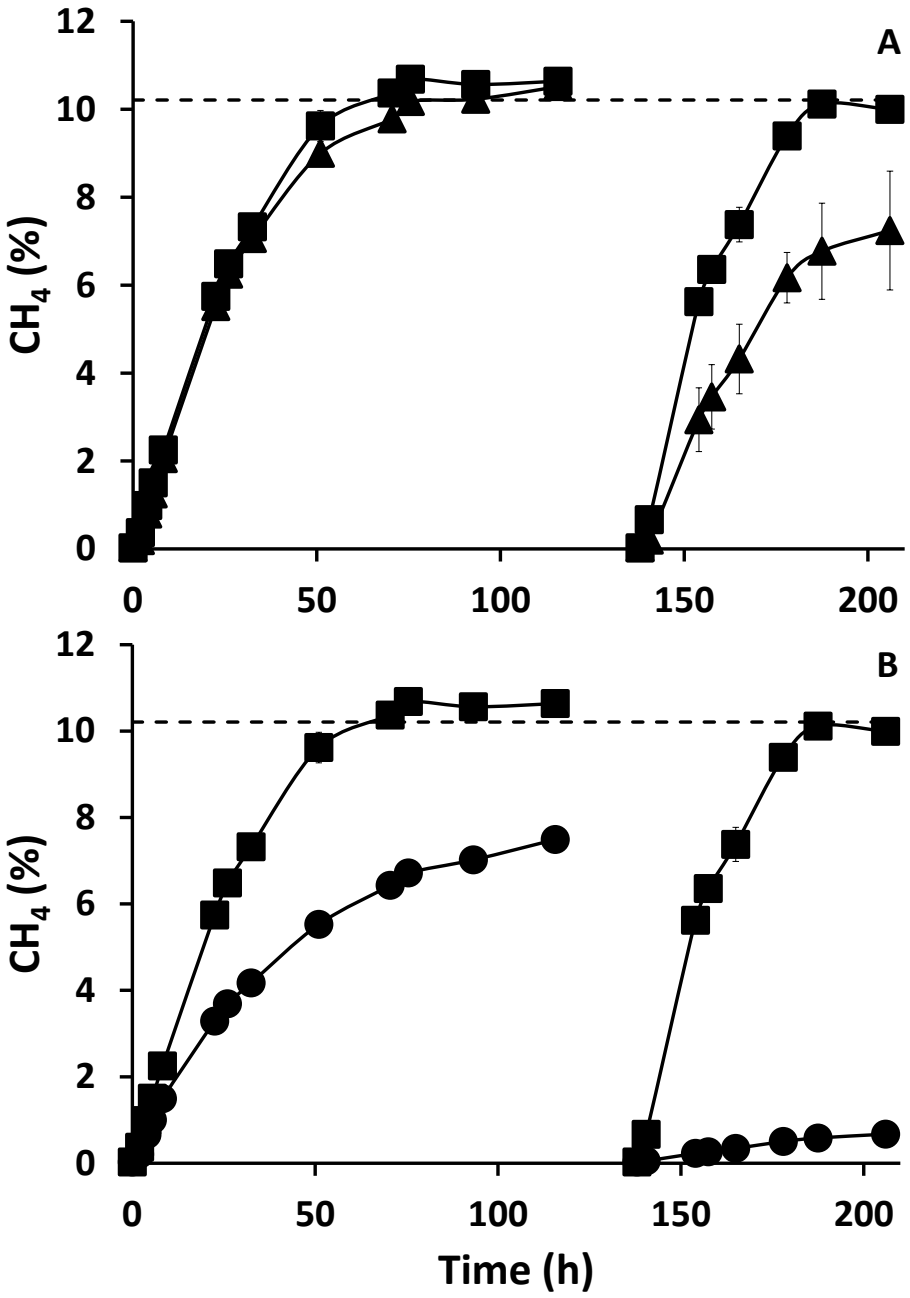

Figure A.1.2. Time course of hydrogenotrophic methane production in the presence of 1,500 mg L^{-1} of CuO NP (**A**) or ZnO NP (**B**). Controls without NPs (■), assays with CuO (▲), and assays with ZnO (●).

ANNEX II ELEMENTAL COPPER NANOPARTICLE TOXICITY TO DIFFERENT TROPHIC GROUPS INVOLVED IN ANAEROBIC WASTEWATER TREATMENT PROCESSES

A.2.1 Residual Cu solubility

A measurement of residual soluble Cu was performed of the all assays supplied either with Cu^0 NP or $CuCl_2$. Figure A.2.1 shows the residual soluble Cu concentration in all the biological media applied in this research as function of added Cu. Results indicated that anammox biological media showed overall more recovery as soluble Cu from the added Cu. As an example, around 20% as soluble Cu was recovered from the highest concentration of Cu^0 NP in the anammox media, whereas all other biological media showed from 10 to less than 1% of recovery as soluble Cu from the highest added concentrations. Similar trends can be observed when comparing other concentrations. Therefore, overall Cu was more soluble in anammox media.

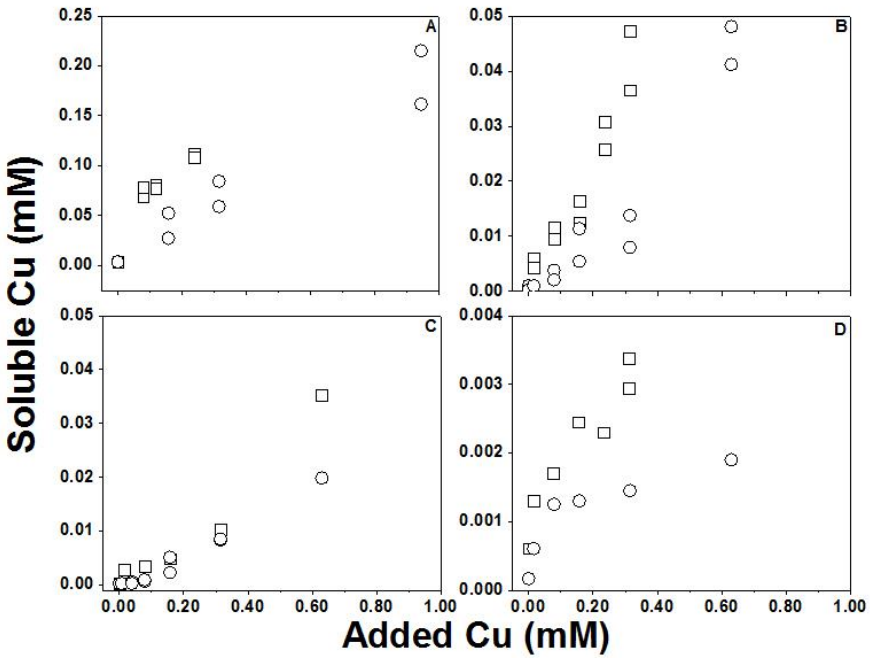

Figure A.2.1 Residual soluble Cu of the annamox (A), denitrification (B), glucose fermentation and methanogenesis (C), and syntrophic propionate oxidation and methanogenesis (D) assays amended with $CuCl_2$ (□) and Cu0 NPs (○)

ANNEX III ROLE OF BIOGENIC SULFIDE IN ATTENUATING ZNO AND CU^0 NANOPARTICLE TOXICITY TO ACETOCLASTIC METHANOGENESIS

A.3.1. Explaining the physical meaning of the inhibition order from the Equation 5.1.

The methanogenesis rate can be explained by Monod kinetics, as follows:

$$\frac{dS}{dt} = -\frac{1}{Y_{X/S}} \cdot \left(\mu_{\max} \cdot X \cdot \frac{S}{K_S + S} - k_d \cdot X \right) \quad [A.3.1]$$

Where S is the substrate consumed (g acetate-COD L^{-1}), μ_{max} is the maximum specific growth rate (d^{-1}), X is the biomass concentration (g VSS L^{-1}), $Y_{X/S}$ is the biomass yield (g VSS g^{-1} COD), K_S is the saturation constant, or Monod constant (g acetate-COD L^{-1}) and k_d is the biomass decay coefficient (d^{-1}). If the experimental time is low, as is the case in batch experiments, the decay rate will be negligible compared to the μ_{max}. So that, Eq. [A.3.1] can be rewritten as:

$$\frac{dS}{dt} = -\frac{1}{Y_{X/S}} \cdot \mu_{\max} \cdot X \cdot \frac{S}{K_S + S} \quad [A.3.2]$$

which represents the classic Monod model. If a non-competitive inhibitor (like all the cationic heavy metals) enters in the system, the Eq. [A.3.2] is modified by the addition of an inhibition term, as follows:

$$\frac{dS}{dt} = -\frac{1}{Y_{X/S}} \cdot \mu_{\max} \cdot X \cdot \frac{S}{K_S + S} \cdot \frac{1}{1 + \left(\frac{I}{K_i} \right)^n} \quad [A.3.3]$$

Where I and K_i are the inhibitor concentration and the inhibition constant, respectively (mM of Cu or Zn), and n is the inhibition order (dimensionless). The equation described in [A.3.3] has been frequently used for describing non-competitive inhibitory effects on anaerobic digestion, referred to toxicants like ammonia, nitrite, sodium or sulfide. In fact, it has been proposed as the reference inhibitory equation in

the IWA-Anaerobic Digestion Model 1. If only the maximum rate is considered instead of the entire methane production curve, Eq. [A.3.3] is reduced to:

$$SMA = SMA_{\max} \cdot \frac{1}{1+\left(\frac{I}{K_i}\right)^n} \quad \text{[A.3.4]}$$

Where *SMA* and SMA_{max} are the specific methanogenic activity and its maximum value, respectively (mg COD g^{-1} VSS d^{-1}). Normalizing the activities by means of a control in absence of the inhibitor, Eq. [A.3.4] is converted into:

$$NMA = NMA_{\max} \cdot \frac{1}{1+\left(\frac{I}{K_i}\right)^n} \quad \text{[A.3.5]}$$

which represents the equation used in the present study for analyzing the inhibitory effect of Cu and Zn NPs on the methanogenesis (Eq. [5.1]). In practice, *n* is usually between 1 and 2. However, there are cases where this value is higher than 2, leading to a typical effect known as *cliff* effect. The following Figure exemplifies the *cliff* effect:

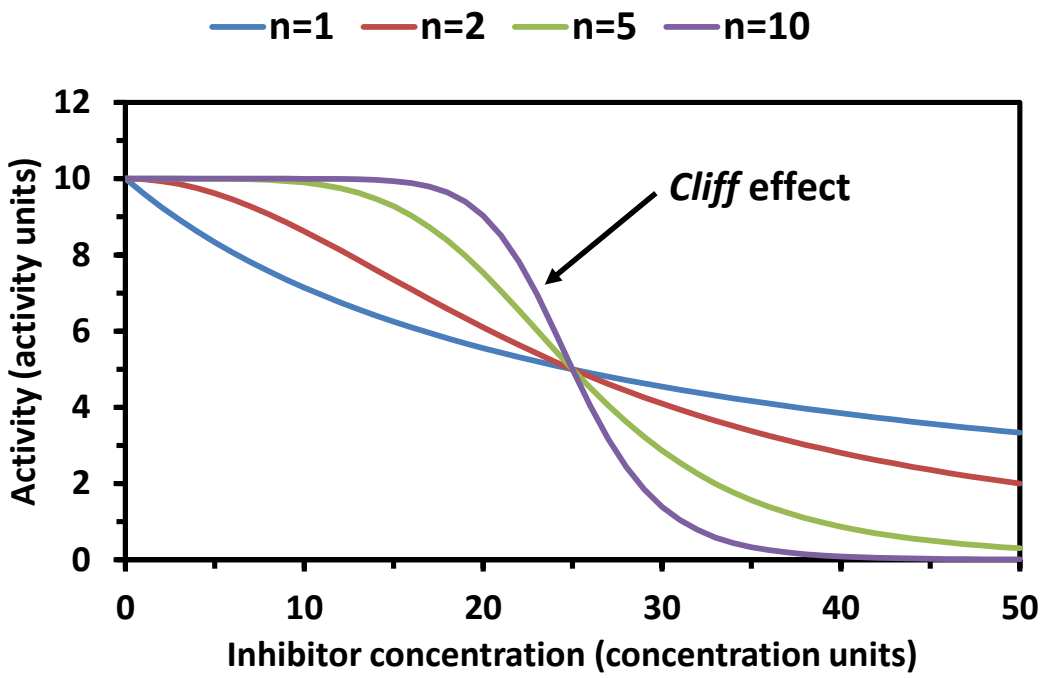

Figure A.3.1: Theoretical effect of an inhibitor on the biomass activity. K_i=25 concentration units.

As can be seen in Figure A.3.1, while the inhibition order is increasing, the shape of the line is becoming more and more pronounced. If the *n* value tends to infinite, the line would be converted into a switch function.

The meaning of a *cliff* function in this study is related with the sudden presence of bioavailable toxicant (Zn and Cu) in the system as the total concentration is incremented. Since both the Zn and Cu concentrations are dependent on the biogenic sulfide production, once the sulfate has been completely reduced and the sequestering capability of the sulfide is exhausted, the bioavailable concentration of both metals increase substantially, and so the inhibitory effect appears suddenly.

A.3.2. Derivation of the model for explaining the long-term inhibition of methanogenesis by Cu and Zn

The methanogenesis rate can be explained by Monod kinetics, following the Eq. [A.3.1]. In optimum conditions, during a batch experiment the decay rate is negligible compared with the μ_{max}. Considering

that every 1 g CH4-COD produced ≈ 1 g acetate-COD consumed, the methanogenic activity (MA) is defined as the maximum COD consumption rate per unit of volume, described by the following equation:

$$MA = V_{\max} = \mu_{\max} \cdot \frac{X}{Y_{X/S}} \quad \text{[A.3.6]}$$

where Y represents the cell yield (mass of cell mass of substrate^{-1}). All other parameters defined in manuscript. The increment of the MA is linearly dependent on the biomass produced. In fact, the term $X/Y_{X/S}$ can be substituted with $S_{consumed}$, which represents the cumulative substrate concentration that has been consumed to obtain the quantity of biomass appearing in the system when the MA is being calculated. An important assumption is MA is directly proportional to X, which means any loss in MA is due to cell death (rather than lowered activity of existing cells). So, Eq. [A.3.6] can be rearranged into:

$$MA = \mu_{\max} \cdot S_{consumed} \quad \text{[A.3.7]}$$

where $S_{consumed}$ is the total cumulative substrate consumed (g COD L^{-1}). If the initial biomass concentration is not negligible then the initial activity cannot be considered as 0, so that Eq. [A.3.7] is modified as follows:

$$MA = \mu_{\max} \cdot S_{consumed} + MA_o \quad \text{[A.3.8]}$$

where MA_o is the initial volumetric activity (mg COD-CH_4 L^{-1} d^{-1}) calculated by performing linear regressions over three cumulative methane production data points. In order to simplify the model, it can be considered that the saturation constant of the acetoclastic methanogenesis is negligible compared with the concentration of acetate used in this study (the K_S recommended by the IWA-ADM-1 model is 150 mg COD L^{-1} [1]. Consequently, the Eq. [A.3.1] can be simplified to:

$$\frac{dS}{dt} = \frac{1}{Y_{X/S}} \left(\mu_{\max} \cdot X - k_d \cdot X \right) \quad \text{[A.3.9]}$$

where k_d represents the biomass deactivation constant (d^{-1}). In this case, the apparent maximum specific growth rate can be defined as:

$$\mu_{app} = \mu_{\max} - k_d \quad \text{[A.3.10]}$$

where μ_{app} is the apparent maximum growth rate or net growth rate.. Therefore, Eq. [A.3.8] is transformed into:

$$MA = \mu_{app} \cdot S_{consummed} + MA_o \quad \text{[A.3.11]}$$

Eq. [A.3.11] implies that, when μ_{app} becomes negative, biomass death rate overcomes the biomass growth rate, and therefore the MA decreases as explained by the progressive action of the inhibitor, which can lead to total cell death. This equation has been used in the present study for analyzing the long term effect of Cu and Zn NPs on the methanogenesis (Eq. [5.3]).

In order to verify the assumption that MA is proportional to X there are two evidences. Firstly, washing the Zn and Cu from sludge after long term exposures does not restore activity (Figure A.3.6) which clearly indicates that the lost activity was due to inactivated cells. Similar results were obtained in column studies of granular sludge exposed to ZnO (Otero-González et al., 2014a). Secondly, during regrowth in the long term Cu exposure experiments, the growth rate that could be estimated with Eq 5.3 corresponded to the expected values for the acetoclastic methanogens *Methanosaete* (Conklin et al., 2006; Dezeeuw, 1985). Such values would not be anticipated if inhibition was just reversed when the bioavailable Cu was depleted.

A.3.3 Data modeling

Non-linear fittings of the data to the Eq. [5.2] were performed by least-square minimization of the error using the Levemberg-Marquardt algorithm. Origin 8.6 software (OriginLab, Northampton, USA) was used. Linear-fittings of the data for calculating the SMA and long-term Cu and Zn toxicity to methanogens (Eq. [5.3]) were performed by linear regression using Excel (Microsoft, Redmond, USA).

A.3.4 Analytical methods

Methane was quantified by gas chromatography with flame ionization detection (Hewlett Packard 5890 Series II) and analysis of soluble metals by inductively coupled plasma-optical emission spectroscopy (ICP-OES Optima 2100 DV, Perkin–Elmer TM, Shelton, CT). The wavelengths used for ICP-OES analysis of were 324.754 and 206.200 for Cu and Zn, respectively. All samples were centrifuged at 13000 rpm and filtered (0.025 µm VSWP, Millipore, Billerica, MA, USA) prior to ICP analysis. Sulfate was analyzed by suppressed conductivity ion chromatography detector (Dionex IC-3000 system, Sunnyvale, CA, USA)

A.3.5. Similar inhibitory effect of ZnO and $ZnCl_2$ on methanogens.

Figure A.3.2 shows an overlap of panels A and B of Figure 1 of the manuscript. This figure evidences that ZnO and $ZnCl_2$ have almost the same inhibitory effect on methanogens. Both ZnO and $ZnCl_2$ remained non-inhibitory for the methanogens in sulfate-containing conditions within the sulfide buffered zone. Whereas, an evident inhibitory was observed for both forms of Zn as soon as the concentration of Zn was greater than the concentration of biogenic sulfide. The same pattern was also observed in sulfate-free conditions. ZnO and $ZnCl_2$ had an inhibitory effect at concentrations >0.02 mM of Zn. These observations strongly suggest that ZnO and $ZnCl_2$ affect methanogens in the same fashion in sulfate-free and sulfate-rich conditions.

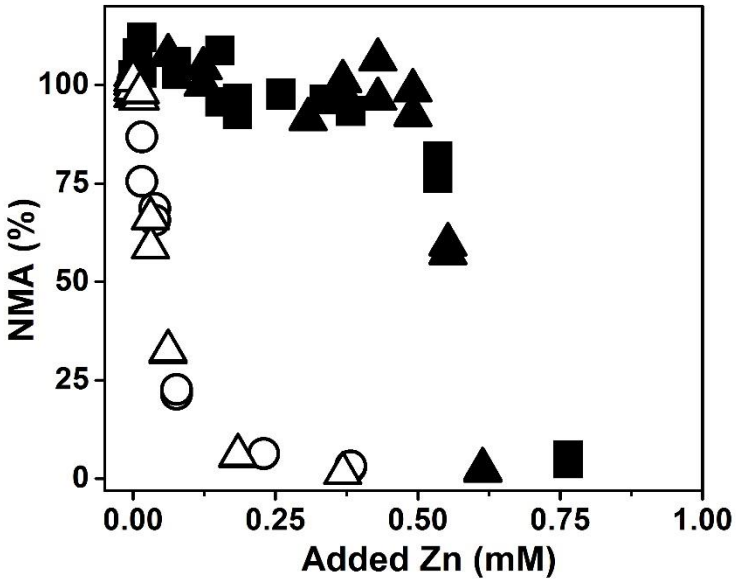

Figure A.3.2. Normalized methanogenic activity of the treatments amended with ZnO NP in sulfate-containing (▲), sulfate-free conditions (△), and with ZnCl2 in sulfate containing (■) and sulfate-free conditions (□). The toxicity response is almost exactly the same for ZnCl2 and ZnO NPs under conditions with or without sulfate

A.3.6. Inhibition effect of Zn and Cu (NPs and salts) on sulfate reduction

An experiment was carried out to explore NP and salt toxicity to sulfate-reducer bacteria by supplying the concentrations that cause inhibition of the acetoclastic methanogens. Figure A.3.3 shows the time course of sulfate consumption at different concentrations of NP and metal. Results indicated that inhibitory concentrations of ZnO and $ZnCl_2$ for methanogens did not decrease the sulfate consumption rate, whereas the highest supplied concentrations of Cu^0 and $CuCl_2$ strongly inhibited sulfate-reduction.

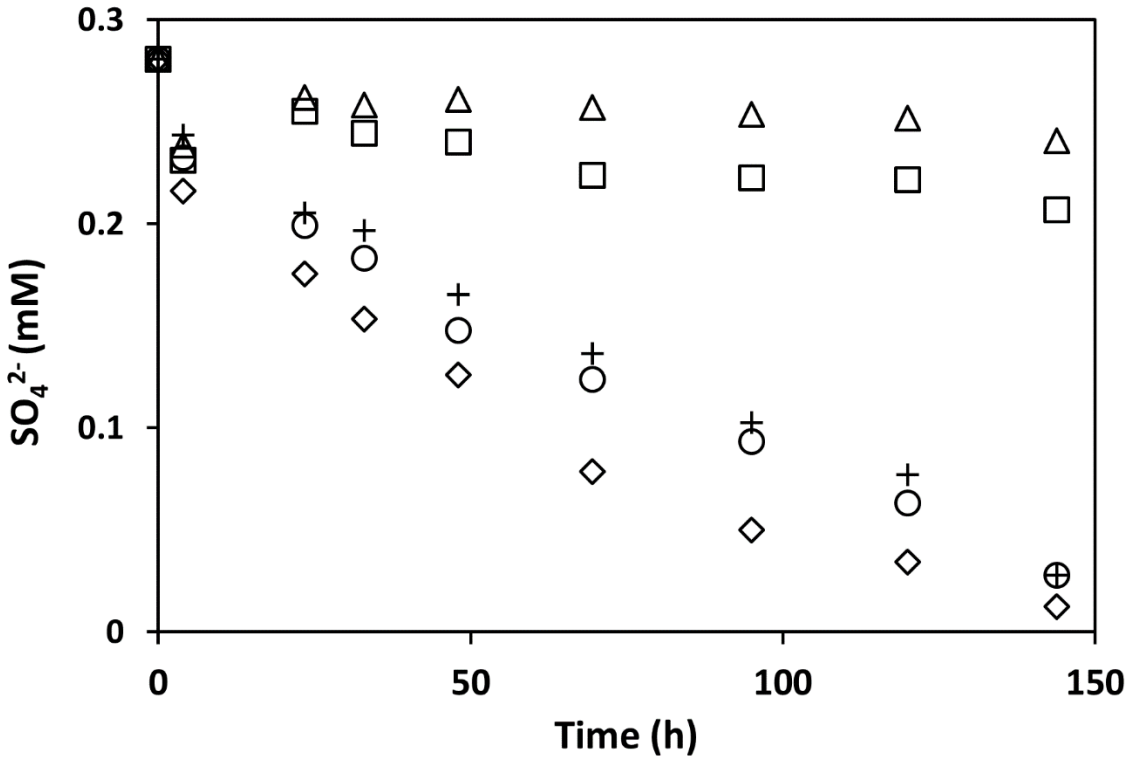

Figure A.3.3. Time course consumption of 0.41 SO_4^{2-} mM by anaerobic sludge at selected concentrations of Zn and Cu that were inhibitory to methanogens. 0 mM (◇), 0.37 $ZnCl_2$ mM (+) 0.8 ZnO mM (○), 0.19 $CuCl_2$ mM (△) Cu^0 0.9mM (□) at different Zn and Cu added concentrations amended with either chlorides or nanoparticles sources.

A.3.7. Source of electron donors for biogenic sulfide production.

An experiment was carried out to determine the source of electron donors used by sulfate-reducer culture by measuring the amount of sulfide produced. Sulfide was analyzed by spectrophotometry using the methylene blue method (Truper & Schlegel, 1964). Figure A.3.4 shows the time course of sulfide production by different electron donors. Results showed that the granular sludge used in this study used endogenous substrates in the biomass as the electron donor to reduce SO_4^{2-}. Acetate had no additional benefit beyond the impact of the endogenous substrate. Results also demonstrate that the sulfate-reducer bacteria of this sludge were able to use H_2 as electron donor as evidenced by an accelerated rate in the treatment with H_2 addition.

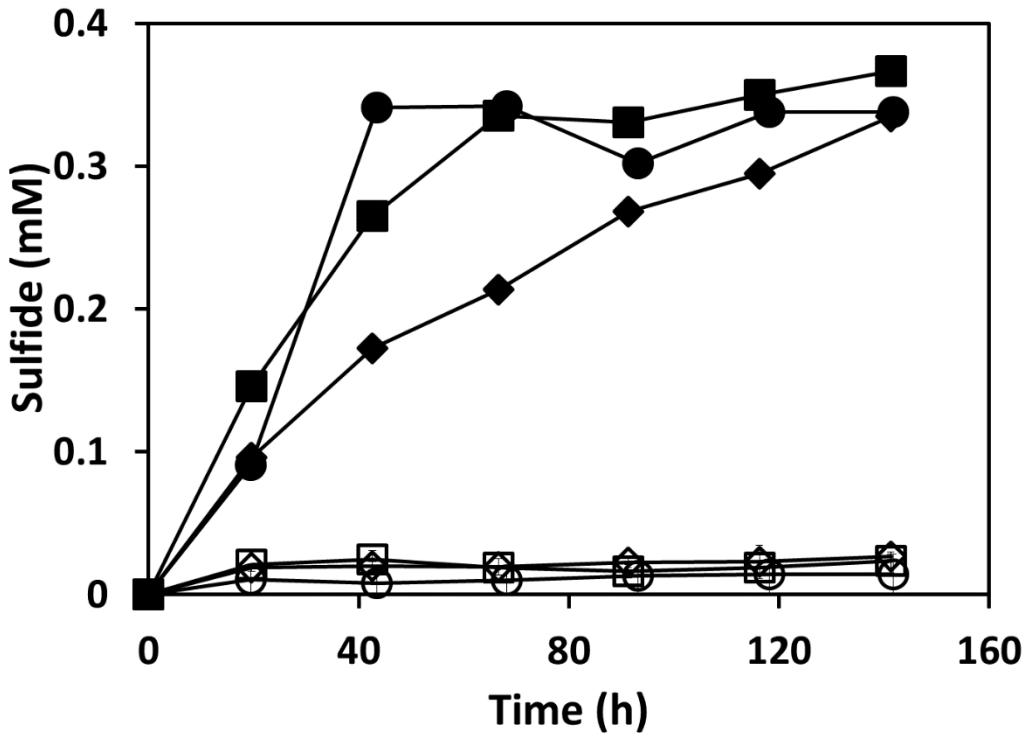

Figure A.3.4. Sulfide production using acetate, endogenic source, and H_2 as electron donors. Sulfate-rich assays supplied with 0.4 mM of sulfate amended with acetate (◆), endogenic source (■) and H_2 (●) as electron donors. And sulfate-free assays amended with acetate (◇), endogenic source (□), and H_2 (○) as electron donors.

A.3.8. Concentration of soluble ions released either by NPs or salts over time.

An analysis of the soluble metals was performed to the long-term assays that were fed with five acetate spikes over a period of 30 days. Figure S5 shows the concentration of soluble metals at different time of the experiment. Overall the results showed that after seven days the concentration of soluble zinc remained constant despite the source (Figure S5 A-B). Conversely, the concentration of soluble Cu progressively decreased over time (Figure S5 C-D).

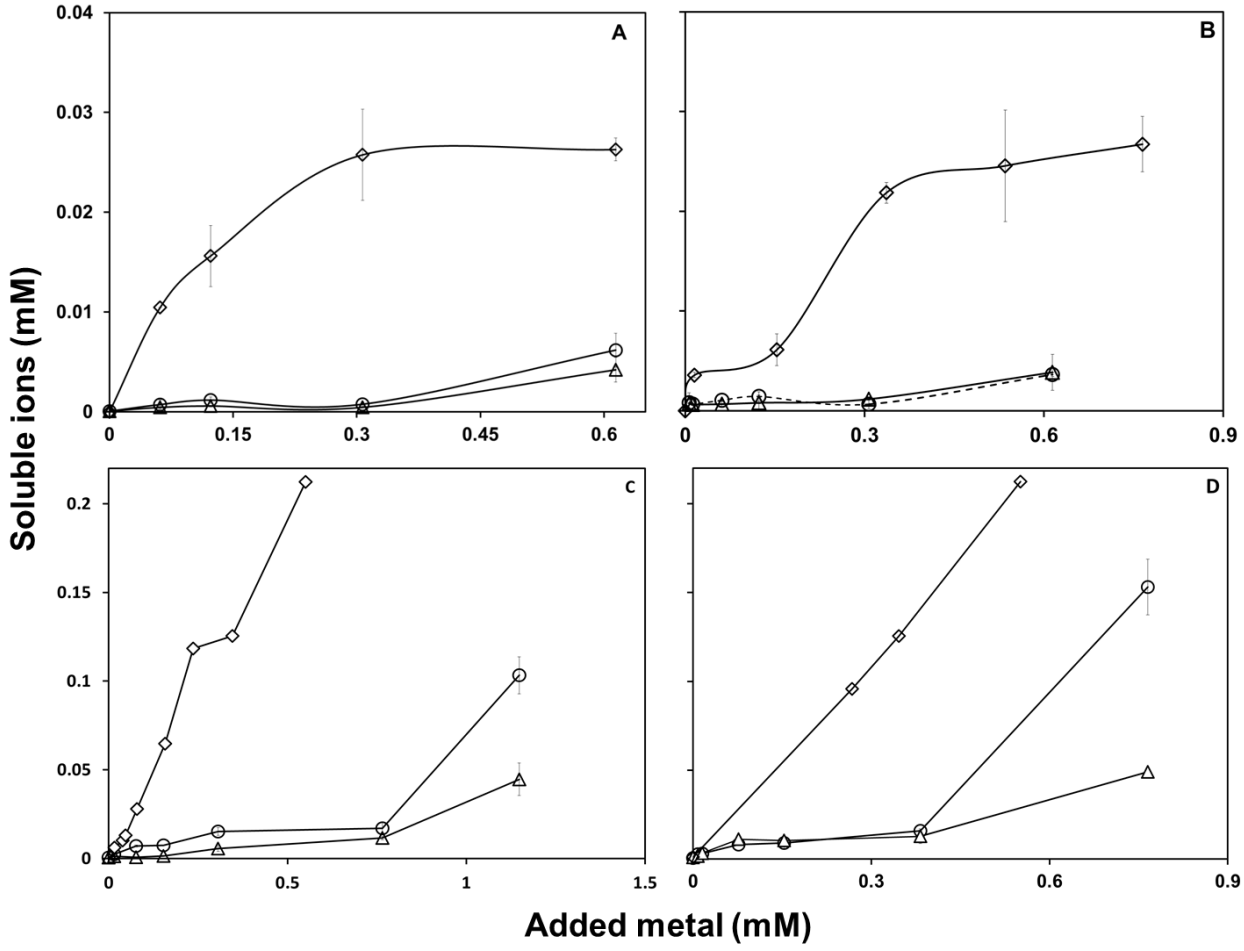

Figure A.3.5 Time 0 (◇), time 7.5 d (○), and time 30 d (△) soluble ZnO-Zn (A), $ZnCl_2$-Zn (B), Cu^0-Cu (C), and $CuCl_2$-Cu(D)

A.3.9. Methanogenic activity in a basal medium rinsed free of metals after the longtime exposure experiment.

In order to confirm that the inhibition was not reversible in the assays that showed complete inhibition, the basal medium of most inhibited assays and the control was exchanged for a basal medium free of metals and the sludge was rinsed out with Milliq water. Figure S6 shows the normalized activity of the 5th and 6th feeding (Metal-free basal medium) of the assays that initially contained inhibitory concentrations of NPs and metals. Results indicated that the assays that were completely inhibited after five feedings of acetate (ZnO, $ZnCl_2$, and $CuCl_2$) remained deactivated after the rinsing. Conversely, a progressive recovery was observed in the assays amended with Cu^0 due to cell growth, which was already evidenced in the 2nd to 5th feedings of acetate.

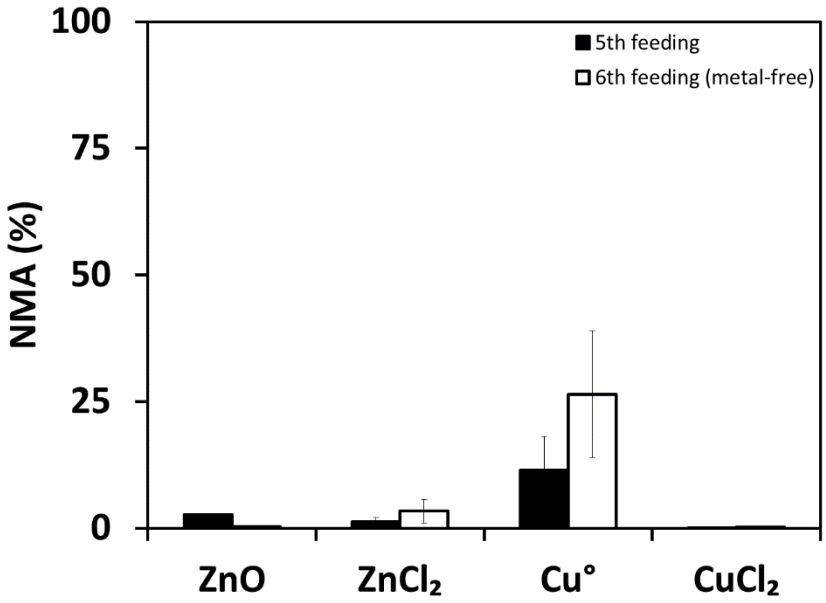

Figure A.3.6. Normalized methanogenic activity of the most inhibited assays in the 5th feeding and 6th feeding (metal-free basal medium). The assays initially contained (mM): ZnO (0.61), $ZnCl_2$ (0.72), Cu^0 (1.18) and $CuCl_2$ (0.79).

ANNEX IV FES ATTENUATES TOXICITY TO METHANOGENS OF ELEMENTAL COPPER AND ZINC OXIDE NANOPARTICLES AND THEIR SOLUBLE METAL ANALOGS

A.4.1. Toxicity of FeS-f and FeS-c.

Figure A.4.1 shows the NMA of the third feeding of acetate in presence of the highest concentration of FeS-f (2.4 mM) and FeS-c (7.2mM) used in the experiments. Results indicated that the NMA was >90% for the assays amended with both FeS-f and FeS-c particles.

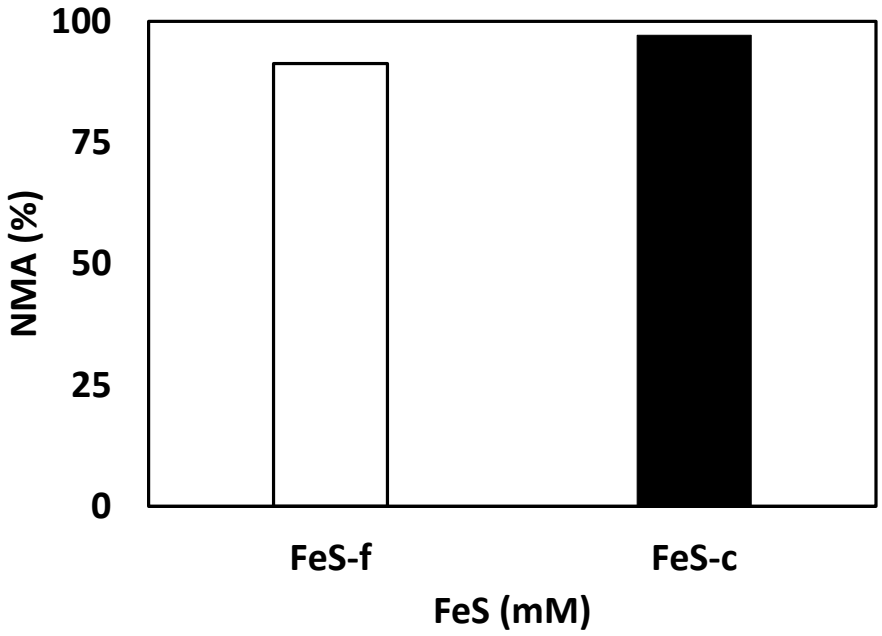

Figure A.4.1. Effect of 2.4 mM of FeS-f (Empty bar) and 7.2 mM of (FeS-c) on the NMA after three feedings of acetate

References

Aitken, R.J., Chaudhry, M.Q., Boxall, A.B.A., Hull, M. 2006. Manufacture and use of nanomaterials: current status in the UK and global trends. *Occup. Med.* **56**(5), 300-306.

Allen, H.E., Fu, G., Deng, B. 1993. Analysis of acid-volatile sulfide (AVS) and simultaneously extracted metals (SEM) for the estimation of potential toxicity in aquatic sediments. *Environ. Toxicol. Chem.*, **12**(8), 1441-1453.

Allison R., V.d.V.a.Y.A. 2012. Effect of silver nanoparticles on soil denitrification kinetics. *Ind. Biotechnol.*, **8**(6), 358-364.

Ankley, G., Thomas, N., Di Toro, D., Hansen, D., Mahony, J., Berry, W., Swartz, R., Hoke, R., Garrison, A.W., Allen, H., Zarba, C. 1994. Assessing potential bioavailability of metals in sediments: A proposed approach. *Environ. Manage.*, **18**(3), 331-337.

Aruoja, V., Dubourguier, H.-C., Kasemets, K., Kahru, A. 2009. Toxicity of nanoparticles of CuO, ZnO and TiO_2 to microalgae Pseudokirchneriella subcapitata. *Sci. Total Environ.*, **407**(4), 1461-1468.

Auffan, M., Rose, J., Bottero, J.-Y., Lowry, G.V., Jolivet, J.-P., Wiesner, M.R. 2009. Towards a definition of inorganic nanoparticles from an environmental, health and safety perspective. *Nat. Nanotechnol.*, **4**(10), 634-641.

Benjamin, M.M. 2002. *Water chemistry*. McGraw-Hill, Boston.

Besser, J.M., Ingersoll, C.G., Giesty, J.P. 1996. Effects of spatial and temporal variation of acid-volatile sulfide on the bioavailability of copper and zinc in freshwater sediments. *Environ. Toxicol. Chem.*, **15**(3), 286-293.

Boxall, A.B.A., Tiede, K., Chaudhry, Q. 2007. Engineered nanomaterials in soils and water: How do they behave and could they pose a risk to human health? *Nanomed.*, **2**(6), 919-927.

Brar, S.K., Verma, M., Tyagi, R.D., Surampalli, R.Y. 2010. Engineered nanoparticles in wastewater and wastewater sludge - Evidence and impacts. *Waste Manage.*, **30**(3), 504-520.

Carlson, C., Hussain, S.M., Schrand, A.M., Braydich-Stolle, L.K., Hess, K.L., Jones, R.L., Schlager, J.J. 2008. Unique Cellular Interaction of Silver Nanoparticles: Size-Dependent Generation of Reactive Oxygen Species. *J. Phys. Chem. B*, **112**(43), 13608-13619.

Casas, A.M., Crecelius, E.A. 1994. Relationship between acid volatile sulfide and the toxicity of zinc, lead and copper in marine sediments. *Environ. Toxicol. Chem.*, **13**(3), 529-536.

Chen, J.L., Ortiz, R., Steele, T.W.J., Stuckey, D.C. 2014. Toxicants Inhibiting Anaerobic Digestion: A Review. *Biotechnol. Adv.* (0).

Chen, X., Mao, S.S. 2007. Titanium dioxide nanomaterials: Synthesis, properties, modifications, and applications. *Chem. Rev.*, **107**(7), 2891-2959.

Chen, Y., Cheng, J.J., Creamer, K.S. 2008. Inhibition of anaerobic digestion process: A review. *Bioresour. Technol.*, **99**(10), 4044-4064.

Choi, O., Cleuenger, T.E., Deng, B., Surampalli, R.Y., Ross, L., Jr., Hu, Z. 2009. Role of sulfide and ligand strength in controlling nanosilver toxicity. *Water Res.*, **43**(7), 1879-1886.

Choi, O., Deng, K.K., Kim, N.-J., Ross Jr, L., Surampalli, R.Y., Hu, Z. 2008. The inhibitory effects of silver nanoparticles, silver ions, and silver chloride colloids on microbial growth. *Water Res.*, **42**(12), 3066-3074.

Conklin, A., Stensel, H.D., Ferguson, J. 2006. Growth kinetics and competition between Methanosarcina and Methanosaeta in mesophilic anaerobic digestion. *Water Environ. Res.*, **78**(5), 486-496.

Dahle, J., Arai, Y. 2014. Effects of Ce(III) and CeO_2 Nanoparticles on Soil-Denitrification Kinetics. *Arch. Environ. Contam. Toxicol.*., 1-9.

Deppenmeier, U. 2002. The unique biochemistry of methanogenesis. *Prog. Nucleic Acid Res. Mol. Biol., Vol 71*, **71**, 223-283.

Dermont, G., Bergeron, M., Mercier, G., Richer-Laflèche, M. 2008. Soil washing for metal removal: A review of physical/chemical technologies and field applications. *J. Hazard. Mater.*, **152**(1), 1-31.

Dezeeuw, W.J. 1985. Acclimatization of anaerobic sludge for UASB reactor start-up. *Neth. J. Agr. Sci.*, **33**(1), 81-84.

Di Toro, D.M., Mahony, J.D., Hansen, D.J., Scott, K.J., Carlson, A.R., Ankley, G.T. 1992. Acid volatile sulfide predicts the acute toxicity of cadmium and nickel in sediments. *Environ. Sci. Technol.*, **26**(1), 96-101.

Di Toro, D.M., Mahony, J.D., Hansen, D.J., Scott, K.J., Hicks, M.B., Mayr, S.M., Redmond, M.S. 1990. Toxicity of cadmium in sediments: The role of acid volatile sulfide. *Environ. Toxicol. Chem.*, **9**(12), 1487-1502.

Franklin, N.M., Rogers, N.J., Apte, S.C., Batley, G.E., Gadd, G.E., Casey, P.S. 2007. Comparative toxicity of nanoparticulate ZnO, bulk ZnO, and $ZnCl_2$ to a freshwater microalga (Pseudokirchneriella subcapitata): The importance of particle solubility. *Environ. Sci. Technol.*, **41**(24), 8484-8490.

Garcia-Saucedo, C., Field, J.A., Otero-Gonzalez, L., Sierra-Alvarez, R. 2011. Low toxicity of HfO_2, SiO_2, Al_2O_3 and CeO_2 nanoparticles to the yeast, Saccharomyces cerevisiae. *J. Hazard. Mater.*, **192**(3), 1572-1579.

Garcia, A., Delgado, L., Tora, J.A., Casals, E., Gonzalez, E., Puntes, V., Font, X., Carrera, J., Sanchez, A. 2012. Effect of cerium dioxide, titanium dioxide, silver, and gold nanoparticles on the activity of microbial communities intended in wastewater treatment. *J. Hazard. Mater.*, **199**, 64-72.

Gerardi, M.H. 2003. Upsets and Unstable Digesters. in: *The Microbiology of Anaerobic Digesters*, John Wiley & Sons, Inc., pp. 121-125.

Golden, J.H., Small, R., Pagan, L., Shang, C., Ragavan, S. 2000. Evaluating and treating CMP wastewater. *Semicond. Int.*, **23**(12), 85-98.

Gomez-Rivera, F., Field, J.A., Brown, D., Sierra-Alvarez, R. 2012. Fate of cerium dioxide (CeO_2) nanoparticles in municipal wastewater during activated sludge treatment. *Bioresour. Technol.*, **108**, 300-304.

Gonzalez-Estrella, J., Puyol, D., Sierra-Alvarez, R., Field, J.A. 2015. Role of biogenic sulfide in attenuating zinc oxide and copper nanoparticle toxicity to acetoclastic methanogenesis. *J. Hazard. Mater.*, **283**(0), 755-763.

Gonzalez-Estrella, J., Sierra-Alvarez, R., Field, J.A. 2013. Toxicity assessment of inorganic nanoparticles to acetoclastic and hydrogenotrophic methanogenic activity in anaerobic granular sludge. *J. Hazard. Mater.*, **260**, 278-285.

Gottschalk, F., Nowack, B. 2011. The release of engineered nanomaterials to the environment. *J. Environ. Monit.*, **13**(5), 1145-1155.

Haaijer, S.C.M., Crienen, G., Jetten, M.S.M., Op den Camp, H.J.M. 2012. Anoxic iron cycling bacteria from an iron sulfide- and nitrate-rich freshwater environment. *Front. Microbiol.*, **3**.

Han, D.S., Orillano, M., Khodary, A., Duan, Y., Batchelor, B., Abdel-Wahab, A. 2014. Reactive iron sulfide (FeS)-supported ultrafiltration for removal of mercury (Hg(II)) from water. *Water Res.*, **53**, 310-321.

Handy, R.D., Owen, R., Valsami-Jones, E. 2008. The ecotoxicology of nanoparticles and nanomaterials: current status, knowledge gaps, challenges, and future needs. *Ecotoxicol.*, **17**(5), 315-325.

Hansen, S.F., Larsen, B.H., Olsen, S.I., Baun, A. 2007. Categorization framework to aid hazard identification of nanomaterials. *Nanotoxicol.*, **1**(3), 243-250.

Jin, P., Bhattacharya, S.K., Williams, C.J., Zhang, H. 1998. Effects of sulfide addition on copper inhibition in methanogenic systems. *Water Res.*, **32**(4), 977-988.

Kahru, A., Dubourguier, H.-C., Blinova, I., Ivask, A., Kasemets, K. 2008. Biotests and biosensors for ecotoxicology of metal oxide nanoparticles: A minireview. *Sens.*, **8**(8), 5153-5170.

Karlsson, H.L., Toprak, M.S., Fadeel, B. 2015. Chapter 4 - Toxicity of Metal and Metal Oxide Nanoparticles. in: *Handbook on the Toxicology of Metals (Fourth Edition)*, (Eds.) G.F. Nordberg, B.A. Fowler, M. Nordberg, Academic Press. San Diego, pp. 75-112.

Karri, S., Sierra-Alvarez, R., Field, J.A. 2006. Toxicity of copper to acetoclastic and hydrogenotrophic activities of methanogens and sulfate reducers in anaerobic sludge. *Chemosphere*, **62**(1), 121-127.

Kartal, B., Maalcke, W.J., de Almeida, N.M., Cirpus, I., Gloerich, J., Geerts, W., den Camp, H., Harhangi, H.R., Janssen-Megens, E.M., Francoijs, K.J., Stunnenberg, H.G., Keltjens, J.T., Jetten, M.S.M., Strous, M. 2011. Molecular mechanism of anaerobic ammonium oxidation. *Nat.*, **479**(7371), 127-U159.

Kim, Y. 2014. Nanowastes treatment in environmental media. *Environ. Health Toxicol.*.

Kiser, M.A., Ryu, H., Jang, H., Hristovski, K., Westerhoff, P. 2010. Biosorption of nanoparticles to heterotrophic wastewater biomass. *Water Res.*, **44**(14), 4105-4114.

Kiser, M.A., Westerhoff, P., Benn, T., Wang, Y., Perez-Rivera, J., Hristovski, K. 2009. Titanium nanomaterial removal and release from wastewater treatment plants. *Environ. Sci. Technol.*, **43**(17), 6757-6763.

Klaine, S.J., Alvarez, P.J.J., Batley, G.E., Fernandes, T.F., Handy, R.D., Lyon, D.Y., Mahendra, S., McLaughlin, M.J., Lead, J.R. 2008. Nanomaterials in the environment: Behavior, fate, bioavailability, and effects. *Environ. Toxicol. Chem.*, **27**(9), 1825-1851.

Lawrence, A.W., McCarty, P.L. 1965. The role of sulfide in preventing heavy metal toxicity in anaerobic treatment. *J. Water Pollut. Control Fed.*, **37**(3), 392-406.

Lee, D.W., El Khoury, Y., Francia, F., Zambelli, B., Ciurli, S., Venturoli, G., Hellwig, P., Daldal, F. 2011a. Zinc inhibition of bacterial cytochrome bc(1) reveals the role of cytochrome b E295 in proton release at the Q(o) site. *Biochem.*, **50**(20), 4263-4272.

Lee, J.-H., Kennedy, D.W., Dohnalkova, A., Moore, D.A., Nachimuthu, P., Reed, S.B., Fredrickson, J.K. 2011b. Manganese sulfide formation via concomitant microbial manganese oxide and thiosulfate reduction. *Environ. Microbiol.*, **13**(12), 3275-3288.

Li, G., Puyol, D., Carvajal-Arroyo, J.M., Sierra-Alvarez, R., Field, J.A. 2014. Inhibition of anaerobic ammonium oxidation by heavy metals. *J. Chem. Technol. Biotechnol.*, n/a-n/a.

Liang, Z., Das, A., Hu, Z. 2010. Bacterial response to a shock load of nanosilver in an activated sludge treatment system. *Water Res.*, **44**(18), 5432-5438.

Liu, G., Wang, D., Wang, J., Mendoza, C. 2011. Effect of ZnO particles on activated sludge: Role of particle dissolution. *Sci. Total Environ.*, **409**(14), 2852-2857.

Lombi, E., Donner, E., Tavakkoli, E., Turney, T.W., Naidu, R., Miller, B.W., Scheckel, K.G. 2012. Fate of zinc oxide nanoparticles during anaerobic digestion of wastewater and post-treatment processing of sewage sludge. *Environ. Sci. Technol.*, **46**(16), 9089-9096.

Luna-delRisco, M., Orupold, K., Dubourguier, H.-C. 2011. Particle-size effect of CuO and ZnO on biogas and methane production during anaerobic digestion. *J. Hazard. Mater.*, **189**(1-2), 603-608.

Luna-Velasco, A., Field, J.A., Cobo-Curiel, A., Sierra-Alvarez, R. 2011. Inorganic nanoparticles enhance the production of reactive oxygen species (ROS) during the autoxidation of L-3,4-dihydroxyphenylalanine (L-dopa). *Chemosphere*, **85**(1), 19-25.

Ma, R., Levard, C., Judy, J.D., Unrine, J.M., Durenkamp, M., Martin, B., Jefferson, B., Lowry, G.V. 2013a. Fate of zinc oxide and silver nanoparticles in a pilot wastewater treatment plant and in processed biosolids. *Environ. Sci. Technol.*, **48**(1), 104-112.

Ma, R., Levard, C., Michel, F.M., Brown, G.E., Lowry, G.V. 2013b. Sulfidation mechanism for zinc oxide nanoparticles and the effect of sulfidation on their solubility. *Environ. Sci. Technol.*, **47**(6), 2527-2534.

McDevitt, C.A., Ogunniyi, A.D., Valkov, E., Lawrence, M.C., Kobe, B., McEwan, A.G., Paton, J.C. 2011. A molecular mechanism for bacterial susceptibility to zinc. *PLoS Pathog.*, **7**(11).

Metcalf, Eddy, Tchobanoglous, G., Burton, F.L., Stensel, H.D. 2003. *Wastewater engineering : treatment and reuse*. McGraw-Hill, Boston; Montréal.

Morse, J.W., Millero, F.J., Cornwell, J.C., Rickard, D. 1987. The chemistry of the hydrogen sulfide and iron sulfide systems in natural waters. *Earth Sci. Rev.*, **24**(1), 1-42.

Mu, H., Chen, Y. 2011. Long-term effect of ZnO nanoparticles on waste activated sludge anaerobic digestion. *Water Res.*, **45**(17), 5612-5620.

Mu, H., Chen, Y., Xiao, N. 2011. Effects of metal oxide nanoparticles (TiO_2, Al_2O_3, SiO_2 and ZnO) on waste activated sludge anaerobic digestion. *Bioresour. Technol.*, **102**(22), 10305-10311.

Mu, H., Zheng, X., Chen, Y., Chen, H., Liu, K. 2012. Response of Anaerobic Granular Sludge to a Shock Load of Zinc Oxide Nanoparticles during Biological Wastewater Treatment. *Environ. Sci. Technol.*, **46**(11), 5997-6003.

Nies, D.H. 1999. Microbial heavy-metal resistance. *Appl. Microbiol. Biotechnol.*, **51**(6), 730-750.

Nowack, B., Bucheli, T.D. 2007. Occurrence, behavior and effects of nanoparticles in the environment. *Environ. Pollut.*, **150**(1), 5-22.

Nyberg, L., Turco, R.F., Nies, L. 2008. Assessing the impact of nanomaterials on anaerobic microbial communities. *Environ. Sci. Technol.*, **42**(6), 1938-1943.

Ochoa-Herrera, V., Leon, G., Banihani, Q., Field, J.A., Sierra-Alvarez, R. 2011. Toxicity of copper(II) ions to microorganisms in biological wastewater treatment systems. *Sci. Total Environ.*, **412**, 380-385.

Ollila, K. 2013. Copper corrosion experiments under anoxic conditions. *Svensk Kärnbränslehantering AB Swedish Nucl. Fuel and Waste Manag. Co*.

Omil, F., Lens, P., Visser, A., Pol, L.W.H., Lettinga, G. 1998. Long-term competition between sulfate reducing and methanogenic bacteria in UASB reactors treating volatile fatty acids. *Biotechnol. and Bioeng.*, **57**(6), 676-685.

Otero-González, L., Field, J.A., Sierra-Alvarez, R. 2014a. Fate and long-term inhibitory impact of ZnO nanoparticles during high-rate anaerobic wastewater treatment. *J. Environ. Manage.*, **135**(0), 110-117.

Otero-González, L., Field, J.A., Sierra-Alvarez, R. 2014b. Inhibition of anaerobic wastewater treatment after long-term exposure to low levels of CuO nanoparticles. *Water Res.*, **58**(0), 160-168.

Patterson, R.R., Fendorf, S., Fendorf, M. 1997. Reduction of hexavalent chromium by amorphous iron sulfide. *Environ. Sci. Technol.*, **31**(7), 2039-2044.

Peng, J.-f., Song, Y.-h., Yuan, P., Cui, X.-y., Qiu, G.-l. 2009. The remediation of heavy metals contaminated sediment. *J. Hazard. Mater.*, **161**(2–3), 633-640.

Puyol, D., Sanz, J.L., Rodriguez, J.J., Mohedano, A.F. 2012. Inhibition of methanogenesis by chlorophenols: a kinetic approach. *New Biotechnol.*, **30**(1), 51-61.

Reed, R.B., Ladner, D.A., Higgins, C.P., Westerhoff, P., Ranville, J.F. 2012. Solubility of nano-zinc oxide in environmentally and biologically important matrices. *Environ. Toxicol. Chem.*, **31**(1), 93-99.

Reith, J.H., Wijffels, R.H. 2003. *Bio-methane & bio-hydrogen : status and perspectives of biological methane and hydrogen production*. Dutch Biol. Hydrogen Found., Petten.

Rittmann, B.E., McCarty, P.L. 2001. *Environmental biotechnology : principles and applications*. McGraw-Hill, Boston.

Roco, M.C. 2011. The long view of nanotechnology development: the National Nanotechnology Initiative at 10 years (vol 13, pg 427, 2011). *J. Nanopart. Res.*, **13**(3), 1335-1335.

Roco, M.C., Mirkin, C.A., Hersam, M.C. 2011. Nanotechnology research directions for societal needs in 2020: summary of international study. *J. Nanopart. Res.*, **13**(3), 897-919.

Sani, R.K., Peyton, B.M., Brown, L.T. 2001. Copper-induced inhibition of growth of Desulfovibrio desulfuricans G20: Assessment of its toxicity and correlation with those of zinc and lead. *Appl. Environ. Microbiol.*, **67**(10), 4765-4772.

Simpson, S.L., Rosner, J., Ellis, J. 2000. Competitive displacement reactions of cadmium, copper, and zinc added to a polluted, sulfidic estuarine sediment. *Environ. Toxicol. Chem.*, **19**(8), 1992-1999.

Solioz, M., Abicht, H.K., Mermod, M., Mancini, S. 2010. Response of Gram-positive bacteria to copper stress. *J. Biol. Inorg. Chem.*, **15**(1), 3-14.

Tapia-Rodriguez, A., Luna-Velasco, A., Field, J.A., Sierra-Alvarez, R. 2010. Anaerobic bioremediation of hexavalent uranium in groundwater by reductive precipitation with methanogenic granular sludge. *Water Res.*, **44**(7), 2153-2162.

Truper, H.G., Schlegel, H.G. 1964. Sulphur metabolism in thiorhodaceae .1. Quantitative measurements on growing cells of chromatium okenii. Anton Van Lee J. M. S., **30**(3), 225-&.

Utgikar, V.P., Tabak, H.H., Haines, J.R., Govind, R. 2003. Quantification of toxic and inhibitory impact of copper and zinc on mixed cultures of sulfate-reducing bacteria. *Biotechnol. Bioeng.*, **82**(3), 306-312.

Wang, J.M., Huang, C.P., Allen, H.E. 2003. Modeling heavy metal uptake by sludge particulates in the presence of dissolved organic matter. *Water Res.*, **37**(20), 4835-4842.

Wang, Z.Y., von dem Bussche, A., Kabadi, P.K., Kane, A.B., Hurt, R.H. 2013. Biological and Environmental Transformations of Copper-Based Nanomaterials. *Acs Nano*, **7**(10), 8715-8727.

Westerhoff, P.K., Kiser, A., Hristovski, K. 2013. Nanomaterial removal and transformation during biological wastewater treatment. *Environ. Eng. Sci.* **30**(3), 109-117.

Yang, Y., Chen, Q., Wall, J.D., Hu, Z. 2012a. Potential nanosilver impact on anaerobic digestion at moderate silver concentrations. *Water Res.*, **46**(4), 1176-1184.

Yang, Y., Xu, M., Wall, J.D., Hu, Z. 2012b. Nanosilver impact on methanogenesis and biogas production from municipal solid waste. *Waste Manage.*, **32**(5), 816-825.

Zayed, G., Winter, J. 2000. Inhibition of methane production from whey by heavy metals - protective effect of sulfide. *Appl. Microbiol. Biotechnol.*, **53**(6), 726-731.

Zhang, Y., Chen, Y., Westerhoff, P., Hristovski, K., Crittenden, J.C. 2008. Stability of commercial metal oxide nanoparticles in water. *Water Res.*, **42**(8-9), 2204-2212.

Zumft, W., Körner, H. 1997. Enzyme diversity and mosaic gene organization in denitrification. Anton Van Lee., **71**(1-2), 43-58.